UNIVERSITY OF CALIFORNIA

Los Angeles

Resistance to Programmed Death Protein 1 Blockade Mediated by Somatic *JAK1/2* Mutations

A dissertation submitted in partial satisfaction of the

requirements for the degree Doctor of Philosophy

in Molecular, Cellular and Integrative Physiology

by

Daniel Sanghoon Shin

2017

ABSTRACT OF THE DISSERTATION

Resistance to Programmed Death Protein 1 Blockade

Mediated by Somatic *JAK1/2* Mutations

by

Daniel Sanghoon Shin

Doctor of Philosophy in Molecular, Cellular and Integrative Physiology

University of California, Los Angeles, 2017

Professor Antoni Ribas, Chair

Blocking programmed death protein 1 (PD-1) negative immune receptor has produced remarkable progress in treating patients with advanced cancers, such as melanoma, lung, head and neck, kidney, bladder, Hodgkin's disease, mismatch repair deficient colon cancer, liver and ovarian cancer with high mutational burden, etc. However, only subset of patients are benefitting from this therapy and substantial portion of patients have relapsed after long durable response. Therefore, it is critical to understand its resistance mechanisms to improve therapeutic efficacy and select right patients for checkpoint blockade immunotherapy. We have identified mutations associated with acquired resistance among 4 patients with advanced melanoma, including *JAK1/2* that resulted in loss of adaptive programmed death protein ligand 1 (PD-L1). We reasoned that this could occur among patients with primary resistance. *JAK1*/*2* inactivating mutations were found in tumor biopsies of 1 of 23 patients with melanoma and in 1 of 16 patients with mismatch repair deficient colon cancer treated with PD-1 blockade. Two out of 48 human melanoma cell lines had *JAK1/2* mutations led to loss of PD-L1 expression upon interferon gamma exposure mediated by disabled interferon gamma receptor signaling pathway.

JAK1/2 loss-of-function alterations in TCGA confer adverse outcomes in patients. sh-RNA screening and chromatin immunoprecipitation approach on interferon signaling genes for selected melanoma cell lines revealed JAK1/2, STAT1/2/3 and IRF-1 are the key molecules involved in PD-L1 expression. RNA-seq analyses for tumors enriched with these genes were associated with clinical response to PD-1 blockade. Therefore, we propose that *JAK1/2* loss-of-function mutations are a genetic mechanism of lack of reactive PD-L1 expression and response to interferon gamma, leading to primary or acquired resistance to PD-1 blockade therapy.

The dissertation of Daniel Sanghoon Shin is approved.

Thomas Graeber

Ming Guo

Siavash Kurdistani

Antoni Ribas, Committee Chair

University of California, Los Angeles

2017

DEDICATION

This dissertation is dedicated to my wife, Hannah Shin, my two daughters, Noelle and Eleanor, and my mother, You Sun Kang and late father Chul Soon Shin.

TABLE OF CONTENTS

List of Figures

Chapter 1:

Chapter 2

Chapter 3

Chapter 4

Chapter 5

Acronyms

BRAF: proto-oncogene B-raf and v-Raf murine sarcoma viral oncogene homolog B

EGFR: Epidermal Growth Factor Receptor

CTLA-4: Cytotoxic T cell Lymphocyte Antigen-4

PD-1: Programmed Death Protein-1 or Programmed Death Protein Receptor-1

PD-L1/2: Programmed Death Protein Ligand 1/2

TCR: T cell Receptor

TNF-α: Tumor Necrosis Factor-alpha

IFN-γ: Interferon Gamma

IL: Interleukin

TIL: Tumor Infiltrating Lymphocyte

SHP-2: Src Homology 2-Containing Tyrosine Phosphatase

ITSM: Immunoreceptor Tyrosine-based Switch Motif

ZAP70: Zeta-chain-associated protein kinase 70

PI3K: Phosphatidylinositol-4,5-bisphosphate 3-kinase

AKT: Protein Kinbase B

CCL4: Chemokine (C-C motif) Ligand 4

TAP1: Transporter associated with Antigen Processing 1

MHC: Major Histocompatibility Complex

B2M: Beta-2-microglobulin

RECIST: Response Evaluation Criteria In Solid Tumors

irRECIST: Immune Related Response Evaluation Criteria In Solid Tumors

LOH: Loss of Heterozygosity

STAT: Signal Transducer and Activator of Transcription

TYK2: Tyrosine Kinase 2

JAK1/2: Januse Kinase 1/2

IRF-1/9: Interferon Regulatory Factor-1/9

CXCL: Chemokine (C-X-C motif) Ligand

IRB: Internal Review Board

IHC: Immunohistochemistry

cGAMP: Cyclic Guanosine Monophosphate–Adenosine Monophosphate

TRAIL: TNF-related Apoptosis-inducing Ligand

HLA: Human Leukocyte Antigen

STING: Stimulator of Inteferon genes

CCLE: Cancer Cell Line Encycolopedia

TCGA: The Cancer Genome Atlas

CRISPR: Clustered regularly interspaced short palindromic repeats

SOCS1/3: Suppressor of Cytokine Signaling 1/3

IDO1: Indoleamine-pyrrole 2,3-dioxygenase 1

ATAC: Assay for Transposase-Accessible Chromatin

Supplementary materials

1. Supplementary Material for chapter 2 - 4

2. Supplementary Table for chapter 4

ACKNOWLEDGMENTS

I first would like to thank my mentor, Dr. Antoni Ribas, for his unfailing guidance and support throughout my fellowship training and PhD course. I also thank my committee members, Dr. Graeber, Dr. Guo and Dr. Kurdistani for their support and collaboration. I especially thank my co-mentor, Dr. Comin-Anduix who has trained me from the first day of joining Dr. Ribas' lab. Thank you to all Ribas' lab members who have been so helpful in many ways.

I thank my family, especially my wife, for their understanding and support through the last 10 years of my journey from residency until today. Without their support, I could not have completed this training. Thank you and love you all.

Chapter 1 contains Figures from review article “Releasing the Brakes on Cancer Immunotherapy” published by Antoni Ribas in New Eng J Med in Oct, 2015. Figures were reproduced with permission.

Chapter 2 was reproduced with the permission from New England Journal of Medicine as per journal copyright policy for thesis dissertation.

Chapter 3 was reproduced with the permission from Cancer Discovery as per journal copyright policy for thesis dissertation.

Chapter 4 was reproduced with the permission from Cell Reports as per journal copyright policy for thesis dissertation.

I would like to thank to the sources of funding that have supported me throughout the training, including Dermatology Scientist Training grant (2014-2015), Tumor Immunology Training grant (2015-2017), Tower Oncology Career Development Award (2015) and Young Investigator Award from Conquer Cancer Foundation/American Society of Clinical Oncology (2016). I also thank to UCLA STAR (Specialty Training and Advanced Research) program for the financial support and academic guidance and UCLA Hematology-Oncology fellowship program.

Finally, I thank to my friends, specially Nico Palaskas who is one of my fellowship classmates, for the mutual encouragement and support throughout STAR program PhD course. I wish the best to all of my friends for their future endeavor.

VITA

Education:

2013-2017	Ph.D Candidate in Molecular, Cellular and Integrative Physiology STAR (Specialty Training and Advanced Research) Program University of California, Los Angeles, USA
2012-2015	Hematology-Medical Oncology Fellowship training. University of California, Los Angeles, USA
2007-2012	Medicine Residency. (Medical Scientist Pathway) Albert Einstein College of Medicine/Jacobi Medical Center, Bronx, NY, USA
2002-2003	Transitional Year (Internship) Kyung Hee University Medical Center, Seoul, Korea
1998-2002	M.D. Medicine Kyung Hee University, Seoul, Korea

Grants and Awards:

2016	Tumor Immunology NIH T32 grant. PI: Dr. Michael Teitell
2016	American Society of Clinical Oncology/Conquer Cancer Foundation Young Investigator Award
2016	Second Annual Immuno-Oncology Young Investigator's Forum, third place in Basic Science.
2015	Tumor Immunology NIH T32 grant. PI: Dr. Michael Teitell
2015	Tower Oncology Foundation Career Development Award
2014	Dermatology Scientist NIH T32 grant. PI: Dr. Robert Modlin

Publications:

Peer Reviewed Articles

1. Angel Garcia-Diaz, **Daniel Sanghoon Shin**, Blanca Homet Moreno, et al. Interferon receptor signaling pathways regulating PD-L1 and PD-2 expression. *Cell Reports*. 19(6), 1189-1201. 9 May 2017
2. **Daniel Sanghoon Shin**, Jesse M. Zaretsky, Helena Escuin-Ordinas, et al: Primary resistance to PD-1 blockade mediated by *JAK1/2* mutations. *Cancer Discovery*, 7(2):188-201, 2017. Epub, 30 November 2016.

3. Jesse M. Zaretsky, Angel Garcia-Diaz, **Daniel S. Shin**, et al: Mutations Associated with Acquired Resistance to PD-1 Blockade in Melanoma. *New England Journal of Medicine* 375(9):819-829. 07/2016
4. Young Kwang Chae, Ayush Arya, Mary-Kate Malecek, **Daniel Sanghoon Shin**, et al: Repurposing metformin for cancer treatment: current clinical studies. *Oncotarget* 03/2016.
5. Antoni Ribas, **Daniel Sanghoon Shin**, Jesse Zaretsky, et al: PD-1 blockade expands intratumoral memory T cells. *Cancer Immunology Research* 01/2016; 4(3).
6. **Daniel Sanghoon Shin**, Antoni Ribas: The evolution of checkpoint blockade as a cancer therapy: What's here, what's next? *Current Opinion in Immunology* 04/2015; 33.
7. **Daniel Sanghoon Shin**, Rongbao Zhao, Andras Fiser, et al: The Role of the Fourth Transmembrane Domain in Proton-Coupled Folate Transporter (PCFT) Function as Assessed by the Substituted Cysteine Accessibility Method. *AJP Cell Physiology* 04/2013; 304(12).
8. **Daniel Sanghoon Shin**, Rongbao Zhao, Andras Fiser, et al: Functional roles of the A335 and G338 residues of the proton-coupled folate transporter (PCFT-SLC46A1) mutated in hereditary folate malabsorption. *AJP Cell Physiology* 07/2012; 303(8):C834-42.
9. Rongbao Zhao, **Daniel Sanghoon Shin**, Andras Fiser, et al: Identification of a functionally critical GXXG motif and its relationship to the folate binding site of the proton-coupled folate transporter (PCFT-SLC46A1). *AJP Cell Physiology* 07/2012; 303(6):C673-81.
10. **Daniel Sanghoon Shin**, Rongbao Zhao, Enghui H Yap, et al: A P425R mutation of the proton-coupled folate transporter causing hereditary folate malabsorption produces a highly selective alteration in folate binding. *AJP Cell Physiology* 02/2012; 302(9):C1405-12.
11. Rongbao Zhao, **Daniel Sanghoon Shin**, Ndeye Diop-Bove, Channa Gila Ovits, I David Goldman: Random Mutagenesis of the Proton-coupled Folate Transporter (SLC46A1), Clustering of Mutations, and the Bases for Associated Losses of Function. *Journal of Biological Chemistry* 05/2011; 286(27):24150-8.
12. **Daniel Sanghoon Shin**, Kris Mahadeo, Sang Hee Min, et al: Identification of novel mutations in the proton-coupled folate transporter (PCFT-SLC46A1) associated with hereditary folate malabsorption. *Molecular Genetics and Metabolism* 05/2011; 103(1):33-7.
13. Rongbao Zhao, **Daniel Sanghoon Shin**, I David Goldman: Vulnerability of the cysteine-less proton-coupled folate transporter (PCFT-SLC46A1) to mutational stress associated with the substituted cysteine accessibility method. *Biochimica et Biophysica Acta* 04/2011; 1808(4):1140-5.
14. **Daniel Sanghoon Shin**, Sang Hee Min, Laura Russell, et al: Functional roles of aspartate residues of the proton-coupled folate transporter (PCFT-SLC46A1); a D156Y mutation causing hereditary folate malabsorption. *Blood* 12/2010; 116(24):5162-9.
15. Kris Mahadeo, Ndeye Diop-Bove, **Daniel Shin**, et al: Properties of the Arg376 residue of the proton-coupled folate transporter (PCFT-SLC46A1) and a glutamine mutant causing hereditary folate malabsorption. *AJP Cell Physiology* 11/2010; 299(5):C1153-61.
16. Rongbao Zhao, Ersin Selcuk Unal, **Daniel Sanghoon Shin**, et al: Membrane topological analysis of the proton-coupled folate transporter (PCFT-SLC46A1) by the substituted cysteine accessibility method. *Biochemistry* 03/2010; 49(13):2925-31.

Chapter 1:

Introduction

1.1 Cancer immunotherapy targeting immune checkpoint

Systemic chemotherapy has been main therapeutic armamentarium for patients with advanced cancers since 1940's when Sydney Farber introduced anti-folate agent to treat pediatric leukemia patients. Many decades of trials and fails, some of the cancers, especially hematologic malignancies could be cured by various combination of systemic chemotherapeutic agents. However, it comes with significant toxicities with marginal benefit for most of patients with advanced solid malignancies. More recently, field of oncology had major advancement to treat patients with targeted agents. Some of cancers, such as BRAF mutated melanoma or EGFR mutated non-small cell lung cancer have somatic mutations or overexpression on tyrosine kinases that driving cancer cells to grow (1-3). Over a decade of studies, targeted agents have shown improved response rate and survival and now these agents are readily available in the clinic. However, the majority of patients will develop resistance to these targeted agents with limited duration of response (4-7).

The concept of utilizing our immune system to fight cancer was introduced more than a century ago when Dr. Coley observed tumor regression with infection after surgery. Since then, efforts to activate the immune system to treat patients with advanced cancers largely had been unsuccessful until the first immune checkpoint blockade agent, anti-Cytotoxic T lymphocyte Antigen 4 (CTLA4) antibody (ipilimumab), was approved for patients with advanced melanoma in 2011 (Figure 1) (8, 9). Shortly after anti-CTLA4 antibody was approved, programmed death protein 1 (PD-1) blocking antibodies (pembrolizumab and nivolumab) were approved for

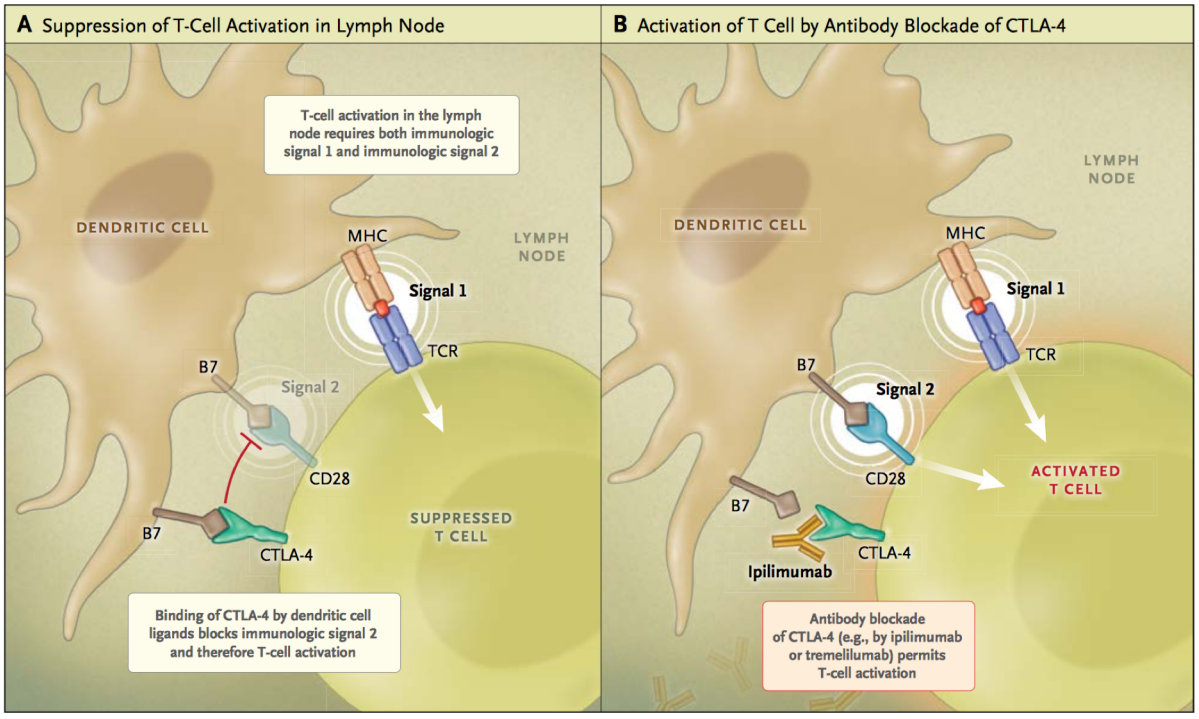

Figure 1. T cell activation in the lymph node. Two immunologic signals are required for T cell activation in the lymph node: stimulation of the T cell receptor (TCR) by the MHC (immunologic signal 1), and stimulation of CD28 by the B7 costimulatory molecule (immunologic signal 2). However, binding of the B7 costimulatory molecules to CTLA-4 blocks immunologic signal 2, and therefore blocks T cell activation. Antibody blockader of CTLA-4, for example, by ipilimumab, derepresses signals by CD28, permitting T cell activation. *Ribas A, N Eng J Med 2015; 373:1490-1492*

patients with advanced melanoma and non-small cell lung cancer in 2014 and its indication has been grown to bladder, head and neck, Hodgkin disease, kidney, mismatch repair deficient colorectal cancer and it continues to growing (10-15). It is considered a major breakthrough in cancer therapeutics given unprecedented durable response rate for patients (Figure 2 and Figure 3) (16, 17) with various types of advanced cancers. Even with this remarkable success, only subset of patients benefitting from this therapy and the field has been putting tremendous efforts to identify biomarker to predict response and improve therapeutic efficacy with various combinatorial strategies (18).

1.2 Blockade of PD-1/PD-L1 axis

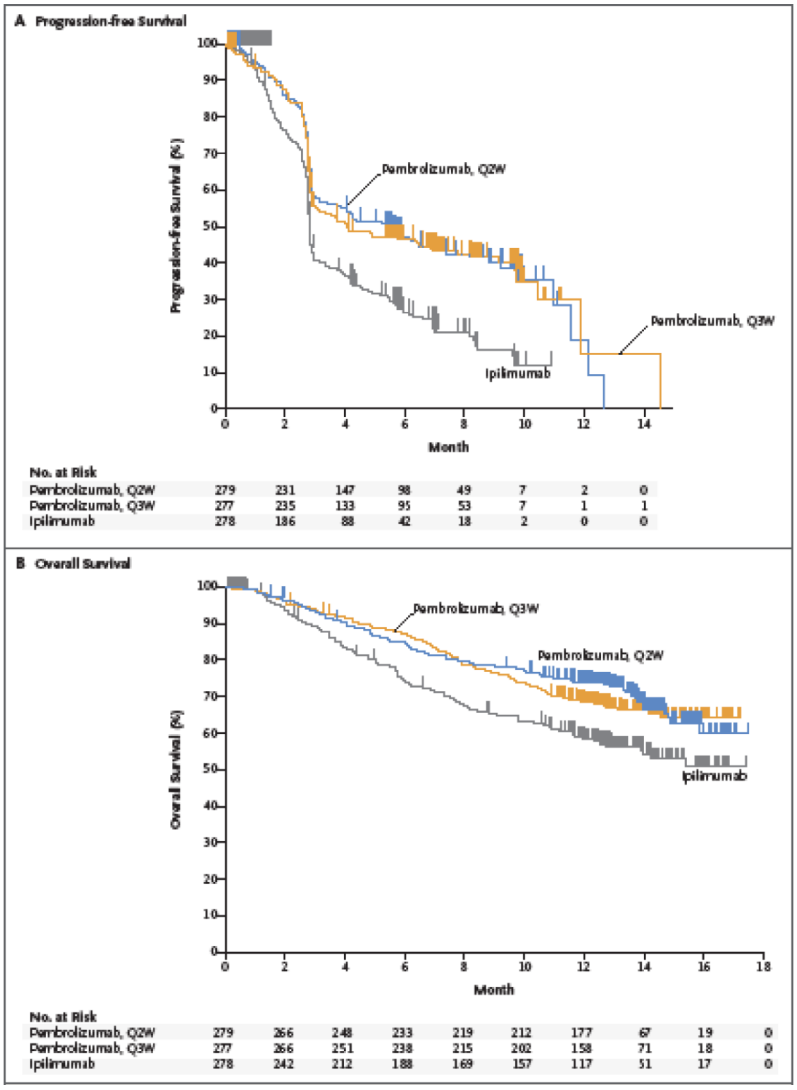

Figure 2. Kaplan-Meier Estimates of progression-free and overall survival. Shown are rates of progression-free survival as of September 3, 2014 (Panel A), and overall survival as of March 3, 2015 (Panel B), in the intention-to-treat population among patients receiving pembrolizumab every 2 weeks (Q2W) or every 3 weeks (Q3W) or ipilimumab. *Robert C et al. N Eng J Med. 2015 Jun 25;372(26):2521-32.*

A. Biology

PD-1 (also known as CD279) is a type I transmembrane receptor protein consisted of 268 amino acids, belongs to the immunoglobulin superfamily (19). It is a co-inhibitory immune checkpoint molecule expressed at the surface of T cells during thymic development and several types of hematopoietic cells following T cell receptor (TCR) signaling and cytokine stimulation (20, 21). Persistent PD-1 expression on T cells may result in T cell exhaustion that characterized by inability to secret cytolytic molecules, such as perforin/granzyme and pro-inflammatory cytokines, such as interferon gamma (IFN-γ), interleukin-2 (IL-2) and tumor necrosis factor alpha (TNF-α) (22-25).

PD-1 has two binding ligands, PD-L1 (B7-H1, CD274) and PD-L2 (B7-DC, CD273), with PD-L1 being better characterized in regulation (25, 26). PD-L1 is inducibly expressed on both hematopoietic cells and non-hematopoietic cells with specific stimulation (20). Cytokines, such

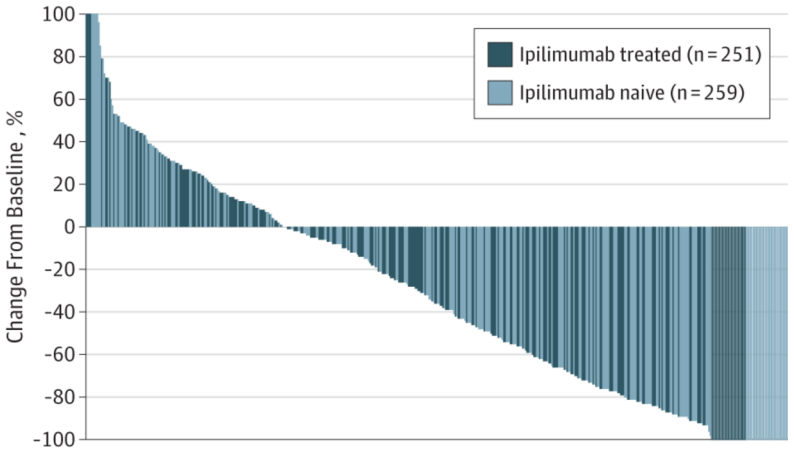

Figure 3. Maximum Percentage of Change From Baseline in Sum of the Longest Diameter of Each Target Lesion in the Full Analysis Set. Reports maximum percentage change from baseline in the sum of the longest diameter of each target lesion, as assessed by RECIST v1.1 by independent central review for patients who had measurable disease at baseline by the same and at least 1 postbaseline tumor assessment (full analysis set, N = 510). Target lesions were defined as all measurable lesions up to a maximum of 2 lesions per organ and 5 lesions in total. Changes greater than 100% were truncated at 100%. *Ribas A et al, 2016 JAMA Apr 19;315(15):1600-9*

as IFN-γ or TNF-α can induce its expression on T cells, B cells, endothelial cells and epithelial cells that involved in maintenance of peripheral tolerance. Inducible PD-L2 expression is somewhat limited to dendritic cells (DCs), macrophage, mast cells and some B cells with IL-4 and interferons.

B. Regulation of PD-1 and its ligands in human malignancy

Persistent expression of PD-1 on T cells is highly suggestive of T cell exhaustion that associated with decreased function or so called ‘anergic state’. This has been observed in many types of tumor infiltrating lymphocytes (TILs) that potentially associated with poor prognosis (27-30). It signifies the important role of PD-1 molecule in mediating anti-tumor activity. PD-L1/L2 expression also showed its prognostic role in some cancers (31-34), PD-L1 being the major ligand that associated with tumor size, lymph node involvement and overall survival. As discussed above, tumor PD-L1 can be expressed with cytokine stimulation, especially IFN-γ, which is particularly important in tumor microenvironment that is most likely associated with T cell infiltration. This is the mechanistic rationale to target PD-1/PD-L1 axis that will be discussed below. PD-L1 also can be expressed with various oncogenic processes (36-40) and its expression without T cell association is unknown significance yet in the context of PD-1 blockade immunotherapy.

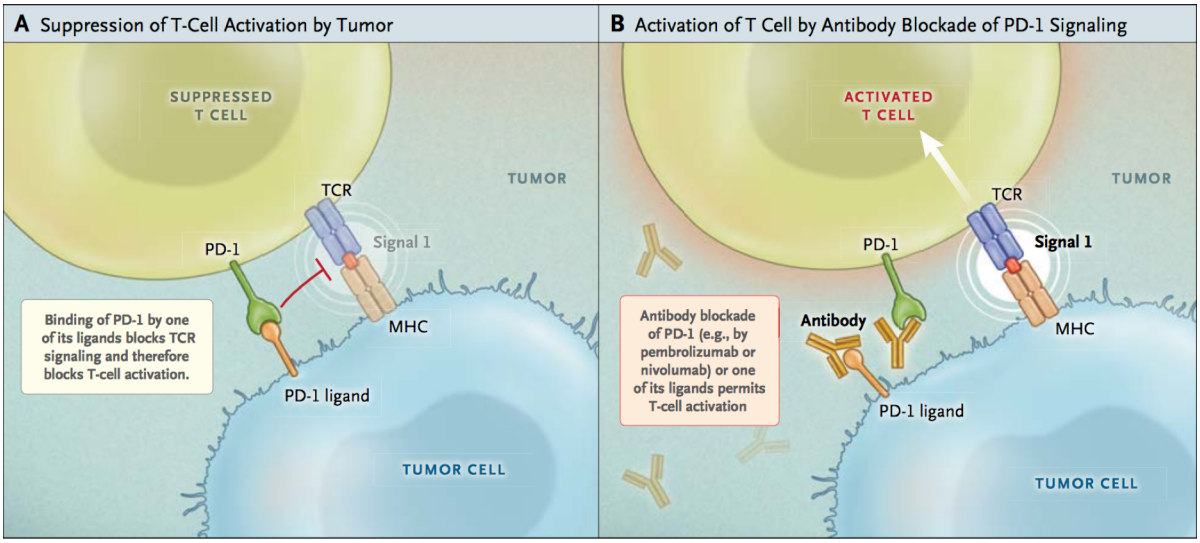

Figure 4. T cell activation in tumor milieu. During long-term antigen exposure, such as occurs in the tumor mileu, the programmed death 1 (PD-1) inhibitor receptor is expressed by T cells (Panel A); it suppresses the effect of TCR on T cell activation. Blockade of PD-1 or its ligand (Panel B) (e.g., pembrolizumab or nivolumab) depresses TCR signaling, thereby permitting T cell activation. *Ribas A, N Eng J Med 2015; 373:1490-1492*

C. Mechanism of action of PD-1 blockade

As discussed above, up-regulation of PD-L1/L2 expression in the presence of activated T cells results in immunosuppressive tumor microenvironment (so called 'adaptive immune resistance') that is the mechanistic basis of targeting PD-1/PD-L1 axis (Figure 4) (9). Binding of PD-L1/L2 to PD-1 receptor leads to phosphorylation of the cytoplasmic domain tyrosines and recruitment of Src homology 2- containing tyrosine phosphatase (SHP-2) to ITSM (Immunoreceptor Tyrosine-based Switch Motif). SHP-2 dephosphorylates TCR-associated CD3ζ and ZAP70 that result in inhibition of downstream signaling, including PI3K and AKT activity that disrupts glucose metabolism and IL-2 and other cytokine secretion (24, 41).

Monoclonal antibodies targeting PD-1/PD-L1 axis to enhance T cell function have been tested in the clinic and produced the unprecedented clinical activity as discussed above. Tumeh et al reported how PD-1 blockade works in patients with advanced melanoma by evaluating tumor biopsies at baseline and on treatment. It showed the density of tumor infiltrating CD8+ T cell at

the tumor invasive margin was strongly predictive to clinical response (42). It demonstrates that PD-1 blockade induces responses by inhibiting adaptive immune resistance that is consistent with scientific rationale to target this axis.

1.3 Biomarker/Patient selection for PD-1/PD-L1 blockade

Identifying who would be likely responding to PD-1 blockade therapy has been important subject over the past several years. Yet, there is no defined maker that can robustly predict response. Tumor baseline PD-L1 expression has been pursued as a potential marker to select patient based on high correlation between its clinical responses. Non-small cell lung cancer incorporates PD-L1 expression level for one of the PD-1 antibodies (pembrolizumab) based on its clinical data. However, clinical responses have been observed among patients who were labeled as negative for PD-L1 expression in tumor biopsies prior to therapy (42, 43). This implies PD-L1 expression is dynamic and tumor heterogeneity that cannot be captured within one biopsy. This also implies complex interaction between many other players in tumor microenvironment, including immune cells (lymphoid and myeloid cells), tumor cells and stromal element as well (44, 45). Non-standardized PD-L1 staining also makes it hard to compare its expression level cross the many clinical trials. Many efforts are underway to define better way to identify patients who would response or not response to PD-1 blockade by taking into accounts this complex equation in tumor microenvironment.

1.4 Resistance mechanisms to PD-1 blockade

Along with biomarker search endeavor, identifying resistance mechanism has been prime importance to overcome the resistance with better therapeutic strategies and patient selection as well. As Tumeh et al showed, T cell infiltration into tumor microenvironment is important factor to predict response. In other words, if the tumor microenvironment is devoid of T cells, the chances of having response from this therapy is low. Spranger et al provided the mechanistic

insight why some cancers are devoid of T cells, via increased WNT/ß-catenin signaling that results in down regulation of CCL4 expression which is the main chemotactic cytokine (46). Hugo et al studied transcriptome data from patients with advanced melanoma who participated anti-PD-1 clinical trial. This study showed that tumors with innate resistance to PD-1 therapy display a transcriptional signature indicating concurrent up regulation of genes involved in the regulation of mesenchymal transition, cell adhesion, extracellular matrix remodeling etc (47).

We are now beginning to understand resistance mechanisms with these studies and clinical studies are already addressing how we can overcome the T cell exclusion in tumor microenvironment by testing various combinatorial treatment with PD-1 blockade. I started projects with the aims to understand the biology of PD-L1 expression in melanoma cell lines to define its role in mediating response and resistance to PD-1 blockade by utilizing clinical samples from anti-PD-1 antibody clinical trial and cell lines panels established in our laboratory.

1.5 References

1. Gray-Schopfer V, Wellbrock C, Marais R. Melanoma biology and new targeted therapy. *Nature* 2007;**445**:851-7.

2. Flaherty KT, Puzanov I, Kim KB et al. Inhibition of mutated, activated BRAF in metastatic melanoma. *N Eng J Med*. 2010 Aug 26; **363**(9):809-19.

3. Lynch TJ, Bell DW, Sordella R et al. Activating mutations in the epidermal growth factor receptor underlying responsiveness of non-small-cell lung cancer to gefitinib. *N Eng J Med*. 2004; **350**(21):2129-39.

4. Chapman PB, Hauschild A, Robert C et al. Improved survival with vemurafenib in melanoma with BRAF V600E mutation. *N Eng J Med*. 2011 Jun 30;**364**(26):2507-16.

5. Larkin J, Ascierto PA, Dreno B et al. Combined vemurafenib and cobimetinib in BRAF-mutated melanoma. *N Eng J Med*. 2014 Nov 13;37(20):1867-76.

6. Long GV, Storyakovskiy D, Gogas H et al. Combined BRAF and MEK inhibition versus BRAF inhibition alone in melanoma. *N Eng J Med*. 2014 Nov 13;**37**(20):1877-88

7. Robert C, Karaszewska B, Schachter J et al. Improved overall survival in melanoma with combined dabrafenib and trametinib. *N Eng J Med*. 2015 Jan 1;**372**(1):30-9.

8. Robert C, Thomas L, Bondarenko I et al. Ipilimumab plus dacarbazine for previously untreated metastatic melanoma. *N Eng J Med*. June 2011; **364**:2517-2526

9. Ribas A. Releasing the brakes on cancer immunotherapy. *N Eng J Med*. 2015 Oct 15;**373(16)**:1490-2.

10. Herbst RS, Soria JC, Kowanetz M et al. Predictive correlates of response to the anti-PD-L1 antibody MPDL3280A in cancer patients. *Nature* **515**, 563-567, doi:10.1038/nature14011, 2014.

11. Powles T, Eder JP, Find GD et al. MPDL3280A (anti-PD-L1) treatment leads to clinical activity in metastatic bladder cancer. *Nature* **515**, 558-562, doi:10.1038/nature13904, 2014.

12. Robert C, Long GV, Brady B et al. Nivolumab in previously untreated melanoma without BRAF mutation. *N Engl J Med* **372**, 320-330, 2015.

13. Le DT, Lram JN, Wang H et al. PD-1 Blockade in Tumors with Mismatch-Repair Deficiency. *N Engl J Med* **372**, 2509-2520, doi:10.1056/NEJMoa1500596, 2015.

14. Ansell SM, Lesokhin AM, Borrello I et al. PD-1 blockade with nivolumab in relapsed or refractory Hodgkin's lymphoma. *N Engl J Med* **372**, 311-319, 2015.

15. Garon EB, Rizvi NA, Hui R. Pembrolizumab for the treatment of non-small cell lung cancer. *N Engl J Med* **372**, 2018-2028, 2015.

16. Robert C, Schachter J, Long GV et al. Pembrolizumab versus ipilimumab in advanced melanoma. *N Eng J Med*. 2015 Jun;**372**(26):2521-32.
17. Ribas A, Hamid O, Daud A et al. Association of pembrolizumab with tumor response and survival among patients with advanced melanoma. *JAMA*. 2016 Apr 19;**315**(15):1600-9.

18. Bu X, Mahoney KM, Freeman GJ. Learning from PD-1 resistance: New combination strategies. *Trends Mol Med*. 2016 Jun;**22(6):**448-51.

19. Ishida Y, Agata Y, Shibahara K et al. Induced expression of PD-1, a novel member of the immunoglobulin gene superfamily, upon programmed cell death. *EMBO J*. 1992;**11(11):**3887-95.

20. Keir ME, Butte MJ, Free,man GJ et al. PD-1 and its ligands in tolerance and immunity. *Annu. Rev. Immunol*. 2008;**26**, 677-704.

21. Schwartz LM, Osbourne BA. Programmed cell death, apoptosis and killer genes. *Immunol Today*. 1993 Dec; **14**(12):582-90.

22. Barber DL, Wherry EJ, Masopust D et al. Restoring function in exhausted CD8 T cells during chronic viral infection. *Nature*. 2006 Feb 9;**439**(7077):682-7.

23. Wherry EJ. T cell exhaustion. *Nat Immunol*. 2011 Jun;**12**(6):492-9.

24. Hofmeyer KA, Jeon J, Zang X. The PD-1/PDL1 (B7-H1) pathway in chronic infection-induced cytotoxic T lymphocyte exhaustion. *J Biomed Biotechnol*. 2011;**2011**;451694.

25. Latchman Y, Wood CR, Chmova T et al. PD-L2 is a second ligand for PD-1 and inhibits T cell activation. *Nat Immunol*. 2001 Mar;**2(**3):261-8.

26. Tseng SY, Otsuj M, Gorski K et al. D7-DC, a new dendritic cell molecule with potent costimulatory properties for T cells. *J Exp Med*. 2001 Apr 2;**193**(7):839-46.

27. Muenst S, Soyal SD, Gao F et al. The presence of programmed death 1 (PD-1)-positive tumor infiltrating lymphocyte is associated with poor prognosis in human breast cancer. Breast *Cancer Res Treat*. 2013 Jun;**139**(3):667-76.

28. French JD, Kotnis GR, Said R et al. Programmed death-1+ T cells and regulatory T cells are enriched in tumor-involved lymph nodes and associated with aggressive features in papillary thyroid cancer. *J Clin Endocrinol Meta*. 2012 Jun;**97**(6):E934-43.

29. Chapon M, Randriamampita C, Maubec E et al. Progressive upregulation of PD-1 in primary and metastatic melanomas associated with blunted TCR signaling in infiltrating T lymphocytes. *J Invest Deramtol*. 2011 Jun;**131**(6):1300-7.

30. Thompson RH, Dong H, Lohse CM et al. PD-1 is expressed by tumor-infiltrating immune cells and is associated with poor outcome for patients with renal cell carcinoma. *Clin Cancer Res*. 2007 Mar;**13**(6):1757-61.

31. Thompson RH, Kuntz SM, Leiovich BC et al. Tumor B7-H1 is associated with poor prognosis in renal cell carcinoma patients with long-term follow-up. *Cancer Res*. 2006 Apr 1;**66**(7):3381-5.

32. Gao Q, Wang XY, Qiu SJ et al. Overexpression of PD-L1 significantly associates with tumor aggressiveness and postoperative recurrence in human hepatocellular carcinoma. *Clin Cancer Res.* 2009 Feb 1;**15**(3):97-9.

33. Gadiot J, Hooijkaas AI, Kaiser AD et al. Overall survival and PD-L1 expression in metastasized malignant melanoma. *Cancer*. 2011 May 15;**117**(10):2192-201.

34. Hino R, Kabashima K, Kato Y et al. Tumor cell expression of programmed cell death-1 ligand 1 is a prognostic factor for malignant melanoma. *Cancer.* 2010 Apr 1;**116**(7):1757-66.

35. Massi D, Brusa D, Merelli B et al. PD-L1 marks a subset of melanomas with a shorter overall survival and distinct genetic and morphological characteristics. Ann Oncol. 2014 Dec;25(12):2433-42.

36. Azuma K, Ota K, Kawahara A et al. Association of PD-L1 overexpression with activating EGFR mutations in surgically resected non-small-cell lung cancer. *Ann Oncol*. 2014 Oct;**25**(10):1935-40.

37. Atefi M, Avramis E, Lassen A et al. Effects of MAPK and PI3K pathways on PD-L1 expression in melanoma. *Clin Cancer Res*. 2014;**20**:3446-57.

38. Katoka K, Shiraishi Y, Takeda Y et al. Abberant PD-L1 expression through 3'-UTR disruption in multiple cancers. *Nature* 2016 Jun 16;**534**(7607):402-6.

39. Kim J, Myers AC, Chen L et al. Constintutive and inducible expression of b7 family of ligands by human airway epithelial cells. Am J Respir Cell Mol Biol. 2005 Sep;33(3):280-9.

40. Jiang X, Zhou J, Giobbie-Hurder A et al. The activation of MAPK in melanoma cells resistant to BRAF inhibition promotes PD-L1 expression that is reversible by MEK and PI3K inhibition. Clin Cancer Res. 2013 Feb 1;19(3):598-609.

41. Parry RV, Chemnitz JM, Frauwirth KA et al. CTLA-4 and PD-1 receptors inhibit T-cell activation by distinct mechanism. *Mol Cell Biol*. 2005 Nov;**25**(21):9543-53.

42. Tumeh PC, Harview CL, Yearley JH et al. PD-1 blockade induces responses by inhibiting adaptive immune resistance. *Nature* 2014 Nov 27;**515**(7528):568-71.

43. Taube JM, Klein A, Brahmer JR et al. Association of PD-1, PD-1 ligands, and other features of the tumor microenvironment with response to anti-PD-1 therapy. *Clin Cancer Res*. 2014 Oct 1;**20**(19):5064-74.

44. Teng MW, Ngiow SF, Ribas A et al. Classifying cancers based on T-cell infiltration and PD-L1. *Cancer Res*. 2015 1;**7**(11):2139-45.

45. Symth MJ, Ngiow SF, Ribas A et al. Combination cancer immunotherapies tailored to the tumor microenvironment. *Nat Rev Clin Oncol*. 2016 Mar;**13**(3):143-58.

46. Spranger S, Bao R, Gajewski TF. Melanoma-intrinsic β-catenin signaling prevents anti-tumor immunity. *Nature*. 2015 Jul 9;**523**(7559):231-5.

47. Hugo W, Zaretsky JM, Sun L et al. Genomic and transcriptomic features of response to anti-PD-1 therapy in mestastatic melanoma. *Cell* 2016 Mar 24;**165**(1):35-44.

Chapter 2:

Mutations Associated with Acquired Resistance to PD-1 Blockade in Melanoma

N Engl J Med 2016; 375:819-829

Mutations Associated with Acquired Resistance to PD-1 Blockade in Melanoma

Jesse M. Zaretsky, B.S., Angel Garcia-Diaz, Ph.D., Daniel S. Shin, M.D., Helena Escuin-Ordinas, Ph.D., Willy Hugo, Ph.D., Siwen Hu-Lieskovan, M.D., Ph.D., Davis Y. Torrejon, M.D., Gabriel Abril-Rodriguez, M.Sc., Salemiz Sandoval, Ph.D., Lucas Barthly, M.Sc., Justin Saco, B.S., Blanca Homet Moreno, M.D., Riccardo Mezzadra, M.Sc., Bartosz Chmielowski, M.D., Ph.D., Kathleen Ruchalski, M.D., I. Peter Shintaku, Ph.D., Phillip J. Sanchez, Ph.D., Cristina Puig-Saus, Ph.D., Grace Cherry, R.N., N.P., Elizabeth Seja, B.A., Xiangju Kong, M.Sc., Jia Pang, B.S., Beata Berent-Maoz, Ph.D., Begoña Comin-Anduix, Ph.D., Thomas G. Graeber, Ph.D., Paul C. Tumeh, M.D., Ton N.M. Schumacher, Ph.D., Roger S. Lo, M.D., Ph.D., and Antoni Ribas, M.D., Ph.D.

ABSTRACT

BACKGROUND

Approximately 75% of objective responses to anti–programmed death 1 (PD-1) therapy in patients with melanoma are durable, lasting for years, but delayed relapses have been noted long after initial objective tumor regression despite continuous therapy. Mechanisms of immune escape in this context are unknown.

METHODS

We analyzed biopsy samples from paired baseline and relapsing lesions in four patients with metastatic melanoma who had had an initial objective tumor regression in response to anti–PD-1 therapy (pembrolizumab) followed by disease progression months to years later.

RESULTS

Whole-exome sequencing detected clonal selection and outgrowth of the acquired resistant tumors and, in two of the four patients, revealed resistance-associated loss-of-function mutations in the genes encoding interferon-receptor–associated Janus kinase 1 (*JAK1*) or Janus kinase 2 (*JAK2*), concurrent with deletion of the wild-type allele. A truncating mutation in the gene encoding the antigen-presenting protein beta-2-microglobulin (*B2M*) was identified in a third patient. *JAK1* and *JAK2* truncating mutations resulted in a lack of response to interferon gamma, including insensitivity to its antiproliferative effects on cancer cells. The *B2M* truncating mutation led to loss of surface expression of major histocompatibility complex class I.

CONCLUSIONS

In this study, acquired resistance to PD-1 blockade immunotherapy in patients with melanoma was associated with defects in the pathways involved in interferon-receptor signaling and in antigen presentation. (Funded by the National Institutes of Health and others.)

From the University of California, Los Angeles (UCLA) (J.M.Z., A.G.-D., D.S.S., H.E.-O., W.H., S.H.-L., D.Y.T., G.A.-R., S.S., L.B., J.S., B.H.M., B.C., K.R., I.P.S., P.J.S., C.P.-S., G.C., E.S., X.K., J.P., B.B.-M., B.C.-A., T.G.G., P.C.T., R.S.L., A.R.), and Jonsson Comprehensive Cancer Center (B.C., B.C.-A., T.G.G., P.C.T., R.S.L., A.R.) — both in Los Angeles; and the Division of Immunology, Netherlands Cancer Institute, Amsterdam (R.M., T.N.M.S.). Address reprint requests to Dr. Ribas at the Department of Medicine, Division of Hematology–Oncology, Jonsson Comprehensive Cancer Center at UCLA, 11-934 Factor Bldg., 10833 Le Conte Ave., Los Angeles, CA 90095-1782, or at aribas@mednet.ucla.edu.

This article was published on July 13, 2016, at NEJM.org.

N Engl J Med 2016;375:819-29.
DOI: 10.1056/NEJMoa1604958

Durable responses in metastatic cancers have been achieved with a variety of immunotherapies such as interleukin-2, adoptive cell transfer of tumor-infiltrating lymphocytes, antibodies that block cytotoxic T-lymphocyte–associated antigen 4 (CTLA4),[1-5] and antibodies that block programmed death 1 (PD-1).[6-10] However, in a recent study, approximately 25% of patients with melanoma who had had an objective response to PD-1 blockade therapy had disease progression at a median follow-up of 21 months.[11]

The mechanisms of immune-resistant cancer progression are mostly unknown. Previous studies involving humans examined the loss of beta-2-microglobulin as a mechanism of acquired resistance to several forms of cancer immunotherapy.[12-14] In preclinical models, defects in the interferon signaling pathway have been proposed as a potential mechanism of cancer escape (insensitivity) to immunotherapy.[15,16] In the current study, we assessed the effect of anti–PD-1 therapy on cancer genomic evolution, including acquired mutations in the genes affecting the interferon pathway and antigen-presentation pathway, in an effort to determine genetic mechanisms of acquired resistance to PD-1 blockade therapy.

Methods

Patients, Response Assessment, and Tumor Biopsies

Of 78 patients with metastatic melanoma who were treated with the anti–PD-1 antibody pembrolizumab at the University of California, Los Angeles (UCLA), 42 had an objective response, of whom 15 went on to have disease progression. Four of these 15 patients met all three selection criteria for this analysis. First, they must have had an objective tumor response while participating in a clinical trial with single-agent pembrolizumab.[6,7,10,11] Tumor responses were evaluated at 12 weeks and confirmed 4 weeks later, and patients were assessed by imaging every 12 weeks thereafter with the use of both the Response Evaluation Criteria in Solid Tumors[17] and the immune-related response criteria.[18] Second, patients had to have late acquired resistance, defined as in situ recurrence or new lesion development, despite continuous dosing, after more than 6 months of tumor response. Third, patients had to have adequate biopsy material for whole-exome sequencing at two time points: before the initiation of pembrolizumab therapy and after disease progression. We processed tumor biopsy samples as described previously to perform pathological analyses, obtain DNA and RNA, and attempt to establish cell lines.[19,20]

Immunohistochemical, Immunofluorescence, Western Blot, and Flow-Cytometric Analyses

Immunohistochemical and immunofluorescence analyses[19] as well as Western blot and flow-cytometric analyses[21] were performed and analyzed as described previously. Full methods are included in the Supplementary Appendix, available with the full text of this article at NEJM.org.

Genetic and Transcriptional-Profiling Analyses

Whole-exome sequencing was performed at the UCLA Clinical Microarray Core with the use of the NimbleGen SeqCap EZ Human Exome Library, version 3.0 (Roche). Mutation calling was performed as described previously.[22] Selected gene-expression profiling on interferon exposure was performed with the use of nCounter (NanoString Technologies). Whole-exome sequencing data have been deposited in the National Center for Biotechnology Information Sequence Read Archive under the accession number SRP076315.

Functional Studies

Patient-derived and previously established human melanoma cell lines were used to analyze recognition by T-cell receptor transgenic T cells[23] with the use of in vitro coculture assays that detect antigen-induced release of interferon-γ assessed by enzyme-linked immunosorbent assay. Cell-proliferation and growth-inhibition assays were performed with the use of an automated live-cell imaging system (IncuCyte, Essen BioScience) with or without exposure to interferons. Full methods are described in the Supplementary Appendix.

Study Oversight

Data generated and collected by the study investigators were analyzed by the last author, who vouches for the completeness and accuracy of the data, analyses, and reported results. Summaries of the clinical protocol have been reported by Hamid et al.[6] and Robert et al.[10]

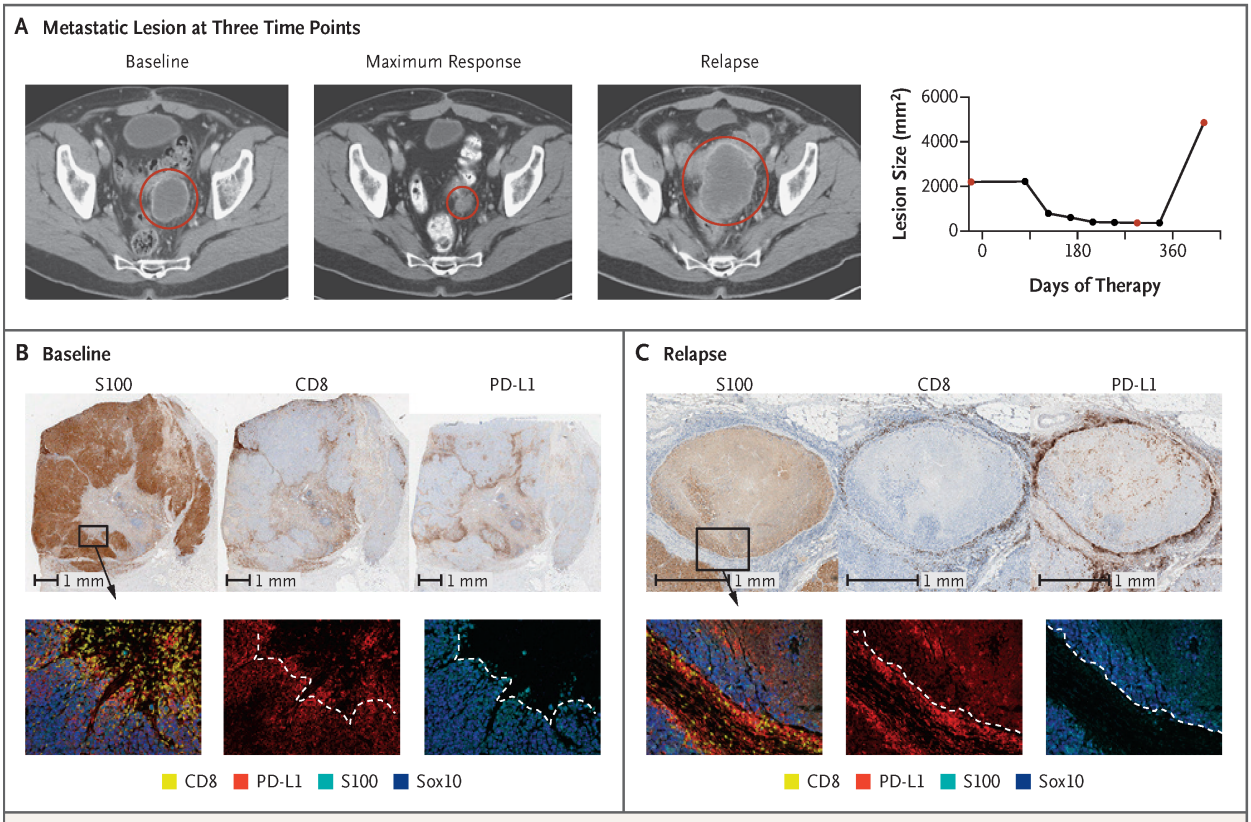

Figure 1. Clinical Pattern of Acquired Resistance to Anti–Programmed Death 1 (PD-1) Therapy in Patient 1.

In Panel A, computed tomographic images show a melanoma small-bowel metastasis at baseline, at the time of maximum response, and at the time of an in situ relapse after a year of minimal residual disease; the red dots in the graph on the right indicate these three time points. Immunohistochemical staining and multiplexed immunofluorescence analysis showed abundant CD8 T-cell infiltrates and programmed death ligand 1 (PD-L1) expression at baseline and again at the time of relapse at the tumor margin in Panels B and C, respectively. In the immunofluorescence images, red indicates PD-L1, yellow CD8 T cells, light blue the melanoma marker S100 (cytoplasmic staining), and dark blue the melanoma marker Sox10 (nuclear staining).

STATISTICAL ANALYSIS

Student's t-test and a two-way analysis of variance were used for cell-culture experiments, with Dunnett's correction applied for multiple comparisons with untreated controls.

RESULTS

CLINICAL COURSE AND IMMUNE INFILTRATES

We analyzed paired tumor samples from four (nonconsecutive) selected patients with metastatic melanoma who had had a relapse while receiving PD-1–inhibition therapy with pembrolizumab (Tables S1 and S2 in the Supplementary Appendix). All four patients met objective criteria for a partial response,[17,18] though with slightly different kinetics (Fig. 1, and Figs. S1, S2, and S3 in the Supplementary Appendix). The mean time to relapse was 624 days (range, 419 to 888). The baseline biopsy samples were obtained just before the initiation of pembrolizumab therapy in Patients 2, 3, and 4, whereas for Patient 1, the only available baseline biopsy sample was obtained before an earlier course of therapy with the BRAF inhibitor vemurafenib. The baseline biopsy samples from Patients 1, 2, and 3 showed preexisting CD8 T-cell infiltrates at the invasive margin that colocalized with programmed death ligand 1 (PD-L1) expression on surrounding macrophages and melanoma cells (Fig. 1B, and Figs. S1B and S2B in the Supplementary Appendix). The biopsy samples obtained at the time of response in Patients 2, 3, and 4 showed a marked increase in intratumoral CD8 T-cell in-

filtrates (Figs. S1C, S2C, and S3C and Table S3 in the Supplementary Appendix; no biopsy sample during therapy was available for Patient 1). At the time of relapse, all four biopsy samples showed CD8 T-cell infiltration and PD-L1 expression concentrated at the tumor margins again (Fig. 1C, and Figs. S1D, S2D, and S3D in the Supplementary Appendix). Multiplex immunofluorescence assays revealed that melanoma cells at the time of relapse in Patients 1 and 2 were negative for PD-L1 even when directly adjacent to T cells, whereas macrophages and stromal cells were positive for PD-L1.

GENETIC CHANGES IN RELAPSE BIOPSY SAMPLES

The pattern of a strong initial response, long dormancy, and rapid late progression led us to hypothesize that relapse in these patients resulted from immune-mediated clonal selection and tumor outgrowth.[24] To identify mutations that might confer immune resistance, we extracted DNA from bulk-tumor biopsy samples or early-passage primary cell lines (Table S2 in the Supplementary Appendix) and performed whole-exome sequencing to compare baseline and matched relapsed tissues. We achieved a median coverage of 149×, and the percent of tumor cells (as compared with stromal cells) was more than 40% in all samples (Table S2 in the Supplementary Appendix). Nonsynonymous mutations for all samples are shown in Table S4 in the Supplementary Appendix.

JAK MUTATIONS WITH CONCURRENT LOSS OF HETEROZYGOSITY AT RELAPSE

We found strong evidence that the relapsed tumors were closely genetically related to their baseline counterparts, despite up to 2 years between biopsies. In the case of Patients 1 and 2, of 1173 and 240 nonsynonymous mutations, respectively, originally identified in the baseline sample, 92.5% and 95.8% were also seen in the resistant tumor (Fig. 2A, and Fig. S4 in the Supplementary Appendix). The relapsing tumors also contained the same chromosomal loss-of-heterozygosity events as the baseline tumors, and all differences were due to further loss in the relapse samples. In the relapse biopsy samples from both patients, we identified new homozygous loss-of-function mutations in the kinases associated with the interferon-receptor pathway, with a Q503* nonsense mutation in the gene encoding Janus kinase 1 (*JAK1*) in Patient 1 (Fig. 2A and 2B) and a F547 splice-site mutation in the gene encoding Janus kinase 2 (*JAK2*) in Patient 2 (Fig. S4 in the Supplementary Appendix). RNA sequencing showed that the *JAK2* splice-site mutation caused intron inclusion, producing an in-frame stop codon 10 bp after exon 12 (Fig. S5 in the Supplementary Appendix). Therefore, both mutations were upstream of the kinase domains and probably truncated the protein or caused nonsense-mediated decay. Neither mutation was seen at baseline in the exome sequencing reads, by Sanger sequencing, or by targeted amplicon resequencing (Fig. S6 in the Supplementary Appendix).

The *JAK2* mutation was the only homozygous mutation (adjusted variant allele frequency, >85%) of 76 new nonsynonymous mutations in Patient 2, and the *JAK1* mutation was 1 of only 3 homozygous mutations among 53 new mutations in Patient 1 (Table S5 in the Supplementary Appendix). To become homozygous, both *JAK* mutations were acquired in the context of a copy-number–neutral nondisjunction event, resulting in loss of the wild-type chromosome and duplication of the mutated allele. This is seen clearly in Patient 1: at relapse, chromosome 1p (containing *JAK1*) showed a decrease in minor-allele frequencies for germline single-nucleotide polymorphisms relative to baseline (Fig. S7 in the

Figure 2 (facing page). Acquired *JAK1* Loss-of-Function Mutation at Relapse, with Accompanying Loss of Heterozygosity.

In Panel A, a Circos plot[25] of Patient 1 shows differences in whole-exome sequencing between the pre-pembrolizumab and post-relapse biopsies. The red circle highlights a new, high-allele-frequency, relapse-specific mutation in the gene encoding Janus kinase 1 (*JAK1*) in the context of chromosomal loss of heterozygosity (asterisk). Each wedge represents a chromosome. In the outer track (black background), each point represents a nonsynonymous mutation, with most detected in both biopsy samples (gray) rather than at relapse only (red) or baseline only (green). The y-axis position indicates the variant allele frequency (VAF) at relapse, unless baseline-specific. The middle and inner tracks show copy-number status for the baseline and relapse biopsy, respectively; dark green in the subtrack indicates loss of heterozygosity. In Panel B, Integrative Genomics Viewer (IGV) plots (top) show that the *JAK1* Q503* nonsense mutation is relapse-specific, and the cBioPortal[26] diagram (bottom) shows that the JAK1 mutation is upstream of the kinase domains.

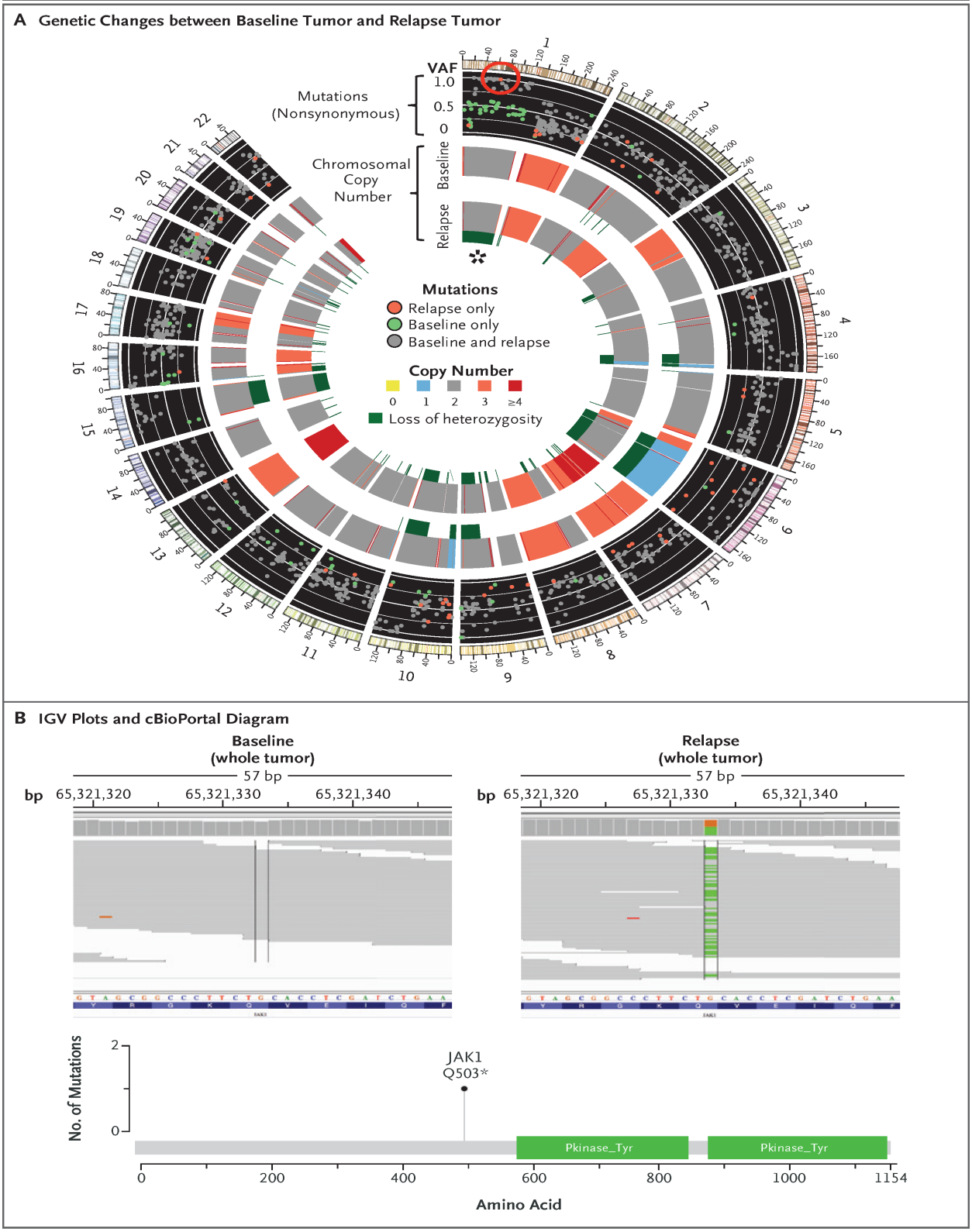
A Genetic Changes between Baseline Tumor and Relapse Tumor
VAF
1.0
0.5
0
Mutations
(Nonsynonymous)
Chromosomal
Copy
Number
Baseline
Relapse
Mutations
Relapse only
Baseline only
Baseline and relapse
Copy Number
0 1 2 3 ≥4
Loss of heterozygosity
B IGV Plots and cBioPortal Diagram
Baseline
(whole tumor)
Relapse
(whole tumor)
57 bp
bp 65,321,320 65,321,330 65,321,340
No. of Mutations
2
0
JAK1
Q503*
Pkinase_Tyr
Pkinase_Tyr
0 200 400 600 800 1000 1154
Amino Acid

Supplementary Appendix), was missing 36 heterozygous baseline mutations (presumably on the lost allele), and contained 20 mutations (presumably on the amplified allele) that became homozygous (adjusted variant allele frequency, >85%, with change of >35 percentage points from baseline). A similar loss-of-heterozygosity event occurred for chromosome 9 in Patient 2 (Fig. S8 and Table S5 in the Supplementary Appendix). Together, these data suggest that the tumors resistant to anti–PD-1 are a relatively homogenous population derived directly from the baseline tumor and that acquisition of the *JAK* mutations was an early founder event before clonal selection and relapse despite the fact that the mutation was not detected in pretreatment tumor tissue.

FUNCTIONAL EFFECTS OF *JAK2* MUTATION

To assess the functional consequences of the observed *JAK* mutations, we focused on the *JAK2* mutation from Patient 2 using two cell lines established at baseline (M420, wild-type *JAK2*) and at the time of relapse (M464, *JAK2* F547 splice-site mutation). Whole-exome sequencing confirmed that the original bulk tumor was well represented by M464 (Fig. S9 in the Supplementary Appendix). Western blot analysis showed that the baseline cell line responded to interferon alfa, beta, and gamma with the expected signal transduction, including an increase in signal transducer and activator of transcription 1 (STAT1) and interferon regulatory factor (IRF) expression, STAT1 phosphorylation (pSTAT1), and the production of downstream interferon targets such as PD-L1, transporter associated with antigen processing 1 (TAP1), and major histocompatibility complex (MHC) class I (Fig. 3A). However, the cell line from the progressing lesion showed a total loss of JAK2 protein (Fig. 3A), resulting in a lack of response to interferon gamma, without change in sensitivity to interferon alfa or beta. This was true of the pSTAT1 response (Fig. 3A) and the expression of PD-L1 and MHC class I molecules (Fig. 3A and 3B). The progressing cell line also failed to up-regulate a wider panel of interferon-induced transcripts involved in antigen presentation and T-cell chemotaxis (Fig. 3C, and Table S6 in the Supplementary Appendix). Together, these data indicate a total loss of functional response to interferon gamma and are consistent with JAK2 being required for signaling through the interferon-γ receptor, as opposed to the interferon-α/β receptor, which uses TYK2 and JAK1.[27-29]

LOSS OF INTERFERON GAMMA–INDUCED GROWTH ARREST THROUGH ACQUIRED *JAK* MUTATIONS

We hypothesized that inactivating *JAK* mutations may result in a functional advantage for the progressive tumors because the lack of interferon signaling either decreased antigen presentation or allowed escape from interferon-induced inhibition of growth. In addition to using M420 and M464, we engineered the human melanoma cell line M407 by means of the CRISPR (clustered regularly interspaced short palindromic repeats)–Cas9 approach to create sublines without expression of *JAK1* or *JAK2* (Figs. S10 and S11 in the Supplementary Appendix). These created truncating mutations analogous to those from Patients 1 and 2, and M407 is positive for HLA-A*02:01 and expresses the cancer–testis antigen NY-ESO-1, which allowed us to model T-cell recognition using T cells genetically modified to express an NY-ESO-1–specific T-cell receptor.[23] M407 and both *JAK*-loss sublines were equally recognized by NY-ESO-1–specific T cells, leading to high levels of interferon-γ production (Fig. 4A).

When cultured in recombinant interferon alfa, beta, or gamma, the M420 and M407 parental cell lines showed interferon-induced growth inhibition in a dose-dependent manner (Fig. S12 in the Supplementary Appendix). However, both the *JAK2*-deficient M464 cell line (from Patient 2 at relapse) and the M407 *JAK2*-knockout subline were insensitive specifically to interferon gamma–induced growth arrest, yet remained sensitive to type I interferons alfa and beta; in contrast, the M407 *JAK1*-mutated subline was resistant to all three interferons (Fig. 4B). This is again consistent with the specific association of *JAK2* with the interferon-γ receptor and the common use of JAK1 by all three interferon receptors.[27-29] As an orthogonal test of these effects, we treated our cell lines with 2′3′-cGAMP (cyclic guanosine monophosphate–adenosine monophosphate); this dinucleotide, which is produced in response to

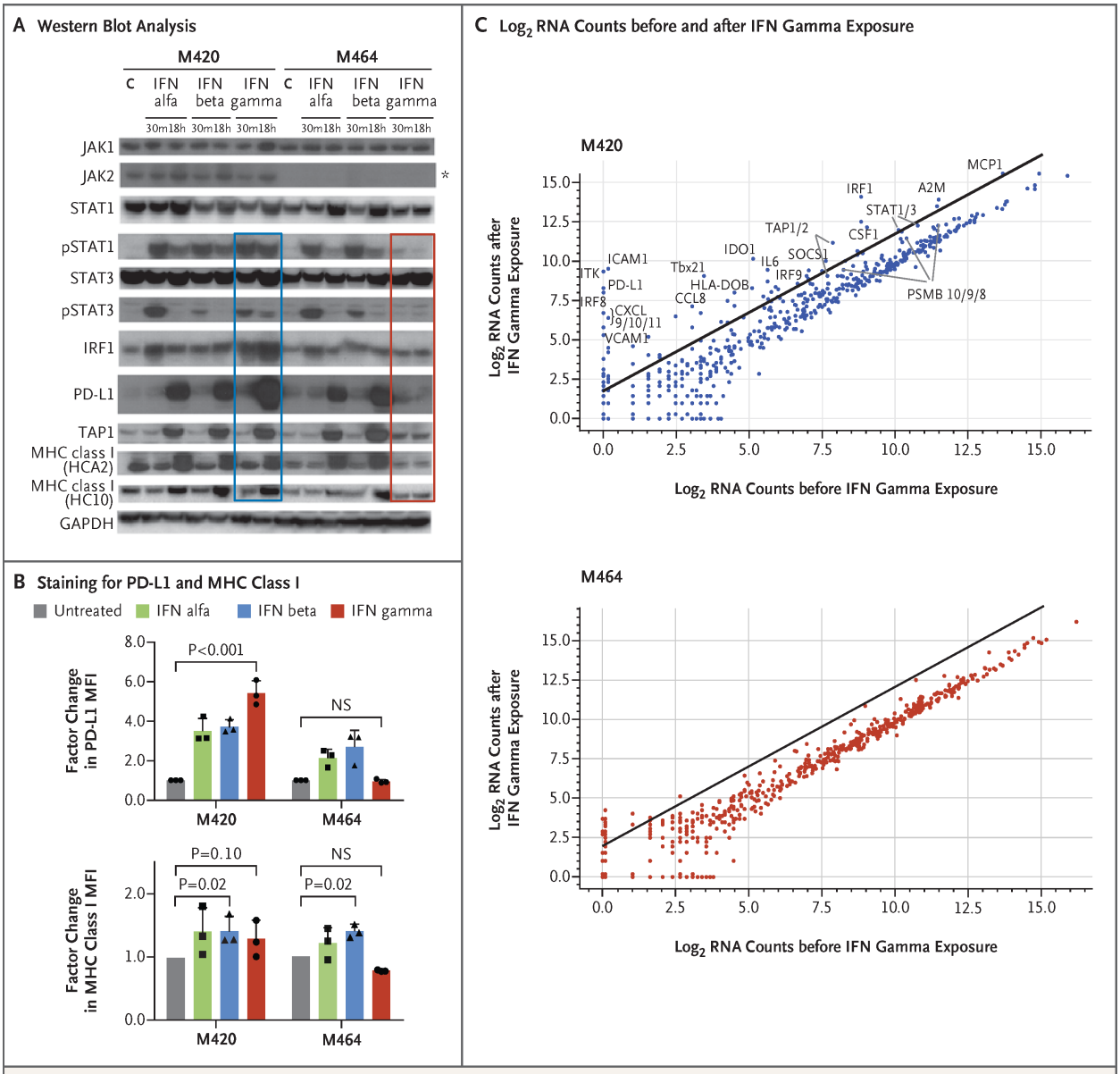

Figure 3. Loss of Interferon Gamma–Induced Signaling and Gene-Expression Changes through Acquired *JAK2* Mutation.

In Panel A, Western blot analysis of lysates from cell lines M420 (Patient 2, baseline) and M464 (Patient 2, relapse) shows Janus kinase (JAK)–signal transducer and activator of transcription (STAT) signaling events and downstream target induction after either 30 minutes (m) or 18 hours (h) of exposure to interferon (IFN) alfa, beta, or gamma (C indicates untreated control). Janus kinase 2 (JAK2) protein expression was absent in the relapse cell line (asterisk), and M464 failed to phosphorylate intermediate signaling components STAT1 and STAT3 or to up-regulate interferon-response targets TAP1, PD-L1, and major histocompatibility complex (MHC) class I after treatment specifically with interferon gamma (red box), as compared with intact signaling in M420 (blue box). There was no change in response to interferon alfa or beta. As shown in Panel B, a lack of response to interferon gamma exposure was also seen in surface staining for PD-L1 and MHC class I by flow cytometry. Each point represents an independent experiment, T bars represent standard deviations, and P values are for a two-way analysis of variance with Dunnett's correction. MFI denotes mean fluorescent intensity, and NS not significant. Panel C shows $\log_2$ RNA counts of expression for 790 immune-related genes on exposure to interferon gamma or vehicle control. The baseline cell line M420 (top) showed up-regulation of many interferon-stimulated genes (line represents an increase by a factor of 4), whereas the *JAK2* mutated progression cell line M464 (bottom) lacked a similar response.

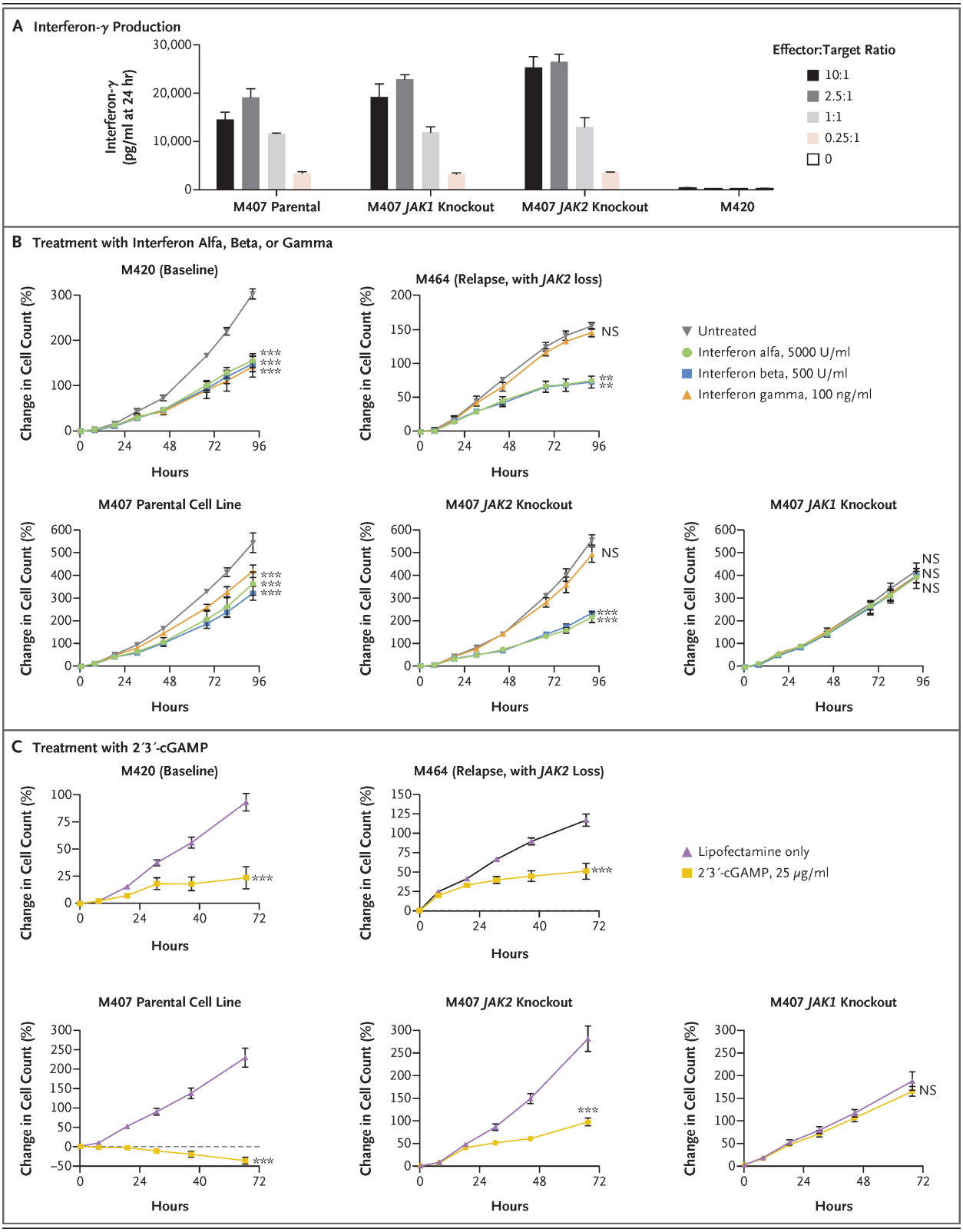
A Interferon-γ Production
Interferon-γ (pg/ml at 24 hr)
30,000
20,000
10,000
0
M407 Parental
M407 JAK1 Knockout
M407 JAK2 Knockout
M420
Effector:Target Ratio
10:1
2.5:1
1:1
0.25:1
0
B Treatment with Interferon Alfa, Beta, or Gamma
M420 (Baseline)
M464 (Relapse, with JAK2 loss)
Change in Cell Count (%)
Hours
***
NS
**
Untreated
Interferon alfa, 5000 U/ml
Interferon beta, 500 U/ml
Interferon gamma, 100 ng/ml
M407 Parental Cell Line
M407 JAK2 Knockout
M407 JAK1 Knockout
C Treatment with 2′3′-cGAMP
M420 (Baseline)
M464 (Relapse, with JAK2 Loss)
Lipofectamine only
2′3′-cGAMP, 25 μg/ml
M407 Parental Cell Line
M407 JAK2 Knockout
M407 JAK1 Knockout

Figure 4 (facing page). Loss of Interferon Gamma–Induced Growth Arrest through Acquired *JAK* Mutations.

In Panel A, the M407 parental cell line as well as the M407 *JAK1*-knockout and *JAK2*-knockout sublines were recognized by NY-ESO-1–specific, HLA-A*02:01–restricted T cells, as assessed by interferon-γ production after 24 hours of in vitro coculture. M420 is negative for HLA-A*02:01 and served as a negative control. In Panel B, cell lines M420 and M407 showed growth inhibition in response to direct in vitro treatment with interferon alfa, beta, or gamma (left), whereas the *JAK2*-deficient counterpart M464 and the M407 *JAK2* knockout were insensitive specifically to interferon gamma (middle). The M407 *JAK1* knockout was insensitive to all three interferons (right). In Panel C, treatment with 2′3′-cGAMP (cyclic guanosine monophosphate–adenosine monophosphate), a direct cytosolic agonist of the stimulator of interferon genes (STING), was able to produce growth arrest in all cell lines, regardless of *JAK2* status, yet had no effect in M407 with *JAK1* knockout. Growth curves represent the percent change in the number of melanoma cells over time as measured by IncuCyte continuous live-cell imaging in one of three independent experiments. I bars in Panels A, B, and C indicate standard deviations for three replicate wells. Three asterisks indicate P<0.001 and two asterisks P<0.01 for the percent change in growth with the treatment shown at the 72-hour end point as compared with the untreated control, with Dunnett's multiple-comparison correction applied in Panel B. NS denotes not significant.

cytosolic double-stranded DNA, directly activates the stimulator of interferon genes (STING) and leads to interferon-β production through activation of interferon regulatory factor 3 (IRF-3).[30] After 2′3′-cGAMP treatment, we observed growth arrest in all cell lines independent of JAK2 status but no effect in the *JAK1*-knockout subline (Fig. 4C). Therefore, the *JAK1* and *JAK2* loss-of-function mutations did not decrease in vitro T-cell recognition but selectively blocked the interferon-γ signaling that leads to cell-growth inhibition, which for *JAK2* loss could be corrected by type I pathway activation or a STING agonist.

FUNCTIONAL EFFECTS OF MUTATION IN THE GENE ENCODING BETA-2-MICROGLOBULIN (*B2M*)

In Patient 3, whole-exome sequencing of the baseline and progressive lesions showed a 4-bp S14 frame-shift deletion in exon 1 of the beta-2-microglobulin component of MHC class I as 1 of only 24 new relapse-specific mutations and the only such mutation that was homozygous (Fig. S13A and S13B in the Supplementary Appendix). Immunohistochemical analysis for MHC class I heavy chains revealed loss of outer-membrane localization as compared with adjacent stroma or the baseline tumor, even though diffuse intracellular staining indicated continued production of MHC class I molecules (Fig. S14 in the Supplementary Appendix). This finding is in line with the role of beta-2-microglobulin in proper MHC class I folding and transport to the cell surface, and its deficiency has long been recognized as a genetic mechanism of acquired resistance to immunotherapy.[12-14] Both the baseline and relapse biopsy samples were negative for MHC class II expression (Fig. S14 in the Supplementary Appendix), which suggests a lack of compensatory MHC up-regulation.

We could not find defined genetic alterations in Patient 4 that had clear potential to result in acquired resistance to T cells, but cancer cells in the baseline and relapse biopsy samples did not express PD-L1 despite proximity to T cells and PD-L1–expressing stroma (Fig. S3D in the Supplementary Appendix). These findings suggest possible nongenetic mechanisms of altered expression of interferon-inducible genes.[16]

DISCUSSION

With the approval of PD-1 checkpoint-blockade agents for the treatment of patients with melanoma, lung cancer, and other cancers, it is anticipated that cases of late relapse after initial response will increase. Understanding the molecular mechanisms of acquired resistance by focused comparison of biopsy samples from paired baseline and relapsing lesions may open options for the rational design of salvage combination therapies or preventive interventions and may guide mechanistic biomarker studies for the selection of patients, before the initiation of treatment, who are unlikely to have a response.

Tumor-infiltrating T cells are the effectors that kill cancer cells during PD-1 blockade therapy.[19,31] We found it striking that after intratumoral CD8 T-cell infiltration during active response, CD8 T cells were usually still present and abundant at the time of relapse, though they were restricted to the tumor margin. This observation suggested to us that the T cells were no longer able to exert their cytotoxic activity, because of either a lack of tumor antigen recognition and activation or a loss of sensitivity to their effector molecules by the cancer cells. The gen-

eral possibilities are loss of mutational or shared tumor antigens that are recognized by T cells, loss of antigen-presenting machinery components (e.g., beta-2-microglobulin and HLA),[12-14] tumor-cell–induced or myeloid-cell–induced inactivation of T-cell signaling,[32,33] or insensitivity to the proapoptotic effects of toxic granules (e.g., perforin and granzymes), death receptors (e.g., Fas and tumor necrosis factor–related apoptosis-inducing ligand [TRAIL]), or interferons.[34] Any of these escape mechanisms would be hypothesized to be fostered by the selective pressure of CD8 attack, which would be particularly active during the new round of immunoediting[35] that is unleashed after PD-1 blockade.

The inactivation of *JAK1* or *JAK2*, as noted in two of the patients, may be particularly advantageous to cancer cells in the context of anti–PD-1 therapy as compared with other immunotherapies. The interferon-induced adaptive expression of PD-L1, which allows the cancer to inactivate adjacent CD8 T cells,[36] would be of no use after the PD-1–PD-L1 interaction is blocked by therapeutic antibodies. We propose that without this benefit, the advantage for cancer cells tilts toward abolishing interferon signaling in order to avoid the detrimental increase in antigen presentation and direct antiproliferative effects.[27] Although we identified inactivating mutations in *JAK1* and *JAK2*, which are receptor-level signaling bottlenecks, interferon insensitivity through other means — such as epigenetic silencing of interferon-signaling components as previously documented in lung-cancer and prostate-cancer cell lines[15,16] or increased expression of negative regulators[37] — might lead to the same end. We also documented one case of beta-2-microglobulin inactivation, which corroborates a previously described mechanism of acquired resistance to cancer immunotherapy in humans through loss of this shared component of all human MHC class I molecules that is required for CD8 T-cell recognition.[12-14]

In conclusion, the nearly identical mechanism of acquisition, functional consequence, and evidence of clonal selection for *JAK1* or *JAK2* mutations in two independent cases with a similar clinical course of acquired resistance suggests that resistance to interferon gamma contributes to immune resistance and escape. This genetic alteration of immune resistance joins the previously described loss of *B2M* in decreasing immune-cell recognition of cancer cells, leading to acquired resistance to cancer immunotherapy. Although we have identified four cases and worked out a potential mechanism of resistance in three of them, additional cases will need to be closely examined to assess the generalizability of these findings.

Supported in part by National Institutes of Health (NIH) grants R35 CA197633, P01 CA168585, 1U54 CA199090, and R01 CA170689 (to Dr. Ribas). Dr. Ribas was supported by the Ressler Family Foundation, the Dr. Robert Vigen Memorial Fund, the Grimaldi Family Fund, the Samuels Family Fund, the Ruby Family Fund, and the Garcia-Corsini Family Fund. Drs. Ribas and Schumacher were supported by a Stand Up To Cancer–Cancer Research Institute Cancer Immunology Dream Team Translational Research Grant (SU2C-AACR-DT1012); Stand Up To Cancer is a program of the Entertainment Industry Foundation administered by the American Association for Cancer Research. Mr. Zaretsky is part of the UCLA Medical Scientist Training Program supported by NIH training grant GM08042. Dr. Shin was supported by the Oncology (5T32CA009297-30), Dermatology (5T32AR058921-05), and Tumor Immunology (5T32CA009120-39) training grants and a Tower Cancer Research Foundation Grant. Dr. Hu-Lieskovan was supported by a Young Investigator Award and a Career Development Award from the American Society of Clinical Oncology, a Tower Cancer Research Foundation Grant, and a Dr. Charles Coltman Fellowship Award from the Hope Foundation. Dr. Homet Moreno was supported in part by the Rio Hortega Scholarship (08/142) from Hospital 12 de Octubre, Madrid. Dr. Torrejon was supported by a grant from the Spanish Society of Medical Oncology for Translational Research in Reference Centers. Dr. Hugo was supported by the American Skin Association. Dr. Graeber was supported by a Melanoma Research Alliance Established Investigator Award (20120279) and an American Cancer Society Research Scholar Award (RSG-12-257-01-TBE). Dr. Lo was supported by the Steven C. Gordon Family Foundation, the Wade F.B. Thompson/Cancer Research Institute Clinic and Laboratory Integration Program Grant, the Ressler Family Foundation, the Grimaldi Family Fund, and the Ian Copeland Melanoma Fund.

Disclosure forms provided by the authors are available with the full text of this article at NEJM.org.

We thank the staff of the Translational Pathology Core Laboratory and Rongqing Guo and Wang Li from UCLA for blood and biopsy processing; Xinmin Li, Ling Dong, Janice Yoshizawa, and Jamie Zhou from the UCLA Clinical Microarray Core for sequencing expertise; and members of Dr. Ribas's laboratory, Pia Kvistborg and Marit van Buuren from the Netherlands Cancer Institute, Jordan Freeman from FLX Bio, and Leticia Corrales and Thomas Gajewski from the University of Chicago for useful discussions.

REFERENCES

1. Atkins MB, Kunkel L, Sznol M, Rosenberg SA. High-dose recombinant interleukin-2 therapy in patients with metastatic melanoma: long-term survival update. Cancer J Sci Am 2000;6:Suppl 1:S11-4.

2. Rosenberg SA, Yang JC, Sherry RM, et al. Durable complete responses in heavily pretreated patients with metastatic melanoma using T-cell transfer immunotherapy. Clin Cancer Res 2011;17:4550-7.

3. Prieto PA, Yang JC, Sherry RM, et al. CTLA-4 blockade with ipilimumab: long-term follow-up of 177 patients with metastatic melanoma. Clin Cancer Res 2012; 18:2039-47.

4. Eroglu Z, Kim DW, Wang X, et al. Long term survival with cytotoxic T lymphocyte-associated antigen 4 blockade using tremelimumab. Eur J Cancer 2015; 51:2689-97.
5. Schadendorf D, Hodi FS, Robert C, et al. Pooled analysis of long-term survival data from phase II and phase III trials of ipilimumab in unresectable or metastatic melanoma. J Clin Oncol 2015;33:1889-94.
6. Hamid O, Robert C, Daud A, et al. Safety and tumor responses with lambrolizumab (anti–PD-1) in melanoma. N Engl J Med 2013;369:134-44.
7. Robert C, Ribas A, Wolchok JD, et al. Anti-programmed-death-receptor-1 treatment with pembrolizumab in ipilimumab-refractory advanced melanoma: a randomised dose-comparison cohort of a phase 1 trial. Lancet 2014;384:1109-17.
8. Ansell SM, Lesokhin AM, Borrello I, et al. PD-1 blockade with nivolumab in relapsed or refractory Hodgkin's lymphoma. N Engl J Med 2015;372:311-9.
9. Robert C, Long GV, Brady B, et al. Nivolumab in previously untreated melanoma without *BRAF* mutation. N Engl J Med 2015;372:320-30.
10. Robert C, Schachter J, Long GV, et al. Pembrolizumab versus ipilimumab in advanced melanoma. N Engl J Med 2015; 372:2521-32.
11. Ribas A, Hamid O, Daud A, et al. Association of pembrolizumab with tumor response and survival among patients with advanced melanoma. JAMA 2016;315: 1600-9.
12. Restifo NP, Marincola FM, Kawakami Y, Taubenberger J, Yannelli JR, Rosenberg SA. Loss of functional beta 2-microglobulin in metastatic melanomas from five patients receiving immunotherapy. J Natl Cancer Inst 1996;88:100-8.
13. D'Urso CM, Wang ZG, Cao Y, Tatake R, Zeff RA, Ferrone S. Lack of HLA class I antigen expression by cultured melanoma cells FO-1 due to a defect in B2m gene expression. J Clin Invest 1991;87:284-92.
14. Sucker A, Zhao F, Real B, et al. Genetic evolution of T-cell resistance in the course of melanoma progression. Clin Cancer Res 2014;20:6593-604.
15. Kaplan DH, Shankaran V, Dighe AS, et al. Demonstration of an interferon gamma-dependent tumor surveillance system in immunocompetent mice. Proc Natl Acad Sci USA 1998;95:7556-61.
16. Dunn GP, Sheehan KC, Old LJ, Schreiber RD. IFN unresponsiveness in LNCaP cells due to the lack of JAK1 gene expression. Cancer Res 2005;65:3447-53.
17. Eisenhauer EA, Therasse P, Bogaerts J, et al. New response evaluation criteria in solid tumours: revised RECIST guideline (version 1.1). Eur J Cancer 2009;45:228-47.
18. Wolchok JD, Hoos A, O'Day S, et al. Guidelines for the evaluation of immune therapy activity in solid tumors: immune-related response criteria. Clin Cancer Res 2009;15:7412-20.
19. Tumeh PC, Harview CL, Yearley JH, et al. PD-1 blockade induces responses by inhibiting adaptive immune resistance. Nature 2014;515:568-71.
20. Nazarian R, Shi H, Wang Q, et al. Melanomas acquire resistance to B-RAF(V600E) inhibition by RTK or N-RAS upregulation. Nature 2010;468:973-7.
21. Atefi M, Avramis E, Lassen A, et al. Effects of MAPK and PI3K pathways on PD-L1 expression in melanoma. Clin Cancer Res 2014;20:3446-57.
22. Shi H, Hugo W, Kong X, et al. Acquired resistance and clonal evolution in melanoma during BRAF inhibitor therapy. Cancer Discov 2014;4:80-93.
23. Robbins PF, Morgan RA, Feldman SA, et al. Tumor regression in patients with metastatic synovial cell sarcoma and melanoma using genetically engineered lymphocytes reactive with NY-ESO-1. J Clin Oncol 2011;29:917-24.
24. Dunn GP, Bruce AT, Ikeda H, Old LJ, Schreiber RD. Cancer immunoediting: from immunosurveillance to tumor escape. Nat Immunol 2002;3:991-8.
25. Krzywinski M, Schein J, Birol I, et al. Circos: an information aesthetic for comparative genomics. Genome Res 2009;19: 1639-45.
26. Cerami E, Gao J, Dogrusoz U, et al. The cBio Cancer Genomics Portal: an open platform for exploring multidimensional cancer genomics data. Cancer Discov 2012; 2:401-4.
27. Bach EA, Aguet M, Schreiber RD. The IFN gamma receptor: a paradigm for cytokine receptor signaling. Annu Rev Immunol 1997;15:563-91.
28. Müller M, Briscoe J, Laxton C, et al. The protein tyrosine kinase JAK1 complements defects in interferon-alpha/beta and -gamma signal transduction. Nature 1993; 366:129-35.
29. Watling D, Guschin D, Müller M, et al. Complementation by the protein tyrosine kinase JAK2 of a mutant cell line defective in the interferon-gamma signal transduction pathway. Nature 1993;366:166-70.
30. Corrales L, Gajewski TF. Endogenous and pharmacologic targeting of the STING pathway in cancer immunotherapy. Cytokine 2016;77:245-7.
31. Pardoll DM. The blockade of immune checkpoints in cancer immunotherapy. Nat Rev Cancer 2012;12:252-64.
32. Finke JH, Zea AH, Stanley J, et al. Loss of T-cell receptor zeta chain and p56lck in T-cells infiltrating human renal cell carcinoma. Cancer Res 1993;53:5613-6.
33. Marvel D, Gabrilovich DI. Myeloid-derived suppressor cells in the tumor microenvironment: expect the unexpected. J Clin Invest 2015;125:3356-64.
34. Marincola FM, Jaffee EM, Hicklin DJ, Ferrone S. Escape of human solid tumors from T-cell recognition: molecular mechanisms and functional significance. Adv Immunol 2000;74:181-273.
35. Dunn GP, Old LJ, Schreiber RD. The three Es of cancer immunoediting. Annu Rev Immunol 2004;22:329-60.
36. Ribas A. Adaptive immune resistance: how cancer protects from immune attack. Cancer Discov 2015;5:915-9.
37. Fish EN, Platanias LC. Interferon receptor signaling in malignancy: a network of cellular pathways defining biological outcomes. Mol Cancer Res 2014;12:1691-703.

Chapter 3:

Primary Resistance to PD-1 Blockade Mediated by *JAK1/2* Mutations

ABSTRACT Loss-of-function mutations in *JAK1/2* can lead to acquired resistance to anti-programmed death protein 1 (PD-1) therapy. We reasoned that they may also be involved in primary resistance to anti–PD-1 therapy. *JAK1/2*-inactivating mutations were noted in tumor biopsies of 1 of 23 patients with melanoma and in 1 of 16 patients with mismatch repair–deficient colon cancer treated with PD-1 blockade. Both cases had a high mutational load but did not respond to anti–PD-1 therapy. Two out of 48 human melanoma cell lines had *JAK1/2* mutations, which led to a lack of PD-L1 expression upon interferon gamma exposure mediated by an inability to signal through the interferon gamma receptor pathway. *JAK1/2* loss-of-function alterations in The Cancer Genome Atlas confer adverse outcomes in patients. We propose that *JAK1/2* loss-of-function mutations are a genetic mechanism of lack of reactive PD-L1 expression and response to interferon gamma, leading to primary resistance to PD-1 blockade therapy.

SIGNIFICANCE: A key functional result from somatic *JAK1/2* mutations in a cancer cell is the inability to respond to interferon gamma by expressing PD-L1 and many other interferon-stimulated genes. These mutations result in a genetic mechanism for the absence of reactive PD-L1 expression, and patients harboring such tumors would be unlikely to respond to PD-1 blockade therapy. *Cancer Discov; 7(2); 188–201. ©2016 AACR.*

See related commentary by Marabelle et al., p. 128.

INTRODUCTION

Blocking the programmed death 1 (PD-1) negative immune receptor results in unprecedented rates of long-lasting antitumor activity in patients with metastatic cancers of different histologies, including melanoma, Hodgkin disease, Merkel cell carcinoma, and head and neck, lung, esophageal, gastric, liver, kidney, ovarian, bladder, and high mutational load cancers with defective mismatch repair, among others, in a rapidly growing list (1–8). This remarkable antitumor activity is explained by the reactivation of tumor antigen–specific T cells that were previously inactive due to the interaction between PD-1 and its ligand PD-L1 expressed by cancer cells (1, 9–12). Upon tumor antigen recognition, T cells produce interferon gamma, which through the interferon gamma receptor, the Janus kinases JAK1 and JAK2, and the signal transducers and activators of transcription (STAT) results in the expression of a large number of interferon-stimulated genes. Most of these genes lead to beneficial antitumor effects, such as increased antigen presentation through inducible proteasome subunits, transporters associated with antigen processing (TAP), and the major histocompatibility complex (MHC), as well as increased production of chemokines that attract T cells and direct tumor growth arrest and apoptosis (13). However, interferon gamma also provides the signal that allows cancer cells to inactivate antitumor T cells by the adaptive expression of PD-L1 (9), thereby specifically escaping their cytotoxic effects (12).

Acquired resistance to PD-1 blockade in patients with advanced melanoma can be associated with loss-of-function mutations with loss of heterozygosity in *JAK1/2* or in beta 2-microglobulin (*B2M*; ref. 14). The complex genetic changes leading to acquired resistance to PD-1 blockade, wherein one *JAK1/2* allele was mutated and amplified and the other was lost, suggest a strong selective pressure induced by the therapeutic immune response. Similar events leading to lack of sensitivity to interferon gamma have been reported in the cancer immune-editing process and acquired resistance to immunotherapy in mouse models (15–17) and in patients treated with the anti–CTLA-4 antibody ipilimumab who did not respond to therapy (18). Therefore, lack of interferon gamma responsiveness allows cancer cells to escape from antitumor T cells, and in the context of anti–PD-1/PD-L1 therapy, results in the loss of PD-L1 expression, the target of PD-1 blockade therapy, which would abrogate the antitumor efficacy of this approach.

In order to explore the role of *JAK1* and *JAK2* disruption in primary resistance to PD-1 blockade therapy, we performed a genetic analysis of tumors from patients with melanoma and colon cancer who did not respond to PD-1 blockade therapy despite having a high mutational load. We identified tumors with homozygous loss-of-function mutations in *JAK1* and *JAK2* and studied the functional effects of deficient interferon gamma receptor signaling that lead to a genetically mediated absence of PD-L1 expression upon interferon gamma exposure.

RESULTS

JAK Loss-of-Function Mutations in Primary Resistance to PD-1 Blockade in Patients with Metastatic Melanoma

Recent data indicate that tumors with a high mutational burden are more likely to have clinical responses to PD-1

[1]University of California, Los Angeles (UCLA), Los Angeles, California. [2]Jonsson Comprehensive Cancer Center, Los Angeles, California. [3]Johns Hopkins Sidney Kimmel Comprehensive Cancer Center, Baltimore, Maryland.

Note: Supplementary data for this article are available at Cancer Discovery Online (http://cancerdiscovery.aacrjournals.org/).

Corresponding Author: Antoni Ribas, Department of Medicine, Division of Hematology-Oncology, UCLA, 11-934 Factor Building, 10833 Le Conte Avenue, Los Angeles, CA 90095-1782. Phone: 310-206-3928; Fax: 310-825-2493; E-mail: aribas@mednet.ucla.edu

doi: 10.1158/2159-8290.CD-16-1223

blockade therapy (6, 19–21). However, in all of these series some patients failed to respond despite having a high mutational load. We performed whole-exome sequencing (WES) of 23 pretreatment biopsies from patients with advanced melanoma treated with anti–PD-1 therapy, which included 14 patients with a tumor response by immune-related RECIST (irRECIST) criteria and 9 without a response (Supplementary Table S1). Even though the mean mutational load was higher in responders than nonresponders, as reported for lung, colon, and bladder cancers (6, 19, 21), some patients with a tumor response had a low mutational load and some patients without a tumor response had a high mutational load (Fig. 1A).

We then assessed whether loss-of-function mutations in interferon receptor signaling molecules, which would prevent adaptive expression of PD-L1, might be present in tumors with a relatively high mutational load that did not respond to therapy. A melanoma biopsy from the patient with the highest mutational load among the 9 nonresponders (patient #15) had a somatic P429S missense mutation in the src-homology (SH2) domain of *JAK1* (Fig. 1B). WES of an early passage cell line derived from this tumor (M431) showed an amplification of chromosome 1p, including the *JAK1* locus, and a 4:1 mutant:wild-type allele ratio was observed at both the DNA and RNA level (Supplementary Fig. S1A–S1E and Supplementary Database S1). None of the tumors from the other 22 patients had homozygous loss-of-function mutations or deletions in the interferon receptor pathway. Rather, the other *JAK2* mutations found in biopsies of responders had low variant allele frequency (VAF) as shown in Fig. 1B and were likely heterozygous. These mutations would not carry the same functional significance, as signaling would still occur upon interferon exposure through the wild-type JAK protein from the nonmutated allele. Two nonresponders had *IFNGR* mutations, also of low allele frequency and therefore uncertain significance. We also analyzed potential mutations in genes involved in the antigen-presenting machinery and did not find any loss-of-function mutations that were homozygous (Supplementary Fig. S2).

As expected, tumors from patients who responded had a higher density of CD8 cells and PD-L1 in the center and invasive tumor margin (Fig. 1C and D). In contrast, the baseline biopsy from patient #15 with a high mutational load but with the *JAK1*^{P429S} missense mutation had undetectable CD8 infiltrates, PD-1 and PD-L1 expression (Supplementary Fig. S3). The amplification of *PD-L1*, *PD-L2*, and *JAK2* (PDJ amplicon), which has been associated with a high response rate in Hodgkin disease (4), was noted only in patient #16, who did not respond to PD-1 blockade therapy despite having the second highest mutational load and a high level of PD-L1 expression (Fig. 1B, D and E).

Functional Analyses of the Role of *JAK* Loss-of-Function Mutations in Regulating PD-L1 Expression

We next sought to characterize the interferon response of M431, the melanoma cell line established from a biopsy of patient #15 with high mutational load and no response to therapy. First, we optimized flow cytometry conditions in selected human melanoma cell lines (Supplementary Figs. S4A–S4F, S5A–S5D, S6A–S6H, and S7A–S7C). PD-L1 expression increased less than 1.5-fold interferon gamma exposure in M431 (Fig. 2A), versus 5.1-fold in M438, a cell line established from patient #8 used as a positive control in this same series. Phosphorylated STAT1 (pSTAT1) was induced at 30 minutes in M431, but the signal dissipated at 18 hours, faster than in cell lines with more durable responses to interferon gamma leading to PD-L1 upregulation (Fig. 2B, C compared with Supplementary Fig. S8A–S8C). These data are consistent with the 4:1 *JAK1* mutant:wild-type allele frequency in the M431 cell line (Supplementary Fig. S1A–S1E).

We then screened a panel of 48 human melanoma cell lines for absolute absence of PD-L1 induction by either type I (alpha and beta) or type II (gamma) interferons. Among the three interferons, interferon gamma most potently induced PD-L1 expression (Fig. 2D; Supplementary Fig. S9A and S9B for type I interferons). Two cell lines had *JAK1/2* homozygous loss-of-function mutations and did not respond to interferon gamma with upregulation of surface PD-L1 expression. M368 had a mutation in *JAK2* (20 out of 22 reads, VAF = 0.91) that is predicted to disrupt and shift the D313 splice-site acceptor in exon 8 by one nucleotide, changing the reading frame, and had loss of the wild-type allele (Fig. 3A; Supplementary Fig. S10A and S10B). M395 had an inactivating *JAK1*^{D775N} kinase domain mutation in exon 17 and loss of the other allele (140 out of 143 reads, variant allele frequency 0.98; Fig. 3B).

We then analyzed signaling in response to interferon alpha, beta, and gamma in these two cell lines. M368, which harbored the *JAK2* loss-of-function mutation, maintained signaling in response to interferon alpha and beta, but did not respond to interferon gamma (Fig. 3C), which resulted in the ability of M368 to upregulate PD-L1 when exposed to interferon alpha and beta, but not to interferon gamma (Fig. 3C; Supplementary Fig. S9A and S9B). M395, which harbored the *JAK1* loss-of-function mutation, did not respond to downstream signaling to interferon alpha, beta, or gamma (Fig. 3D), and equally did not upregulate PD-L1 in response to any of these cytokines (Fig. 3D; Supplementary Fig. S9A and S9B). We were able to retrieve the tumor from which the cell line M395 had been established, and this tumor exhibited an absence of CD8 infiltration similar to the finding in patient #15 with a *JAK1* loss-of-function mutation who did not respond to anti–PD-1 therapy (Supplementary Fig. S11). Taken together, these data are consistent with the knowledge that JAK1 (disabled in M395) is required to propagate signaling downstream of the interferon alpha/beta and gamma receptors, whereas JAK2 (disabled in M368) is required for signaling downstream only from the interferon gamma receptor (22–24).

To assess a causal relationship between loss of adaptive PD-L1 expression and loss-of-function *JAK* mutations, we transduced the M395 and M431 cell lines with a lentivirus vector expressing *JAK1* wild-type (Supplementary Fig. S12A–S12C). Reintroduction of wild-type JAK1 rescued PD-L1 expression in M395 cells, which exhibited a 4-fold increase in PD-L1 surface expression after interferon gamma exposure (Fig. 3E). For M431, the magnitude of change in PD-L1 expression after 18-hour interferon gamma exposure for M431 was modest after reintroducing the JAK1 wild-type protein (approximately 2-fold, compared with a 1.5-fold in the untransduced cell line; Fig. 3F). However, the difference between untransduced and

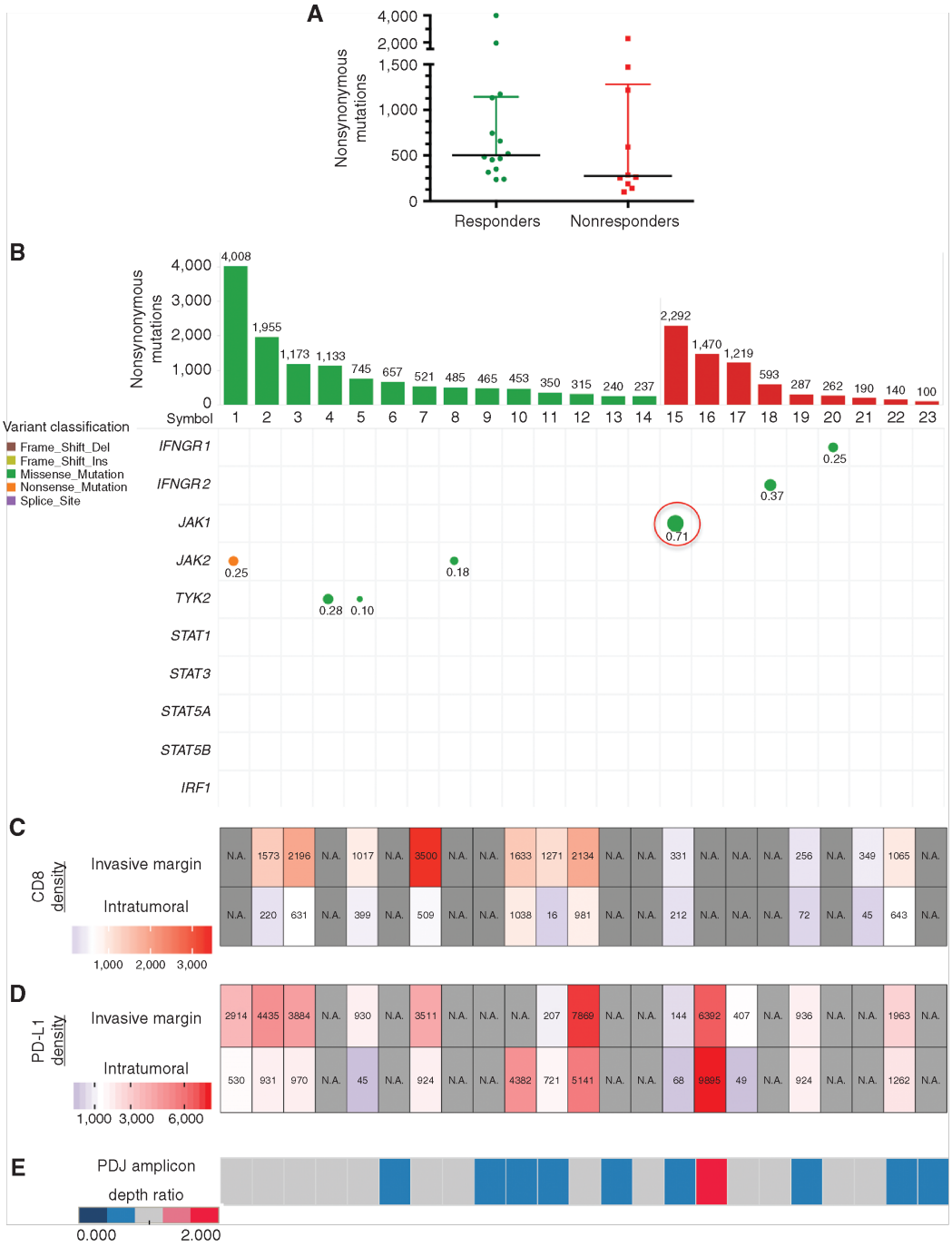

Figure 1. Mutational load and mutations in the interferon signaling pathway among patients with advanced melanoma with or without response to anti–PD-1 blockade therapy. **A,** Total nonsynonymous mutations per tumor from biopsies of patients with response ($n = 14$) or without response ($n = 9$) to anti–PD-1 per RECIST 1.1 criteria (median 503 vs. 274, $P = 0.27$ by Mann–Whitney). Median and interquartile range are shown, with value for each individual tumor shown as dots. **B–D,** Each column corresponds to an individual case from **A**. **B,** Depiction of mutational load (bar graph) and mutations in interferon receptor pathway genes. The size of circles and adjacent labels represents the tumor VAF after adjustment for stromal content. Color represents predicted functional effect. Green, missense; orange, nonsense. Red circle highlights amplified *JAK1* mutation in one patient who did not respond to anti–PD-1 therapy. All the tumor sequences were compared to normal germline sequences. **C,** Heat map of the density of CD8 T cells in the invasive margin or intratumor compartment analyzed in baseline tumor biopsies by immunohistochemistry. **D,** Heat map of density of PD-L1 expression in available tissue samples. **E,** Genetic amplification of the chr9p24.1 (*PD-L1*, *PD-L2*, and *JAK2* locus, termed the PDJ amplicon) was noted in one biopsy from a nonresponding patient. Heat map represents average read depth ratio versus paired germline normal.

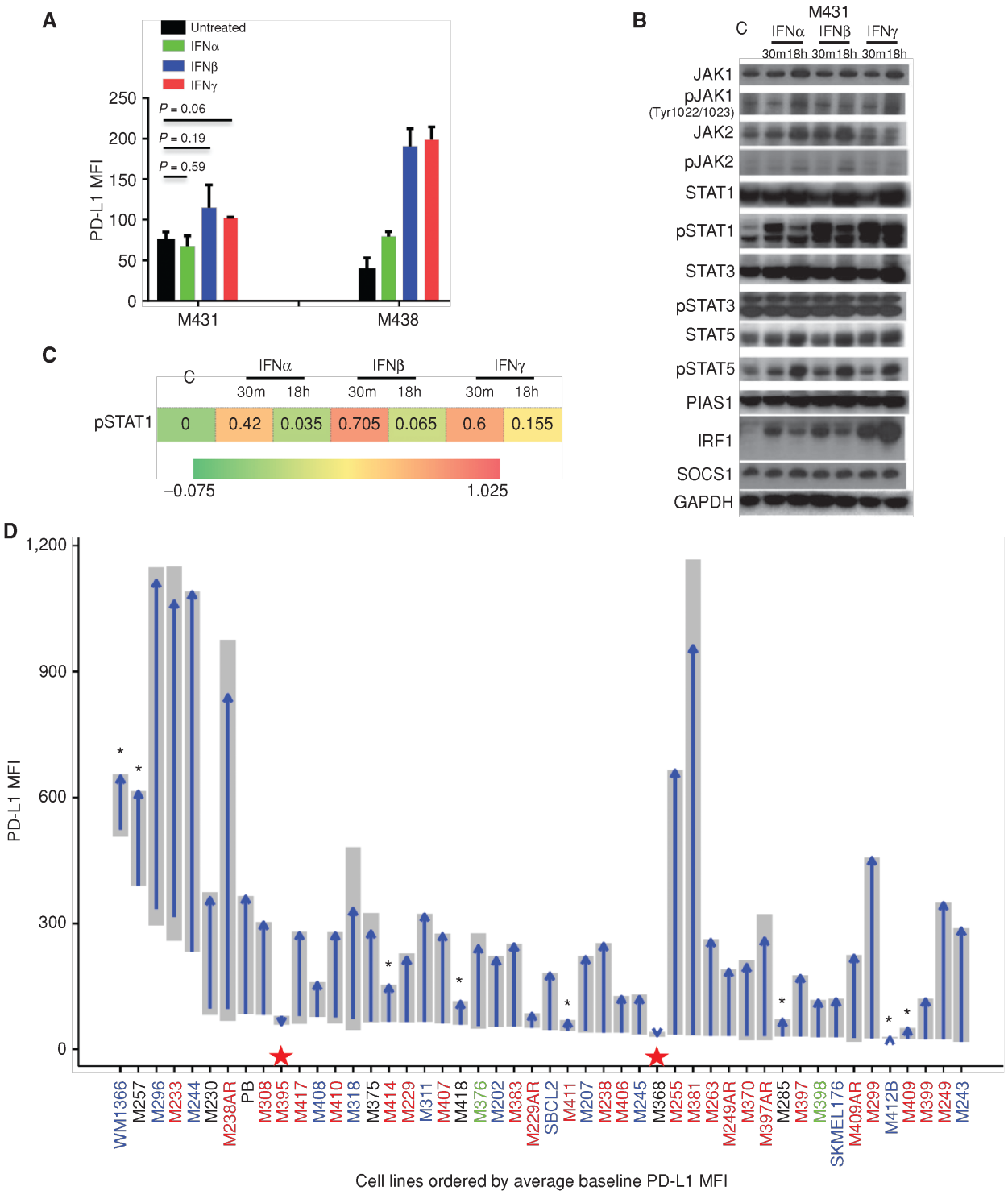

Figure 2. Altered interferon signaling with *JAK1* loss-of-function mutation in M431 and interferon gamma-inducible PD-L1 expression by 48 melanoma cell lines. **A,** Mean fluorescent intensity (MFI) of PD-L1 expression by flow cytometry upon interferon alpha, beta, or gamma exposure over 18 hours in M431 (established from patient #15) compared with M438 (established from patient #8). **B,** Corresponding Western blot analyses for M431 upon interferon exposure for 30 minutes or 18 hours. **C,** Phosphorylated STAT1 (pSTAT1) flow cytometry for M431 upon interferon exposure for 30 minutes or 18 hours (same color scale as in Fig. 3C and D, Supplementary Fig. S8A-S8C). The numbers in the heat map of pSTAT1 indicate the average Arcsinh ratio from two independent phospho-flow cytometry experiments. **D,** PD-L1 response to interferon gamma. Blue arrows represent average change from baseline upon interferon gamma exposure. Grey shades show the full range of measured values ($n = 2$ or 3). Red stars indicate cell lines with no response due to having a JAK loss-of-function mutation, and black stars indicate cell lines with poor response to interferons. Red, *BRAF* mutated; blue, *NRAS* mutated; green, *BRAF* and *NRAS* mutated; black, *BRAF* wild-type, *NRAS* wild-type.

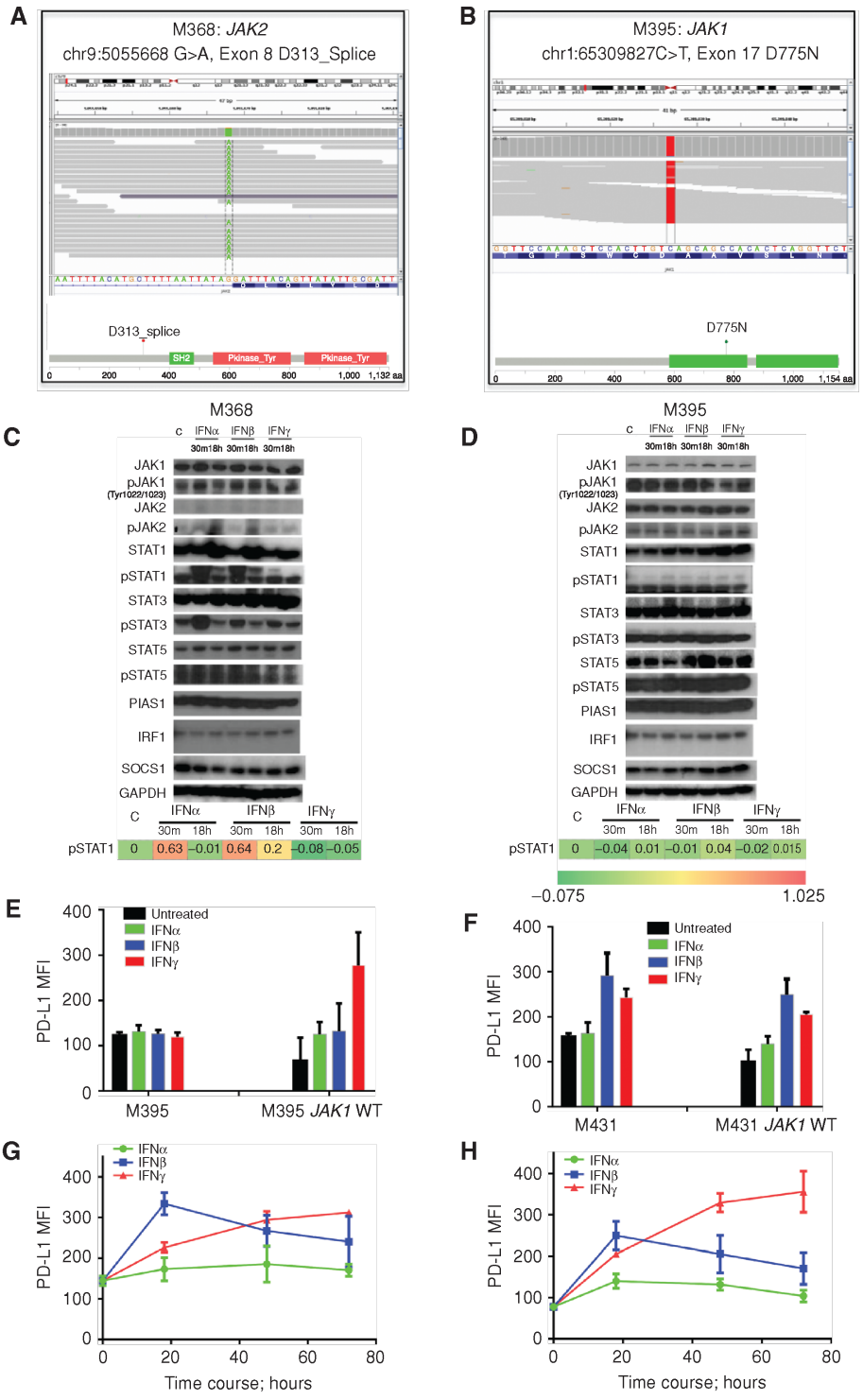

Figure 3. Defects in the interferon receptor signaling pathway with *JAK* homozygous loss-of-function mutations in M368 and M395. **A** and **B,** Exome sequencing data showing *JAK2*^{D313} spice-site mutation in exon 8 in M368 (**A**), and *JAK1*^{D775N} kinase domain mutation in exon 17 in M395 (**B**). Top, individual sequencing reads using the Integrated Genomics Viewer; bottom, position relative to kinase domains using the cBioPortal Mutation Mapper. **C** and **D,** For each cell line, cells were cultured with interferon alpha, interferon beta, or interferon gamma for either 30 minutes or 18 hours, or with vehicle control (c, first column from the left in Western blots and phospho-flow data). Phosphorylated STAT1 (pSTAT1) detected by Western blotting (top) or phospho-flow cytometry data (bottom). The numbers in the heat map of pSTAT1 indicate the average Arcsinh ratio from two independent phospho-flow experiments. Blots represent two independent replicate experiments. **E** and **F,** PD-L1 expression after interferon exposure on M395 and M431 after *JAK1* wild-type (WT) lentiviral transduction respectively. **G** and **H,** Time course PD-L1 expression for M431 and *JAK1* wild-type lentiviral vector transduced M431, respectively.

JAK1 wild-type transduced M431 was more distinct when observed over a longer time course (Fig. 3G and 3H).

JAK Loss-of-Function Mutations in Primary Resistance to PD-1 Blockade in Patients with Metastatic Colon Carcinoma

To determine whether *JAK1/2* loss-of-function mutations are present and relate to response to PD-1 blockade therapy in another cancer histology, we analyzed WES data from 16 biopsies of patients with colon cancer, many with a high mutational load resultant from mismatch-repair deficiency (6). One of the biopsies of a rare patient with high mutational load with neither an objective response nor disease control with anti–PD-1 had a homozygous *JAK1*^{W690*} nonsense loss-of-function mutation, expected to truncate the protein within the first kinase domain, and an accompanying loss of heterozygosity at the *JAK1* locus (Fig. 4A–D). No mutations in antigen presentation machinery were detected in this sample (Supplementary Fig. S13). Although we observed other interferon pathway and antigen presentation mutations in the high mutational load patients with a response to therapy in this cohort, they appeared to be heterozygous by allele frequency (adjusted VAF < 0.6) after adjustment for stromal content. Most were splice-site mutations or frameshift insertions/deletions unlikely to create a dominant-negative effect. Several samples bore two mutations in *JAK1/2* or *B2M*, but either retained at least one wild-type copy (subjects #4 and #5), were too far apart to determine cis versus trans status (subject #6), or were of uncertain significance (subject #1, both near c-terminus).

Frequency of *JAK* Loss-of-Function Mutations in Cell Lines of Multiple Histologies

We then analyzed data from the Cancer Cell Line Encyclopedia (CCLE) from cBioPortal to determine the frequency of homozygous putative loss-of-function mutations in *JAK1/2* in 905 cancer cell lines (25). For this analysis, we considered a homozygous mutation when the VAF was 0.8 or greater, as previously described (26). Approximately 0.7% of cell lines have loss-of-function mutations that may predict lack of response to interferons (Fig. 5A and 5B). The highest frequency of mutations was in endometrial cancers, as described previously (26). None of these cell lines had *POLE* or *POLD1* mutations, but microsatellite instability and DNA-damage gene mutations were present in the *JAK1/2* mutant cell lines (Supplementary Fig. S14). The frequency of *JAK1/2* mutations across all cancers suggests that there is a fitness gain with loss of interferon responsiveness.

JAK1/2 Loss-of-Function Alterations in The Cancer Genome Atlas

Analysis of WES, RNA sequencing (RNA-seq), and reverse-phase protein array (RPPA) data from tissue specimens from 472 patients in The Cancer Genome Atlas (TCGA) Skin Cutaneous Melanoma dataset revealed that 6% (28 of 472) and 11% (50 of 472) harbored alterations in *JAK1* and *JAK2*, respectively. These include loss-of-function alterations in either *JAK1* or *JAK2* that would putatively diminish JAK1 or JAK2 signaling (homodeletions, truncating mutations, or gene or protein downregulation).

There was no survival difference in patients in the TCGA Skin Cutaneous Melanoma dataset harboring any *JAK1* or *JAK2* alteration (Fig. 6A). However, when considering only loss-of-function *JAK1* or *JAK2* alterations (homodeletions, truncating mutations, or gene or protein downregulation), patients with tumors that had *JAK1* or *JAK2* alterations had significantly decreased overall survival ($P = 0.009$, log-rank test). When considered separately, the 8 patients with truncating mutations in *JAK1* or *JAK2* and the 18 patients with *JAK1* or *JAK2* gene or protein downregulation also had significantly decreased overall survival ($P = 0.016$ and $P < 0.001$, respectively).

To assess the relevance of these findings in a broader set of malignancies, we examined the frequency of *JAK1* and *JAK2* alterations and their association with clinical outcome in TCGA datasets for four common malignancies (breast invasive carcinoma, prostate adenocarcinoma, lung adenocarcinoma, and colorectal adenocarcinoma). Similar to findings in melanoma, alterations in *JAK1* were found in 6%, 8%, 10%, and 10% of patients with breast invasive carcinoma, prostate adenocarcinoma, lung adenocarcinoma, and colorectal adenocarcinoma, respectively. Likewise, alterations in *JAK2* were found in 12%, 7%, 12%, and 5% of these respective malignancies.

Consistent with our findings in melanoma, *JAK1* or *JAK2* alterations as a whole were not associated with a difference in survival in any of the four additional TCGA datasets. However, for patients with breast invasive carcinoma harboring truncating mutations, there was an association with decreased survival ($P = 0.006$, log-rank test; Fig. 6B). Likewise, patients with prostate adenocarcinoma harboring truncating mutations had worse overall survival ($P = 0.009$, log-rank test; Fig. 6C), with a similar trend noted in patients harboring any loss-of-function *JAK1* or *JAK2* alterations ($P = 0.083$, Fig. 6C). We did not observe differences in survival in patients with lung adenocarcinoma or colorectal adenocarcinoma harboring *JAK1* or *JAK2* loss-of-function alterations, when considered either separately or as a whole (Supplementary Fig. S15A and S15B).

DISCUSSION

For this work, we hypothesized that if cancer cells evolved to disable inducible PD-L1 expression upon interferon exposure due to selective immune pressure as demonstrated in preclinical models of cancer immune-editing (15, 16), then it would be superfluous to attempt to treat these cases with anti–PD-1/PD-L1 antibody therapy (Supplementary Fig. S16A and S16B). The premise of therapy with anti–PD-1– or anti–PD-L1–blocking antibodies is that T cells with specificity for cancer antigens recognize their target on cancer cells and produce interferon gamma. The cancer cell then finds a way to specifically protect itself from the T-cell attack by reactively expressing PD-L1 upon interferon gamma signaling. This reactive process is termed adaptive immune resistance, and it requires signaling through the interferon gamma receptor (12). By understanding this process, it is then logical to anticipate that a genetically acquired insensitivity to interferon gamma signaling could represent an immune resistance mechanism; these tumors would be expected to be incapable of upregulating either antigen-presenting machinery or PD-L1 even in the presence of a robust preexisting repertoire of tumor-specific T cells. With a genetic mechanism of lack

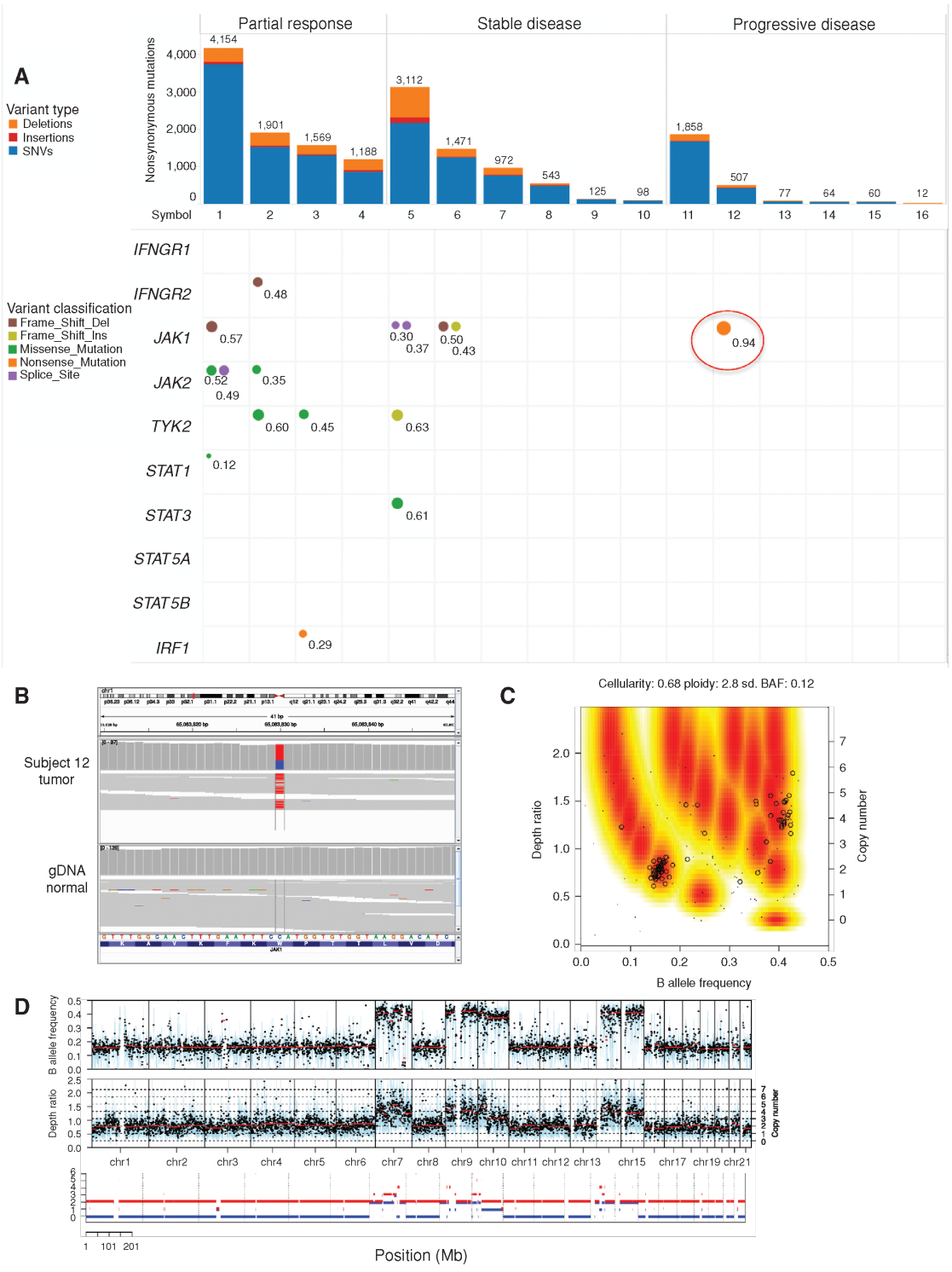

Figure 4. Mutational burden of somatic, protein-altering mutations per subject from WES for patients with advanced colon cancer who participated in PD-1 blockade clinical trial. **A,** Similar to Fig. 1B, bar graph shows mutational load in individual cases [fraction single nucleotide variants (SNV), blue; insertions, red; deletions, orange] divided by response to PD-1 blockade therapy. Bottom panel depicts mutations, insertions, or deletions in the interferon receptor pathway. Color represents predicted functional effect. The size of circles and adjacent labels correspond to tumor VAF after adjusting for stromal content. Red circle highlights homozygous nonsense mutation in *JAK1* from one patient who did not respond to anti–PD-1 therapy. **B,** Sequencing reads of *JAK1* mutation in nonresponder subject #12. **C,** Mutation observed in 51 reads out of 80 (VAF 0.64), which corresponds to a homozygous mutation (adjusted VAF 0.94) when adjusted for a tumor purity of 68%. **D,** Copy-number profile reveals loss of heterozygosity across most of the genome, including chromosome 1/*JAK1*.

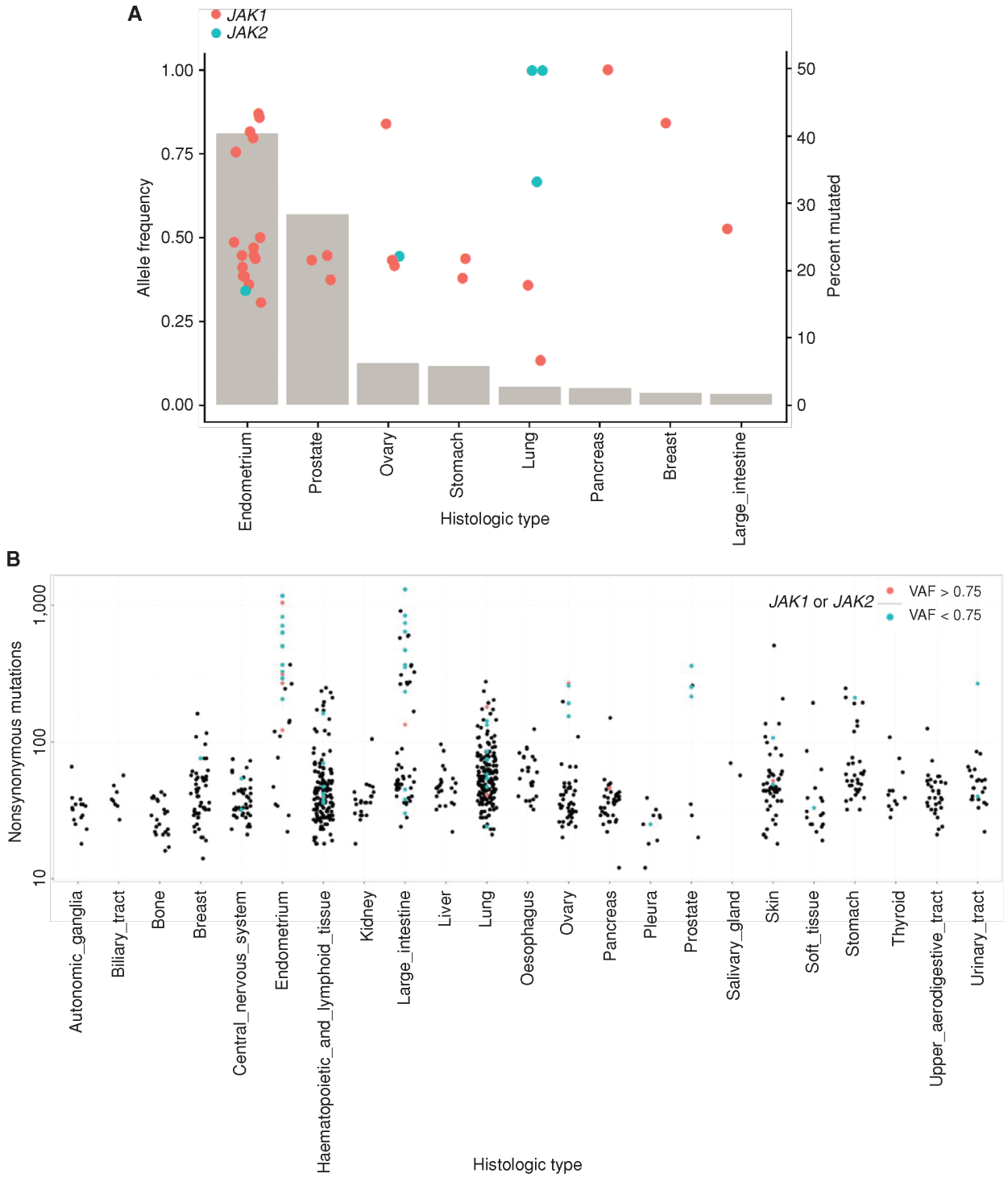

Figure 5. Analysis of *JAK1* and *JAK2* mutations in the CCLE database. **A,** Variant allele frequency (left axis, red and blue points) and percentage of tumors with mutations in *JAK1* or *JAK2* (right axis, gray bars) in the CCLE database from the cBioPortal. **B,** Nonsynonymous mutational burden was analyzed for individual cell lines (each dot represents cell line) and plotted for each histologic type. *JAK1* or *JAK2* mutated cell lines were color coded (red, VAF>0.75; blue, VAF<0.75).

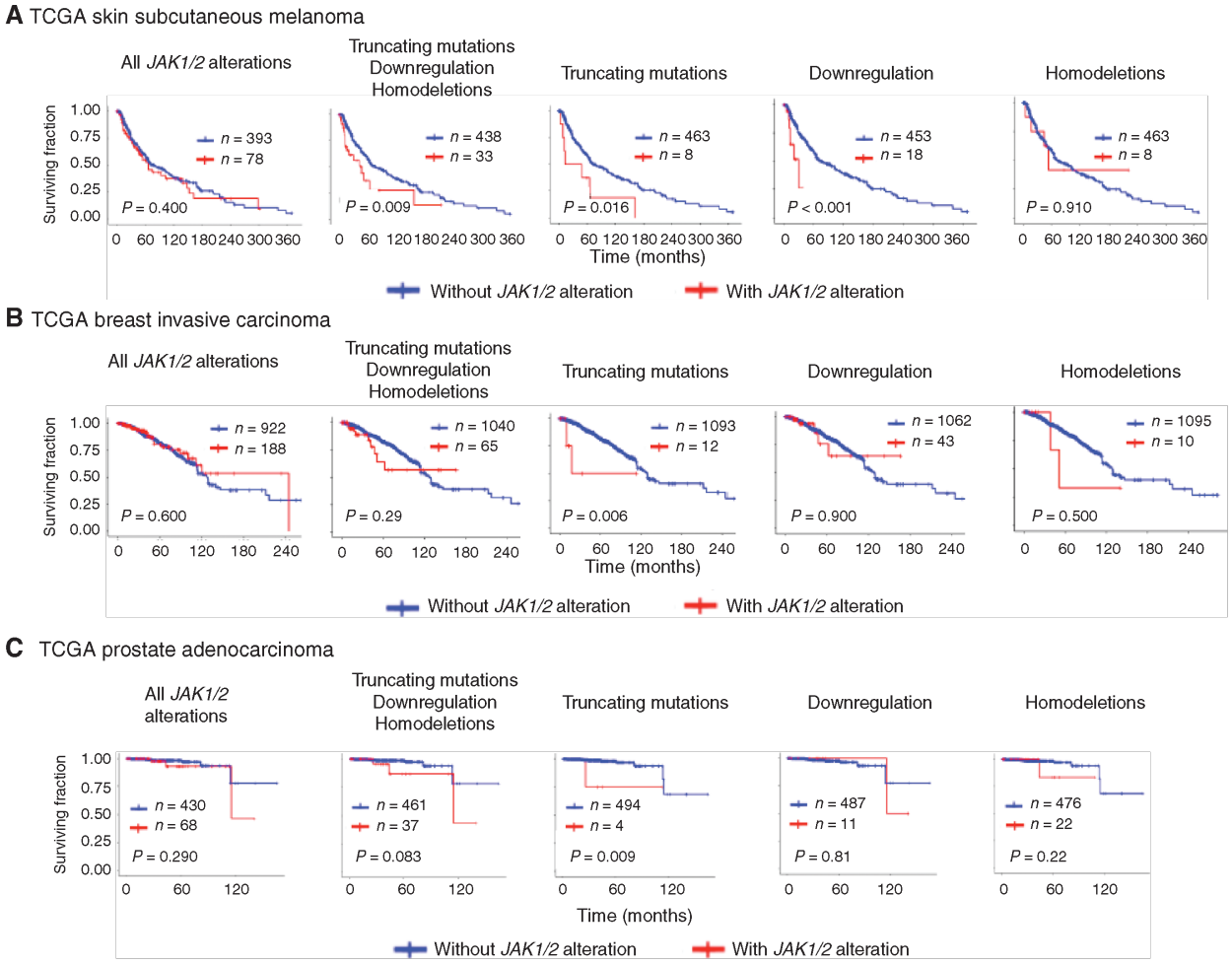

Figure 6. Frequency of *JAK1* and *JAK2* alterations and their association with overall survival in TCGA datasets. Kaplan–Meier survival analysis of TCGA skin cutaneous melanoma (**A**), breast invasive carcinoma (**B**), and prostate adenocarcinoma (**C**) provisional datasets, comparing control patients (blue) and patients harboring specified alterations in *JAK1* and *JAK2* (red). Frequency and distribution of combined *JAK1* and *JAK2* alterations are shown within each set of Kaplan–Meier plots. Significance testing of overall survival was performed using log-rank analysis.

of interferon gamma signaling, a T-cell response with interferon gamma production would not lead to reactive PD-L1 expression and therefore these would be cases that would be considered constitutively PD-L1 negative.

JAK kinases mediate signaling from many cytokine receptors, but the commonality between *JAK1* and *JAK2* homozygous loss-of-function mutations is that they are both required for signaling upon exposure to interferon gamma (27). Interferon gamma is a major cytokine produced by T cells upon recognizing their cognate antigen, and it has multiple effects on target cells. In the setting of acquired resistance to PD-1 blockade therapy in patients who progressed while on continuous anti–PD-1 therapy, the tumor's insensitivity to interferon gamma provides a selective advantage for the relapsed cancer to grow, as it no longer is sensitive to the antiproliferative effects of interferon gamma (14). In that setting, T cells continued to recognize cancer cells with *JAK1* or *JAK2* mutations despite the known role of interferon gamma signaling in upregulating a series of genes involved in the antigen-presenting machinery. However, as the baseline expression of MHC class I, proteasome subunits and TAP transporters is unchanged, tumor antigen presentation to T cells was not impaired (14).

In primary resistance to checkpoint blockade therapy with the anti–CTLA-4 antibody ipilimumab, there is a higher frequency of mutations in the several molecules involved in the interferon signaling pathway (18). It is hypothesized that cancer cells lacking interferon receptor signaling would have a selective advantage because they evade T cells activated by CTLA-4 blockade, in particular through decreased antigen presentation and resistance to the antiproliferative effects of interferons. The same processes may have an important role in the lack of response to anti–PD-1 therapy in the cancers with *JAK1/2* loss-of-function mutations in our series, as antitumor T cells would be anticipated to have lower ability to recognize and kill cancer cells. Loss-of-function mutations in *JAK1/2* would likewise prevent the antitumor activity of any immunotherapy that results in the activation of T cells to attack cancer cells. But in the setting of anti–PD-1/PD-L1 therapy, it has the

additional important effect of preventing PD-L1 expression upon interferon gamma exposure, thereby making it futile to pharmacologically inhibit the PD-L1/PD-1 interaction.

As the interferon gamma receptor pathway downstream of JAK1/2 controls the expression of chemokines with a potent chemoattractant effect on T cells, such as CXCL9, CXCL10, and CXCL11 (28), it is possible that an important effect of *JAK1/2* loss may result in a lack of T-cell infiltrates. Indeed, both the patient in the melanoma series with a *JAK1* loss of function and the biopsy from which we had derived a melanoma cell line with a *JAK1* mutation were completely devoid of T-cell infiltrates. As preexisting T cells in the tumor are a requisite for response to anti–PD-1 therapy (11), a *JAK1/2* mutation may result in lack of response not only because PD-L1 cannot be reactively expressed but also because the cancer fails to attract T cells due to lack of chemokine production.

Beyond a genetic mutation that prevented expression of *JAK1/2*, it is also possible that epigenetic silencing of *JAK*s could result in lack of response to interferon gamma, as previously reported for the LNCaP cell line (29). In this case, loss of JAK1/2 expression could then be corrected with exposure to a demethylating agent. This evidence suggests that the frequency of loss of function in *JAK1/2* may be higher than can be estimated by exome-sequencing analyses, as it could occur epigenetically, and in these cases it would provide an option for pharmacologic intervention.

In conclusion, we propose that *JAK1/2* mutations that lead to loss of interferon gamma signaling and prevent adaptive PD-L1 expression upon interferon gamma exposure represent an immunoediting process that defines patients with cancer who would not be good candidates for PD-1 blockade therapy. This mechanism would add to other multiple explanations that may lead to primary resistance to PD-1 blockade therapy, including a tumor that lacks antigens that can be a target for a T-cell response, the presence of immune suppressive factors in the tumor microenvironment that exclude T cells in tumors or that lead to alteration of T-cell function, presence of immune suppressive cells such as T regulatory or myeloid-derived suppressor cells, or cancers that have specific genetic signaling or transcriptomes that are not permissive to T-cell infiltrates (20, 30, 31). The recognition that *JAK1/2* loss-of-function mutations would lead to lack of response to PD-1 blockade therapy could be incorporated in oncogenic sequencing panels used to select patients for precision cancer treatments.

METHODS

Tumor Samples

Tumor biopsies were obtained from a subset of patients enrolled in a phase I expansion clinical trial with pembrolizumab after signing a written informed consent (32). Patients were selected for this analysis by having adequate tumor biopsy samples and clinical follow-up. Baseline biopsies of metastatic tumors were obtained within 30 days of starting on treatment, except for one in a patient with an eventual complete response (Fig. 3B, subject #4) collected after 84 days on treatment. Samples were immediately fixed in formalin followed by paraffin embedding, and when there was an additional sterile piece of the tumor, processed for snap-freezing in liquid nitrogen and to establish a cell line as previously described (33–35). Tumor biopsy and peripheral blood cell collection and analyses were approved by UCLA Institutional Review Boards 11-001918 and 11-003066.

Treatment and Response Assessment

Patients received single-agent pembrolizumab intravenously in one of three dosing regimens: 2 mg/kg every 3 weeks (2Q3W), 10 mg/kg every 3 weeks (10Q3W), or 10 mg/kg every 2 weeks (10Q2W; ref. 32). Tumor responses to pembrolizumab were evaluated at 12 weeks after the first infusion (confirmed at 16 weeks), and every 12 weeks thereafter. The RECIST version 1.1 was used to define objective clinical responses. The protocol was allowed to proceed beyond initial progression at the restaging scans at 12 weeks and have repeated imaging scans 4 weeks later following the immune-related response criteria (irRC; ref. 36).

IHC Staining

For CD8 T-cell density, 5 of the 11 cases were reanalyzed blindly from IHC samples already used in our prior work (11), and the other 6 cases were newly stained cases also analyzed blindly. Slides were stained with hematoxylin and eosin, S100, CD8, CD68, PD-1, and PD-L1 at the UCLA Anatomic Pathology IHC Laboratory. Immunostaining was performed on Leica Bond III autostainers using Leica Bond ancillary reagents and the REFINE polymer DAB detection system as previously described (11). Cell density (cells/mm^2) in the invasive margin or intratumoral area was calculated using the Indica Labs Halo platform as previously described (11).

Cell Lines, Cell Culture, and Conditions

Patient-derived melanoma cell lines were generated as reported previously and characterized for their oncogenic mutational status (33–35). Each melanoma cell line was thawed and maintained in RPMI-1640 medium supplemented with 10% FBS, 100 units/mL penicillin, and 100 μg/mL streptomycin at 37°C in a humidified atmosphere of 5% CO_2. Cells were subject to experimental conditions after reaching two passages from thawing. Cell lines were periodically authenticated using GenePrint 10 System (Promega) and were matched with the earliest passage cell lines. Selected melanoma cell lines were subjected to *Mycoplasma* tests periodically (every 2–3 months) with the MycoAlert Mycoplasma Detection Kit (Lonza).

Surface Flow Cytometry Analysis for PD-L1 and MHC Class I

Melanoma cells were seeded into 6-well plates on day 1, ranging from 420,000 to 485,000 depending on their doubling time, targeting 70% to 80% of confluence at the time of trypsinization after 18 hours of exposure to interferons. For 48-hour exposure, 225,000 to 280,000 cells were seeded, and 185,000 to 200,000 cells were seeded for 72-hour exposure. After trypsinization, cells were incubated at 37°C for 2 hours with media containing different concentrations of interferons. Concentrations of each interferon were determined after optimization process (dose–response curves were generated with representative cell lines as shown in Supplementary Fig. S5B–S5D). After 2 hours of incubation, the media were removed by centrifugation and cells were resuspended with 100% FBS and stained with APC anti–PD-L1 antibody on ice for 20 minutes. The staining was halted by washing with 3 mL of PBS, which was removed by centrifugation at 500 × *g* for 4 minutes. The cells were resuspended with 300 μL of PBS, and 7-AAD for dead cell discrimination was added to samples prior to data acquisition by LSRII. The data were analyzed by FlowJo software (Version 10.0.8r1, Tree Star Inc.). Experiments were performed at least twice for each cell line; some cell lines with high assay variability were analyzed three times.

Phosphoflow Signaling Analyses

Cells were seeded into two 6-well plates for each cell line for single phospho-proteomics study. After 30-minute or 18-hour exposure to interferon alpha, beta, or gamma, cells were trypsinized and resuspended with 1 mL of PBS per 1 to 3 million cells and stained with live/dead agent at room temperature in the dark for 30 minutes.

Cells were then fixed with paraformaldehyde at room temperature for 10 minutes in the dark, permeabilized by methanol, and stained with pSTAT1. Cells were incubated at room temperature in the dark for 30 minutes, washed with phospho-flow cytometry buffer, and resuspended with 300 to 500 μL of the same buffer and analyzed with an LSRII. The flow cytometry standard (FCS) files obtained by LSRII were analyzed using the online flow cytometry program (Cytobank; ref. 37). The raw FCS files were deconvoluted into four different conditions, three of which were exposed to interferon alpha, beta, and gamma and compared with an untreated condition at each time point. Data represented as Arcsinh ratio, which is one of transformed ratio of cytometry data (inverse hyperbolic sine) analyses; each data point was compared with its control [Value = arcsinh((x − control)/scale_argument)].

Western Blot Analyses

Selected melanoma cells were maintained in 10-cm cell culture dishes and exposed to interferon alpha, beta, or gamma (same concentrations as above) for 30 minutes or 18 hours. Western blotting was performed as described previously (38). Primary antibodies included pJAK1 (Tyr1022/1023), pJAK2 (Tyr221), pSTAT1 (Tyr701), pSTAT3 (Tyr705), pSTAT5 (Tyr695), and their total proteins; PIAS1, IRF1, SOCS1, and GAPDH (all from Cell Signaling Technology). Antibodies were diluted to 1:1,000 ratio for each blot. Immunoreactivity was revealed with an ECL-Plus Kit (Amersham Biosciences Co.), using the ChemiDoc MP system (Bio-rad Laboratories).

Lentiviral Vector Production and Gene Transfer

Lentivirus production was performed by transient cotransfection of 293T cells (ATCC). The lentiviral vectors pLenti-C-mGFP and pLenti-C-JAK1-mGFP were purchased from Origen (cat# RC213878L2). In brief, T175 tissue culture flasks coated with poly-L-lysine (Sigma Aldrich) containing 6×10^6 293T cells were used for each transfection. The constructs required for the packaging of third-generation self-inactivating lentiviral vectors pLenti-C-mGFP and pLenti-C-JAK1-mGFP (60 μg), pMDLGg/p (39 μg), pRSV-REV (15 μg), and pMD.G (21 μg) were dissolved in water in a total volume of 2.7 mL. A total of 300 μL of 2.5 mol/L $CaCl_2$ (Sigma Aldrich) was added to the DNA mixture. A total of 2.8 mL of the DNA/$CaCl_2$ mix was added dropwise to 2.8 mL of 2× HBS buffer, pH 7.12 (280 nmol/L NaCl, 1.5 mmol/L Na_2HPO_4, 100 mmol/L HEPES). The DNA/$CaPO_4$ suspension was added to each flask and incubated in a 5% CO_2 incubator at 37°C overnight. The next morning, the medium was discarded, the cells were washed, and 15 mL DMEM with 10% FBS containing 20 mmol/L HEPES (Invitrogen) and 10 mmol/L sodium butyrate (Sigma Aldrich) was added, and the flask was incubated at 37°C for 8 to 12 hours. After that, the cells were washed once, and 10 mL fresh DMEM medium with 20 mmol/L HEPES was added onto the 293T cells, which were further incubated in a 5% CO_2 incubator at 37°C for 12 hours. The medium supernatants were then collected, filtered through 0.2 μmol/L filters, and cryopreserved at minus 80°C. Virus supernatant was added at different concentrations into 6-well plates containing 5×10^5 cells per well. Protamine sulphate (Sigma Aldrich) was added at a final concentration of 5 μg/mL, and the transduction plates were incubated at 37°C in 5% CO_2 overnight.

Whole-Exome Sequencing

Exon capture and library preparation were performed at the UCLA Clinical Microarray Core using the Roche Nimblegen SeqCap EZ Human Exome Library v3.0 targeting 65 Mb of genome. Paired-end sequencing (2 × 100 bp) was carried out on the HiSeq 2000 platform (Illumina) and sequences were aligned to the UCSC hg19 reference using BWA-mem (v0.7.9). Sequencing for tumors was performed to a target depth of 150× (actual min. 91×, max. 162×, mean 130×). Preprocessing followed the Genome Analysis Toolkit (GATK) Best Practices Workflow v3, including duplicate removal (PicardTools), indel realignment, and base quality score recalibration.

Somatic mutations were called by comparison to sequencing of matched normals for the PD1-treated whole-tumor patient samples. Methods were modified from ref. 39; specifically, the substitution the GATK-HaplotypeCaller (HC, v3.3) for the UnifiedGenotyper. gVCF outputs from GATK-HC for all 23 tumor/normal exomes, and cell lines M395 and M431, were jointly genotyped and submitted for variant quality score recalibration. Somatic variants were determined using one-sided Fisher exact test (P value cutoff ≤ 0.01) between tumor/normal pairs with depth >10 reads. Only high-confidence mutations were retained for final consideration, defined as those identified by at least two out of three programs [MuTect (v1.1.7; ref. 40), Varscan2 Somatic (v2.3.6; ref. 41), and the GATK-HC] for single nucleotide variants, and those called by both Varscan2 and the GATK-HC for insertions/deletions. Variants were annotated by Oncotator (42), with nonsynonymous mutations for mutational load being those classified as nonsense, missense, splice_site, or nonstop mutations, as well as frame_shift, in_frame_, or start_codon altering insertions/deletions. Adjusted variant allele frequency was calculated according to the following equation:

$$VAF\ adjusted = n_{mut}/CN_t = VAF*[1+(2*Stromal\ Fraction)/(Tumor\ Fraction*Local\ Copy\ Number)]$$

This is an algebraic rearrangement of the equation used in the clonal architecture analysis from McGranaham and colleagues (43) to calculate the fraction of mutated chromosomal copies while adjusting for the diluting contribution of stromal chromosomal copies. Local tumor copy number (CN_t) tumor fraction (purity, or p) and stromal fraction (1 − p) were produced by Sequenza (44), which uses both depth ratio and SNP minor B-allele frequencies to estimate tumor ploidy and percent tumor content, and perform allele-specific copy-number variation analysis.

PDJ amplification was considered tumor/normal depth ratio ≥ 2 standard deviations above length-weighted genome average. BAM files for the 16 colorectal cases were previously mapped to hg18, and sequencing and analysis were performed at Personal Genome Diagnostics. After preprocessing and somatic variant calling, positions were remapped to hg19 using the Ensembl Assembly Converter before annotation.

M431 and M395 were compared with matched normal samples, the other 47 cell lines lacked a paired normal sample. For detection of potential *JAK1* or *JAK2* mutations, variants were detected using the Haplotype Caller, noted for membership in dbSNP 146 and allele frequency from the 1000 Genomes project, and confirmed by visual inspection with the Integrated Genomics Viewer.

RT-PCR

Forward 5′-AACCTTCTCACCAGGATGCG-3′ and reverse 5′-CTCAGCACGTACATCCCCTC-3′ primers were designed to perform RT-PCR (700 base pair of target PCR product to cover the P429 region of the JAK1 protein) on the M431 cell line. Total RNA was extracted by the *mir*Vana miRNA Isolation Kit, with phenols as per the manufacturer's protocol (Thermo Fischer Scientific). RT-PCR was performed by utilizing ThermoScript RT-PCR Systems (Thermo Fisher Scientific, cat# 11146-057). PCR product was subject to Sanger sequencing at the UCLA core facility.

TCGA Analysis

To determine the relevance of *JAK1* and *JAK2* alterations in a broader set of patients, we queried the TCGA skin cutaneous melanoma provisional dataset for the frequency of genetic and expression alterations in *JAK1* and *JAK2*. We then extended our query to the breast invasive carcinoma, prostate adenocarcinoma, lung adenocarcinoma, and colorectal adenocarcinoma provisional TCGA datasets. We then examined the association of various *JAK1* and *JAK2* alterations with overall survival for each dataset. The results are based upon data generated by the TCGA Research Network and made available through the NCI Genomic Data Commons and cBioPortal (45, 46).

The mutation annotation format (MAF) files containing *JAK1* and *JAK2* mutations in the TCGA datasets were obtained from the

Genomic Data Commons. In addition, mutations, putative copy-number alterations, mRNA expression, protein expression, and survival data were obtained using the cBioPortal resource. The putative copy-number alterations (homodeletion events, in particular) available in cBioPortal were obtained from the TCGA datasets using Genomic Identification of Significant Targets in Cancer (GISTIC; ref. 47). The mRNA expression data available in cBioPortal were obtained from the TCGA datasets using RNA-seq (RNA Seq V2 RSEM). Upregulation and downregulation of *JAK1* and *JAK2* mRNA expression were determined using an mRNA *z*-score cutoff of 2.0. Protein expression data available in cBioPortal were obtained from the TCGA dataset using RPPA, with a *z*-score threshold of 2.0.

Mutation data between the MAF files and data from cBioPortal were combined. Genetic and expression alterations were characterized in one of six categories: amplifications, homodeletions, single-nucleotide polymorphisms, truncating mutations (stop codons and frameshift insertions and deletions), mRNA or protein downregulation, and mRNA or protein upregulation. The frequency of *JAK1* and *JAK2* alterations was determined using combined data from the *.MAF file and cBioPortal. Kaplan–Meier survival curves were generated in R, using the "survminer" package and the "ggsurvplot" function. Overall survival was determined using log-rank analysis.

Statistical Analysis

Statistical comparisons were performed by the unpaired two-tailed Student *t* test (GraphPad Prism, version 6.0 for Windows). Mutational load was compared by unpaired two-sided Mann–Whitney test. R programming was utilized to generate arrow graphs of PD-L1/MHC class I expression upon interferon exposures and the CCLE *JAK1/2* mutation frequency graph.

Disclosure of Potential Conflicts of Interest

B. Chmielowski reports receiving speakers bureau honoraria from Genentech and Janssen and is a consultant/advisory board member for Merck, Genentech, Eisai, Immunocore, BMS, and Amgen. D.T. Le reports receiving commercial research grants from Merck and BMS, and is a consultant/advisory board member for Merck. D.M. Pardoll reports receiving a commercial research grant from BMS. L.A. Diaz has ownership interest (including patents) in Personal Genome Diagnostics and PapGene, and is a consultant/advisory board member for Merck and Cell Design labs. No potential conflicts of interest were disclosed by the other authors.

Authors' Contributions

Conception and design: D.S. Shin, A. Garcia-Diaz, R.S. Lo, B. Comin-Anduix, A. Ribas

Development of methodology: D.S. Shin, H. Escuin-Ordinas, A. Garcia-Diaz, S. Sandoval, D.Y. Torrejon, G. Abril-Rodriguez, L.A. Diaz, Jr, P.C. Tumeh, R.S. Lo, A. Ribas

Acquisition of data (provided animals, acquired and managed patients, provided facilities, etc.): D.S. Shin, J.M. Zaretsky, S. Hu-Lieskovan, D.Y. Torrejon, B. Chmielowski, G. Cherry, E. Seja, I.P. Shintaku, D.T. Le, D.M. Pardoll, L.A. Diaz, Jr, P.C. Tumeh, A. Ribas

Analysis and interpretation of data (e.g., statistical analysis, biostatistics, computational analysis): D.S. Shin, J.M. Zaretsky, S. Hu-Lieskovan, A. Kalbasi, C.S. Grasso, W. Hugo, N. Palaskas, B. Chmielowski, D.M. Pardoll, L.A. Diaz, Jr, P.C. Tumeh, T.G. Graeber, R.S. Lo, B. Comin-Anduix, A. Ribas

Writing, review, and/or revision of the manuscript: D.S. Shin, J.M. Zaretsky, S. Hu-Lieskovan, A. Kalbasi, C.S. Grasso, W. Hugo, D.Y. Torrejon, N. Palaskas, G. Parisi, B. Chmielowski, D.T. Le, D.M. Pardoll, P.C. Tumeh, T.G. Graeber, R.S. Lo, B. Comin-Anduix, A. Ribas

Administrative, technical, or material support (i.e., reporting or organizing data, constructing databases): H. Escuin-Ordinas, S. Sandoval, B. Berent-Maoz, P.C. Tumeh, A. Ribas

Study supervision: B. Comin-Anduix, A. Ribas

Other (assisted with Western blot work): A. Azhdam

Acknowledgments

We acknowledge the UCLA Translational Pathology Core Laboratory (TPCL); Rongqing Guo, Jia Pang, and Wang Li from UCLA for blood and biopsy processing; and Matt Klinman, Thinle Chodon, and Charles Ng for establishing some of the cell lines.

Grant Support

This study was funded in part by the NIH grants R35 CA197633 and P01 CA168585, the Parker Institute for Cancer Immunotherapy (PICI), the Dr. Robert Vigen Memorial Fund, the Ruby Family Fund, and the Garcia-Corsini Family Fund (to A. Ribas); and P01 CA168585, the Ressler Family Fund, the Samuels Family Fund, and the Grimaldi Family Fund (to A. Ribas and R.S. Lo). D.S. Shin was supported by the Oncology (5T32CA009297-30), Dermatology (5T32AR058921-05), and Tumor Immunology (5T32CA009120-39 and 4T32CA009120-40) training grants, a 2016 Conquer Cancer Foundation ASCO Young Investigator Award, and a Tower Cancer Research Foundation Grant. A. Ribas and D.M. Pardoll were supported by a Stand Up To Cancer – Cancer Research Institute Cancer Immunology Dream Team Translational Research Grant (SU2C-AACR-DT1012). Stand Up To Cancer is a program of the Entertainment Industry Foundation administered by the American Association for Cancer Research. J.M. Zaretsky is part of the UCLA Medical Scientist Training Program supported by NIH training grant GM08042. S. Hu-Lieskovan was supported by a Conquer Cancer Foundation ASCO Young Investigator Award, a Conquer Cancer Foundation ASCO Career Development Award, and a Tower Cancer Foundation Research Grant. G. Parisi was supported by the V Foundation-Gil Nickel Family Endowed Fellowship in Melanoma Research and also in part by the Division of Medical Oncology and Immunotherapy (University Hospital of Siena). T.G. Graeber was supported by an American Cancer Society Research Scholar Award (RSG-12-257-01-TBE), a Melanoma Research Alliance Established Investigator Award (20120279), and the National Center for Advancing Translational Sciences UCLA CTSI Grant UL1TR000124. R.S. Lo was supported by the Steven C. Gordon Family Foundation and the Wade F.B. Thompson/Cancer Research Institute CLIP Grant. L.A. Diaz and D.T. Le were funded from the Swim Across America Laboratory and the Commonwealth Fund at Johns Hopkins. W. Hugo was supported by the 2016 Milstein Research Scholar Award from the American Skin Association and by the 2016 AACR-Amgen, Inc., Fellowship in Clinical/Translational Cancer Research (16-40-11-HUGO).

Received November 1, 2016; revised November 28, 2016; accepted November 28, 2016; published OnlineFirst November 30, 2016.

REFERENCES

1. Herbst RS, Soria JC, Kowanetz M, Fine GD, Hamid O, Gordon MS, et al. Predictive correlates of response to the anti-PD-L1 antibody MPDL3280A in cancer patients. Nature 2014;515:563–7.
2. Powles T, Eder JP, Fine GD, Braiteh FS, Loriot Y, Cruz C, et al. MPDL3280A (anti-PD-L1) treatment leads to clinical activity in metastatic bladder cancer. Nature 2014;515:558–62.
3. Robert C, Long GV, Brady B, Dutriaux C, Maio M, Mortier L, et al. Nivolumab in previously untreated melanoma without BRAF mutation. N Engl J Med 2015;372:320–30.
4. Ansell SM, Lesokhin AM, Borrello I, Halwani A, Scott EC, Gutierrez M, et al. PD-1 blockade with nivolumab in relapsed or refractory Hodgkin's lymphoma. N Engl J Med 2015;372:311–9.

5. Robert C, Schachter J, Long GV, Arance A, Grob JJ, Mortier L, et al. Pembrolizumab versus ipilimumab in advanced melanoma. N Engl J Med 2015;372:2521–32.
6. Le DT, Uram JN, Wang H, Bartlett BR, Kemberling H, Eyring AD, et al. PD-1 blockade in tumors with mismatch-repair deficiency. N Engl J Med 2015;372:2509–20.
7. Garon EB, Rizvi NA, Hui R, Leighl N, Balmanoukian AS, Eder JP, et al. Pembrolizumab for the treatment of non-small-cell lung cancer. N Engl J Med 2015;372:2018–28.
8. Nghiem PT, Bhatia S, Lipson EJ, Kudchadkar RR, Miller NJ, Annamalai L, et al. PD-1 blockade with pembrolizumab in advanced merkel-cell carcinoma. N Engl J Med 2016;374:2542–52.
9. Pardoll DM.The blockade of immune checkpoints in cancer immunotherapy. Nature reviews Cancer 2012;12:252–64.
10. Taube JM, Anders RA, Young GD, Xu H, Sharma R, McMiller TL, et al. Colocalization of inflammatory response with B7-h1 expression in human melanocytic lesions supports an adaptive resistance mechanism of immune escape. Sci Transl Med 2012;4:127ra37.
11. Tumeh PC, Harview CL, Yearley JH, Shintaku IP, Taylor EJ, Robert L, et al. PD-1 blockade induces responses by inhibiting adaptive immune resistance. Nature 2014;515:568–71.
12. Ribas A. Adaptive immune resistance: how cancer protects from immune attack. Cancer Discov 2015;5:915–9.
13. Bach EA, Aguet M, Schreiber RD. The IFN gamma receptor: a paradigm for cytokine receptor signaling. Annu Rev Immunol 1997;15:563–91.
14. Zaretsky JM, Garcia-Diaz A, Shin DS, Escuin-Ordinas H, Hugo W, Hu-Lieskovan S, et al. Mutations associated with acquired resistance to PD-1 blockade in melanoma. N Engl J Med 2016;375:819–29.
15. Dunn GP, Bruce AT, Ikeda H, Old LJ, Schreiber RD. Cancer immunoediting: from immunosurveillance to tumor escape. Nat Immunol 2002;3:991–8.
16. Kaplan DH, Shankaran V, Dighe AS, Stockert E, Aguet M, Old LJ, et al. Demonstration of an interferon gamma-dependent tumor surveillance system in immunocompetent mice. Proc Natl Acad Sci U S A 1998;95:7556–61.
17. Mazzolini G, Narvaiza I, Martinez-Cruz LA, Arina A, Barajas M, Galofre JC, et al. Pancreatic cancer escape variants that evade immunogene therapy through loss of sensitivity to IFNgamma-induced apoptosis. Gene Ther 2003;10:1067–78.
18. Gao J, Shi LZ, Zhao H, Chen J, Xiong L, He Q, et al. Loss of IFN-gamma pathway genes in tumor cells as a mechanism of resistance to Anti-CTLA-4 Therapy. Cell 2016;167:397–404 e9.
19. Rizvi NA, Hellmann MD, Snyder A, Kvistborg P, Makarov V, Havel JJ, et al. Cancer immunology. Mutational landscape determines sensitivity to PD-1 blockade in non-small cell lung cancer. Science 2015;348:124–8.
20. Hugo W, Zaretsky JM, Sun L, Song C, Moreno BH, Hu-Lieskovan S, et al. Genomic and transcriptomic features of response to Anti-PD-1 therapy in metastatic melanoma. Cell 2016;165:35–44.
21. Rosenberg JE, Hoffman-Censits J, Powles T, van der Heijden MS, Balar AV, Necchi A, et al. Atezolizumab in patients with locally advanced and metastatic urothelial carcinoma who have progressed following treatment with platinum-based chemotherapy: a single-arm, multicentre, phase 2 trial. Lancet 2016;387:1909–20.
22. Rodig SJ, Meraz MA, White JM, Lampe PA, Riley JK, Arthur CD, et al. Disruption of the Jak1 gene demonstrates obligatory and nonredundant roles of the Jaks in cytokine-induced biologic responses. Cell 1998;93:373–83.
23. Muller M, Briscoe J, Laxton C, Guschin D, Ziemiecki A, Silvennoinen O, et al. The protein tyrosine kinase JAK1 complements defects in interferon-alpha/beta and -gamma signal transduction. Nature 1993;366:129–35.
24. Watling D, Guschin D, Muller M, Silvennoinen O, Witthuhn BA, Quelle FW, et al. Complementation by the protein tyrosine kinase JAK2 of a mutant cell line defective in the interferon-gamma signal transduction pathway. Nature 1993;366:166–70.
25. Barretina J, Caponigro G, Stransky N, Venkatesan K, Margolin AA, Kim S, et al. The cancer cell line encyclopedia enables predictive modelling of anticancer drug sensitivity. Nature 2012;483:603–7.
26. Ren Y, Zhang Y, Liu RZ, Fenstermacher DA, Wright KL, Teer JK, et al. JAK1 truncating mutations in gynecologic cancer define new role of cancer-associated protein tyrosine kinase aberrations. Scientific reports 2013;3:3042.
27. Platanias LC. Mechanisms of type-I- and type-II-interferon-mediated signalling. Nat Rev Immunol 2005;5:375–86.
28. Fish EN, Platanias LC. Interferon receptor signaling in malignancy: a network of cellular pathways defining biological outcomes. Mol Cancer Res 2014;12:1691–703.
29. Dunn GP, Sheehan KC, Old LJ, Schreiber RD. IFN unresponsiveness in LNCaP cells due to the lack of JAK1 gene expression. Cancer Res 2005;65:3447–53.
30. Spranger S, Bao R, Gajewski TF. Melanoma-intrinsic beta-catenin signalling prevents anti-tumour immunity. Nature 2015;523:231–5.
31. Sharma P, Allison JP. The future of immune checkpoint therapy. Science 2015;348:56–61.
32. Ribas A, Hamid O, Daud A, Hodi FS, Wolchok JD, Kefford R, et al. Association of pembrolizumab with tumor response and survival among patients with advanced melanoma. JAMA 2016;315:1600–9.
33. Nazarian R, Shi H, Wang Q, Kong X, Koya RC, Lee H, et al. Melanomas acquire resistance to B-RAF(V600E) inhibition by RTK or N-RAS upregulation. Nature 2010;468:973–7.
34. Atefi M, Avramis E, Lassen A, Wong DJ, Robert L, Foulad D, et al. Effects of MAPK and PI3K Pathways on PD-L1 expression in melanoma. Clin Cancer Res 2014;20:3446–57.
35. Wong DJ, Robert L, Atefi MS, Lassen A, Avarappatt G, Cerniglia M, et al. Antitumor activity of the ERK inhibitor SCH722984 against BRAF mutant, NRAS mutant and wild-type melanoma. Mol Cancer 2014;13:194.
36. Wolchok JD, Hoos A, O'Day S, Weber JS, Hamid O, Lebbe C, et al. Guidelines for the evaluation of immune therapy activity in solid tumors: immune-related response criteria. Clin Cancer Res 2009;15:7412–20.
37. Kotecha N, Krutzik PO, Irish JM. Web-based analysis and publication of flow cytometry experiments. Current protocols in cytometry/editorial board, J Paul Robinson managing editor [et al] 2010;Chapter 10:Unit10 7.
38. Escuin-Ordinas H, Atefi M, Fu Y, Cass A, Ng C, Huang RR, et al. COX-2 inhibition prevents the appearance of cutaneous squamous cell carcinomas accelerated by BRAF inhibitors. Mol Oncol 2014;8:250–60.
39. Shi H, Hugo W, Kong X, Hong A, Koya RC, Moriceau G, et al. Acquired resistance and clonal evolution in melanoma during BRAF inhibitor therapy. Cancer Discov 2014;4:80–93.
40. Cibulskis K, Lawrence MS, Carter SL, Sivachenko A, Jaffe D, Sougnez C, et al. Sensitive detection of somatic point mutations in impure and heterogeneous cancer samples. Nat Biotechnol 2013;31:213–9.
41. Koboldt DC, Zhang Q, Larson DE, Shen D, McLellan MD, Lin L, et al. VarScan 2: somatic mutation and copy number alteration discovery in cancer by exome sequencing. Genome research 2012;22:568–76.
42. Ramos AH, Lichtenstein L, Gupta M, Lawrence MS, Pugh TJ, Saksena G, et al. Oncotator: cancer variant annotation tool. Human mutation 2015;36:E2423–9.
43. McGranahan N, Furness AJ, Rosenthal R, Ramskov S, Lyngaa R, Saini SK, et al. Clonal neoantigens elicit T cell immunoreactivity and sensitivity to immune checkpoint blockade. Science 2016;351:1463–9.
44. Favero F, Joshi T, Marquard AM, Birkbak NJ, Krzystanek M, Li Q, et al. Sequenza: allele-specific copy number and mutation profiles from tumor sequencing data. Ann Oncol 2015;26:64–70.
45. Cerami E, Gao J, Dogrusoz U, Gross BE, Sumer SO, Aksoy BA, et al. The cBio cancer genomics portal: an open platform for exploring multidimensional cancer genomics data. Cancer Discov 2012;2:401–4.
46. Gao J, Aksoy BA, Dogrusoz U, Dresdner G, Gross B, Sumer SO, et al. Integrative analysis of complex cancer genomics and clinical profiles using the cBioPortal. Sci Signal 2013;6:pl1.
47. Beroukhim R, Getz G, Nghiemphu L, Barretina J, Hsueh T, Linhart D, et al. Assessing the significance of chromosomal aberrations in cancer: methodology and application to glioma. Proc Natl Acad Sci U S A 2007;104:20007–12.

Chapter 4:

Interferon Receptor Signaling Pathways Regulating PD-L1 and PD-L2 Expression

Cell Reports 19, 1189-1201, 2017

Interferon Receptor Signaling Pathways Regulating PD-L1 and PD-L2 Expression

Angel Garcia-Diaz,[1,*] Daniel Sanghoon Shin,[1] Blanca Homet Moreno,[1,2] Justin Saco,[1] Helena Escuin-Ordinas,[1] Gabriel Abril Rodriguez,[1] Jesse M. Zaretsky,[1] Lu Sun,[3] Willy Hugo,[3] Xiaoyan Wang,[4] Giulia Parisi,[1] Cristina Puig Saus,[1] Davis Y. Torrejon,[1] Thomas G. Graeber,[5,6,7] Begonya Comin-Anduix,[7,8] Siwen Hu-Lieskovan,[1] Robert Damoiseaux,[5,9] Roger S. Lo,[3,5,7] and Antoni Ribas[1,5,7,8,10,*]

[1]Division of Hematology-Oncology, Department of Medicine, David Geffen School of Medicine, University of California, Los Angeles (UCLA), Los Angeles, CA 90095, USA

[2]Division of Translational Oncology, Carlos III Health Institute, 28029 Madrid, Spain
[3]Division of Dermatology, Department of Medicine, UCLA, Los Angeles, CA 90095, USA
[4]Statistics Core, Department of Medicine, UCLA, Los Angeles, CA 90095, USA
[5]Department of Molecular and Medical Pharmacology, UCLA, Los Angeles, CA 90095, USA
[6]Crump Institute for Molecular Imaging, UCLA, Los Angeles, CA 90095, USA
[7]Jonsson Comprehensive Cancer Center, UCLA, Los Angeles, CA 90095, USA
[8]Division of Surgical Oncology, Department of Surgery, UCLA, Los Angeles, CA 90095, USA
[9]California NanoSystems Institute, UCLA, Los Angeles, CA 90095, USA
[10]Lead Contact

*Correspondence: agdiaz@ipb.csic.es (A.G.-D.), aribas@mednet.ucla.edu (A.R.)
http://dx.doi.org/10.1016/j.celrep.2017.04.031

SUMMARY

PD-L1 and PD-L2 are ligands for the PD-1 immune inhibiting checkpoint that can be induced in tumors by interferon exposure, leading to immune evasion. This process is important for immunotherapy based on PD-1 blockade. We examined the specific molecules involved in interferon-induced signaling that regulates PD-L1 and PD-L2 expression in melanoma cells. These studies revealed that the interferon-gamma-JAK1/JAK2-STAT1/STAT2/STAT3-IRF1 axis primarily regulates PD-L1 expression, with IRF1 binding to its promoter. PD-L2 responded equally to interferon beta and gamma and is regulated through both IRF1 and STAT3, which bind to the PD-L2 promoter. Analysis of biopsy specimens from patients with melanoma confirmed interferon signature enrichment and upregulation of gene targets for STAT1/STAT2/STAT3 and IRF1 in anti-PD-1-responding tumors. Therefore, these studies map the signaling pathway of interferon-gamma-inducible PD-1 ligand expression.

INTRODUCTION

The signaling pathway resulting in adaptive expression of PD-L1 and PD-L2 upon exposure to interferons is of high importance for the clinical development of PD-1 blockade therapies for cancer. Upon tumor antigen recognition by T cells, the released interferons trigger the inducible expression of PD-L1 by cancer cells or other tumor microenvironment cells, thereby inhibiting the antitumor immune response in a process known as adaptive immune resistance. Adaptive immune resistance allows the specific inhibition of T cell recognition of cancer while it spares the rest of the immune responses to other antigens, avoiding a systemic immune-suppressive state (Pardoll, 2012; Ribas, 2015). Interferons were first described in the 1950s as agents that interfere with viral replication (Isaacs and Lindenmann, 1957), and signaling from the interferon receptors has been well characterized (Domanski and Colamonici, 1996; Novick et al., 1994; Velazquez et al., 1992). Janus kinase (JAK) and signal transducer and activators of transcription (STAT) are the main signaling pathways mediating interferon-induced gene expression (Darnell et al., 1994; Velazquez et al., 1992) and resulting in the activation of interferon-stimulated response elements (ISREs) (Darnell et al., 1994; Kessler et al., 1988) and gamma interferon activation sites (GASs) (Decker et al., 1991; Lew et al., 1991). There is a renewed interest in interferon signaling given its key role in regulating PD-1 ligand expression and emerging evidence of its role in primary and acquired resistance to immune checkpoint blockade therapy for cancer (Shin et al., 2017; Gao et al., 2016; Zaretsky et al., 2016).

Type I interferons (alpha, beta, and omega) bind to interferon receptor type 1, which is composed of two subunits, IFNAR1 and IFNAR2, and they signal through JAK1 and TYK2, which phosphorylate STAT1, STAT2, and STAT3, as well as other STAT family members, depending on the cellular context. Activated phosphorylated STAT1 (pSTAT1) typically dimerizes with pSTAT2 to form the ISGF3 complex together with the interferon regulatory factor 9 (IRF9) (Smith et al., 2005). This complex binds at the genomic level to the ISRE sequences to control a long list of interferon-induced genes (Friedman and Stark, 1985). Type I interferons can also trigger phosphorylation and subsequent activation of homo- or hetero-dimers of STAT1, STAT3, STAT4, STAT5, and STAT6.

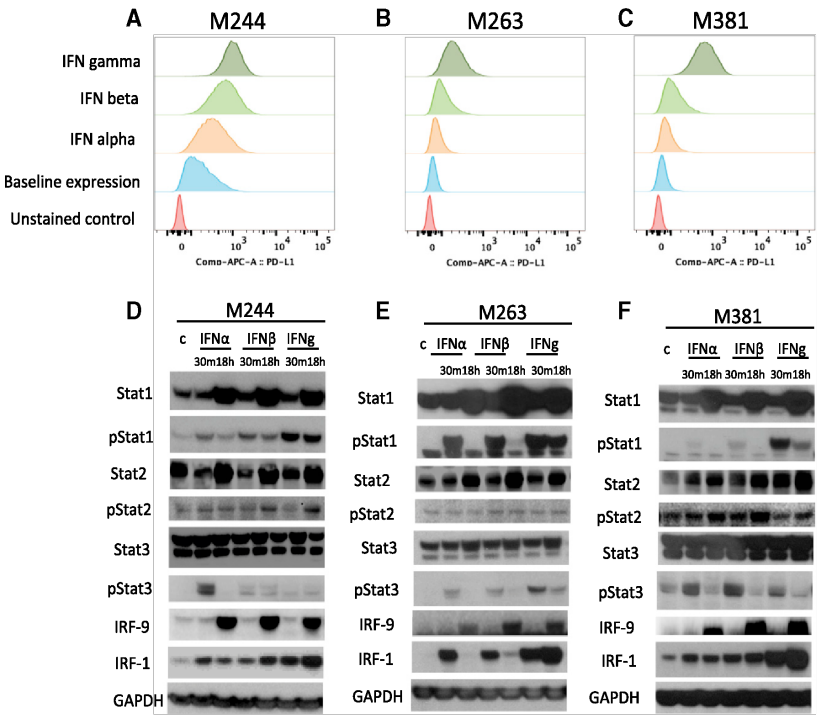

Figure 1. Induction of PD-L1 by Interferon Alpha, Beta, and Gamma

(A–C) Flow cytometry analysis of PD-L1 surface expression upon interferon treatment in the human melanoma cell lines M244 (A), M263 (B), and M381 (C) exposed to interferon alpha, beta, or gamma for 18 hr. Histograms represent changes in mean fluorescence intensity by flow cytometry compared to baseline.

(D–F) Western blot analysis of interferon receptor signaling proteins in M244 (D), M263 (E), and M381 (F), including a set of proteins involved in interferon signaling pathways. Basal and activated (phosphorylated) states of the proteins are included to compare the induction trough these different mediators. The first lane of each panel represents untreated control cells. Each cell line was exposed 30 min or 18 hr with interferon alpha, beta, or gamma, respectively.

Type II interferon gamma binds to the interferon gamma receptor, leading to phosphorylation of JAK1 and JAK2, with receptor phosphorylation followed by receptor attachment and phosphorylation of STAT1 in most cells and STAT3 in some cells. The activated dimers then accumulate in the nucleus to act as transcription factors (Schroder et al., 2004; Aaronson and Horvath, 2002). There, they bind to the GAS elements present in most interferon gamma inducible genes, such as the IRF1 gene (Platanias, 2005). Negative regulators of interferon signaling, such as the suppressor of cytokine signaling protein family (SOCS; mostly SOCS1 and SOCS3) are involved in negative feedback regulation of cytokines that signal mainly through JAK2 binding, thereby modulating the activity of both STAT1 and STAT3 (Qing and Stark, 2004).

PD-1 has two known ligands, PD-L1 (CD274 or B7-H1) and PD-L2 (CD273 or B7-DC), and both have been reported to be expressed on cell surfaces upon exposure to interferons, in particular interferon gamma (Kim et al., 2005; Dong et al., 2002; Tseng et al., 2001). Evidence has been generated for the role of STAT1 and STAT3, as well as the downstream transcription factor IRF1, in regulating the surface expression of PD-L1 upon interferon gamma exposure (Lee et al., 2006; Loke and Allison, 2003). However, there has not been a systematic analysis of the molecules involved in this signal transduction pathway. Given the importance of this process, we undertook a detailed analysis of molecules responsible for interferon receptor signaling and mapping of the PD-L1 and PD-L2 promoters to define the specific signaling that regulates their expression. Our studies demonstrate the key roles of signaling through the interferon-gamma-JAK1/JAK2-STAT1/STAT2/STAT3-IRF1 axis, resulting in binding of the IRF1 transcription factor to the PD-L1 promoter and weaker binding to the PD-L2 promoter, which is also regulated by STAT3 in melanoma cells.

RESULTS

Interferon Receptor Signal Transduction Pathway Regulating PD-L1 Expression

We analyzed the interferon-inducible surface expression of PD-L1 in three human melanoma cell lines, M244, M263, and M381, using flow cytometry (Figures 1A–1C). In all three cell lines, upregulation of PD-L1 was strongest with interferon gamma. Western blot analysis in the three cell lines (Figures 1D–1F) revealed the induction of proteins and phosphorylated proteins involved in the JAK-STAT signaling pathway, including STAT1/pSTAT1, STAT2/pSTAT2, and STAT3/pSTAT3 and increased expression of IRF1 and IRF9. Induction of pSTAT1 and IRF1 was consistently stronger upon interferon gamma exposure compared to interferon alpha or beta exposure. pSTAT1, pSTAT3, and IRF9 induction was also observed through interferon alpha and beta, consistent with the canonical type I interferon signaling pathway (Ivashkiv and Donlin, 2014). We also analyzed interferon receptor mRNA expression in these three lines. Expression of interferon receptor type II was higher than that of interferon receptor type I (Figure S1), which could explain in part the increased sensitivity of these cells lines to interferon gamma. Interestingly, IFNGR1 expression correlated with the PD-L1 induction under interferon gamma stimulation.

Interferon Receptor Pathway shRNA Screen to Define Signaling Molecules Involved in PD-L1 Regulation

To analyze PD-L1 regulation upon interferon gamma exposure, we generated reporter cell lines with luciferase expression downstream of the PD-L1 promoter to be used in a small hairpin RNA (shRNA) screen. The human melanoma cell lines M244, M263, and M381 were infected with a lentiviral vector carrying the PD-L1 promoter driving a polycistronic reporter cassette expressing both a DsRed-expressDR protein and firefly luciferase linked by a 2A picornavirus sequence (Figure 2A). This vector also included an elongation factor alpha promoter (EF1a)-BSD cassette as selectable marker. Cells were also transduced with

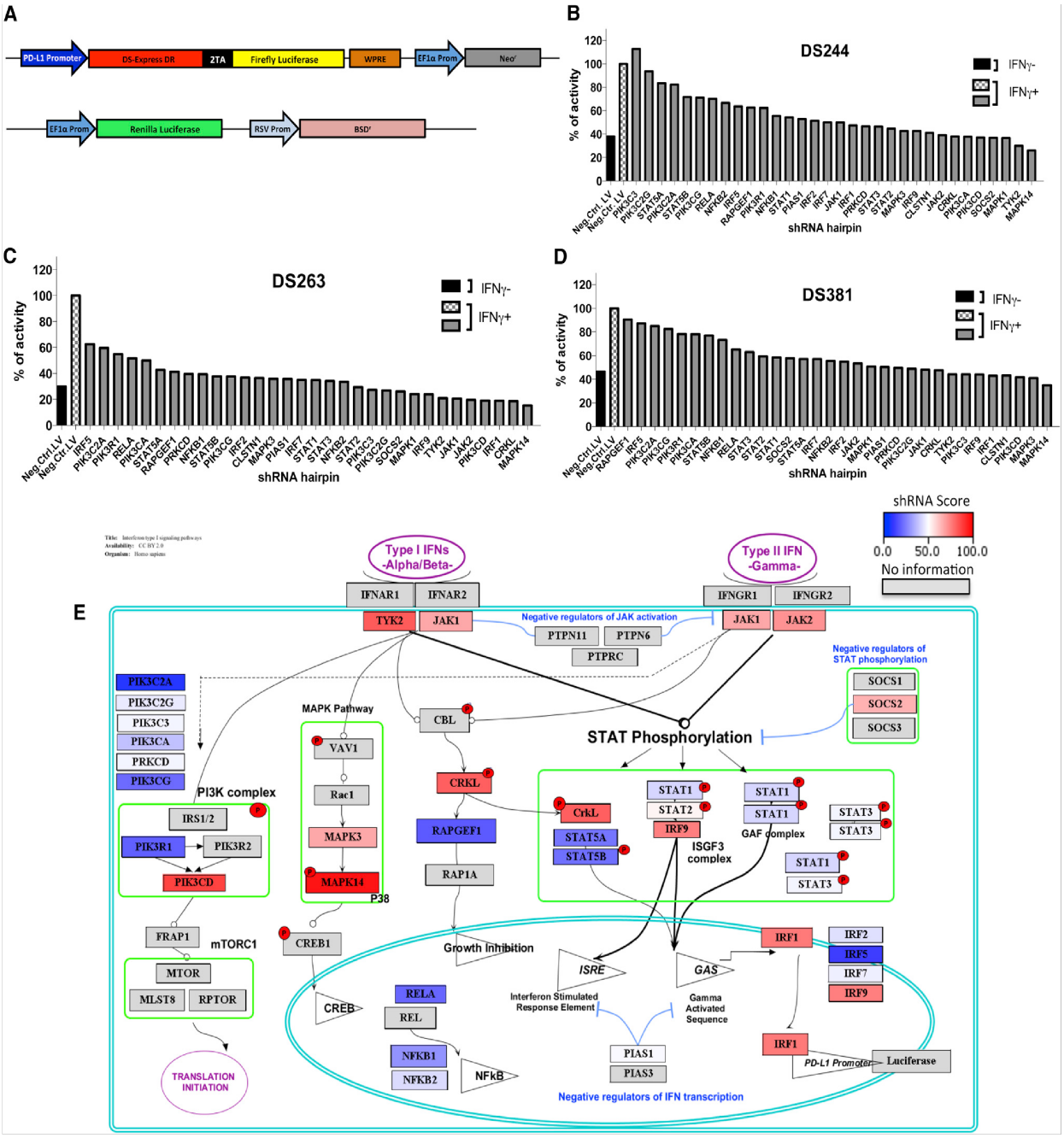

Figure 2. Effects on PD-L1 Reporter Expression upon shRNA Silencing of 33 Genes Involved in the Interferon Signaling Pathway

(A) Schematic representation of the PD-L1Prom-DSRed-FireflyLuciferase/Neo and EF1AProm-Renilla luciferase/RSV-BSD constructs used to generate the reporter melanoma cell lines. Reporter cells contain the PD-L1 promoter driving the expression of a DSRedDR-T2A-Firefly luciferase cassette and also an EF1-alpha promoter driving the Renilla luciferase gene used for normalization.

(B–D) Normalized luciferase reporter expression of each cell line, M244 (B), M263 (C), and M381 (D), transduced with different sets of lentiviral shRNA hairpins. Black and checkered white bars represent the cells transduced with a lentiviral control containing no shRNA, with (black) or without (checkered) interferon gamma treatment. Gray bars represent the expression level of the cells transduced with a set of lentiviral shRNA hairpins with interferon gamma treatment to compare changes upon the interferon gamma induction of PD-L1 expression. Results are represented as a percentage of luciferase expression compared with the interferon-gamma-treated negative control.

(E) Schematic representation of the interferon receptor signaling pathway depicting the hits taking into account the redundant siRNA/shRNA activity (RSA) score obtained for each factor in the three reporter cell lines. Color heatmap represents the summed rank score, with red indicating the greatest impact on interferon-gamma-induced PD-L1 reporter activity and dark blue the least impact. Spatial orientation places each gene in the context of its signaling pathway.

a second vector used for assay signal normalization containing a constitutively expressed EF1-alpha promoter driving Renilla luciferase and RSV-Neo as selectable marker. After transduction and antibiotic selection, double stably transduced melanoma cell lines were validated for interferon gamma response and reporter expression (Figure S2).

In order to screen for individual targets known or anticipated to be involved in interferon receptor signaling and related pathways, we selected 180 shRNA hairpins targeting 33 genes to carry out the shRNA screen of known interferon receptor pathway signaling molecules. The doubly transduced reporter cell lines were then additionally transduced with the 180 shRNA lentiviral vectors. A non-hairpin-containing vector was used as a negative control. Transduced cells were induced for 8 hr with 100 U/mL interferon gamma, and firefly luciferase expression was normalized to the Renilla luciferase signal and the percentage of transduction of each virus. A redundant small interfering RNA (siRNA) activity (RSA) statistical analysis was performed to compensate for the effects of nonfunctional hairpins.

Inhibition of several genes involved in both type I and type II interferon signaling strongly affected PD-L1 reporter expression (Figures 2B–2D). We calculated the percentage of inhibition for each hairpin, and we assigned a score depending on the effect of each silenced gene on the reporter expression in the three different cell lines. We then rank listed the silenced genes that had the strongest global effect in inhibiting PD-L1 expression. Each gene was then represented in a color heatmap in a schematic representation of the interferon receptor signaling pathways (Figure 2E). The data suggest that there are two converging bottlenecks in the signaling pathway: at the upstream tyrosine kinases JAK1, JAK2, and TYK2 and at the downstream transcription factors IRF1 and IRF9. In between, silencing of STAT1, STAT2, or STAT3 had a moderate effect on the PD-L1 reporter expression, suggesting redundancy in the signaling at this level. There was a strong effect in PD-L1 expression when silencing MAK14 (p38), CRKL, and phosphatidylinositol 3-kinase (PI3K), which have been previously reported to be involved in modulating interferon signaling pathways (Platanias et al., 1999). However, when we knocked out these three genes using CRISPR/Cas9, we could not detect a detrimental effect on PD-L1 expression upon interferon gamma exposure (Figure S3); therefore, we believe these were off-target effects of the shRNA screen. We finally confirmed the role of JAK1, JAK2, STAT1, and IRF1 silencing in inhibiting PD-L1 expression using M381 cells stably transduced with shRNAs and analyzed by qPCR (Figure S4), and for JAK1 and JAK2, we have previously reported that their CRISPR/Cas9 knockout results in loss of PD-L1 upregulation upon interferon gamma exposure (Zaretsky et al., 2016).

IRF1 Is the Key Factor for PD-L1 Promoter Function

Analysis of the PD-L1 promoter sequence using the MotEvo algorithm (Pachkov et al., 2007) revealed putative binding sites for STAT1/STAT3, STAT2/STAT5, and IRF1 (Figure 3A). We performed site-directed mutagenesis to delete the STAT1/STAT3, STAT2/STAT5, and IRF1 putative binding sites in a PD-L1 promoter firefly luciferase reporter plasmid. Transiently transfected M381 cells were exposed to interferon gamma, and luciferase activity was quantitated (Figure 3B). Deletion of the IRF1 site dramatically decreased the expression of the PD-L1 reporter construct upon interferon gamma induction. Deletion of the putative STAT2/STAT5 site also affected interferon-gamma-induced luciferase expression, but at a lower level than IRF1. It should be noted that the proximity of these two sequences might be affecting the same activity. On the other hand, deletion of the STAT1/STAT3 putative binding site resulted in strong activation of the PD-L1 reporter upon interferon gamma induction. These data suggest the binding of a putative repressor factor at this level or the presence of genomic elements as silencers or insulator/boundary elements that could block the action of distal enhancers.

In order to confirm the binding of the predicted factors to the specific sequence sites, we carried out chromatin immunoprecipitation (ChIP) assays at the PD-L1 promoter. We confirmed IRF1 binding to the PD-L1 promoter in an interferon-gamma-inducible manner at a level that was much stronger than the positive control HLA-B promoter (Figure 3C). We also detected IRF1 binding to the PD-L1 promoter upon interferon beta exposure but at lower rates than under interferon gamma treatment (Figure S5A). ChIP analysis using STAT3 antibodies did not reveal direct binding of this factor at the PD-L1 promoter in M381 melanoma cells (Figure S5B), which is different from the reported binding of STAT3 to the PD-L1 promoter in a chimeric nucleophosmin (NPM)/anaplastic lymphoma kinase (ALK) T cell lymphoma (ALK-TCL) (Marzec et al., 2008).

The JAK1/JAK2-STAT1/STAT2/STAT3-IRF1 Axis Controls PD-1 Ligand and Antigen-Presenting Machinery upon Interferon Gamma Exposure

In order to analyze the relevant genes activated at transcriptional level by interferon gamma, we analyzed transcripts of 750 immune-related genes that capture the great majority of known interferon response genes (Table S2). Upon interferon gamma exposure of the three melanoma cell lines, there was strong activation of PD-L1 transcripts compared with PD-L2 (Figures 4A–4C). We documented a very repetitive pattern of activation of JAK2, STAT1, STAT2, STAT3, IRF1, IRF9, and SOCS1 transcription upon interferon gamma stimulation. All of these molecules are known to be involved in the JAK-STAT signaling pathway downstream of the interferon gamma receptor (Aaronson and Horvath, 2002).

We also observed upregulation of a second group of genes (light-blue labels) related to immunoregulation and the antigen processing-presentation machinery through major histocompatibility complex (MHC) class I, including the transporters associated with antigen processing 1 and 2 (TAP1/TAP2) and the proteasome subunit beta types 8, 9, and 10 (PSMB9/LMP2, PSMB8/LMP7, and PSMB10/LMP10). Most of these genes are also known to be regulated by interferon gamma. TAP1 and PSMB9 share a bidirectional promoter activated through the interferon gamma-STAT1-IRF1 axis (Saha et al., 2010), and they work at the antigen-processing and antigen-presentation level through the immunoproteasome.

In order to confirm the importance of the JAK1/JAK2-STAT1/STAT3-IRF1 axis, we analyzed the expression profile induced by

Figure 3. Transient Luciferase Reporter Assays and ChIP Analysis for the PD-L1 Promoter in M381 Melanoma Cells

(A) Sequence of the PD-L1 promoter showing the position of the most representative putative binding sites of the promoter, STAT1/STAT3, STAT2/STAT5, and IRF1.

(B) PD-L1 promoter transient reporter assay including deletions of the putative binding sites. Results are represented as normalized relative luciferase units (RLUs).

(C) ChIP assay in M381 cells at the PD-L1 promoter (gray), the HLA-B promoter as a positive control (white), and the human tRNA-Leu anti-codon (TAG) as irrelevant sequence for IRF1 binding (negative control). Results are represented as percent enrichment relative to input. Asterisks denote significance in an unpaired t test (*$p < 0.005$, **$p < 0.001$), and error bars denote SD.

interferon gamma in three additional human melanoma cell lines with altered interferon receptor signaling (Figures 4D–4F). M368 has a *JAK2* loss-of-function mutation and M395 has a *JAK1* loss-of-function mutation, and we tested the effect of pharmacological JAK2 inhibition in M233, which is a good interferon gamma responder cell line (Shin et al., 2015, 2017). Interferon-related gene expression was tested in each cell line with or without interferon gamma exposure, and M233 was treated with or without co-incubation with the JAK2 inhibitor CEP33779 (Stump et al., 2011).

The *JAK1* mutated M395 cell line was strongly affected and dramatically failed to upregulate most of the previously seen interferon-inducible genes, such as JAK2, STAT1, STAT3, IRF1, PD-L1, and PD-L2, although it still conserved some degree of interferon gamma activation for some genes. The *JAK2* mutated M368 cell line presented a complete loss of the interferon gamma induction of the JAK-STAT genes, IRF1, and both PD-1 ligands. The antigen-presentation-related group of genes had equally flat responses to interferon gamma. To confirm the critical role of JAK2 in regulating interferon response, we treated the good responder M233 with the JAK2 inhibitor CEP-33779, which led to a downregulation of STAT3, IRF1, and the two PD-1 ligands, as well as some of the antigen-presentation-related group of genes, such as TAP1 and TAP2. Other interesting genes that were not induced are the chemokine CXCL10 and the interferon-inducible metabolic immune suppressor indoleamine 2,3-dioxygenase-1 (IDO1). These results confirm the importance of the JAK1/JAK2-STAT1/STAT2/STAT3-IRF1 axis in the PD-L1 induction upon interferon gamma exposure.

PD-L1 and PD-L2 Differential Regulation

Given the observations of different regulation of PD-L2 compared to PD-L1, we extended our studies to the PD-L2 promoter function and expression pattern. Flow cytometry analysis of

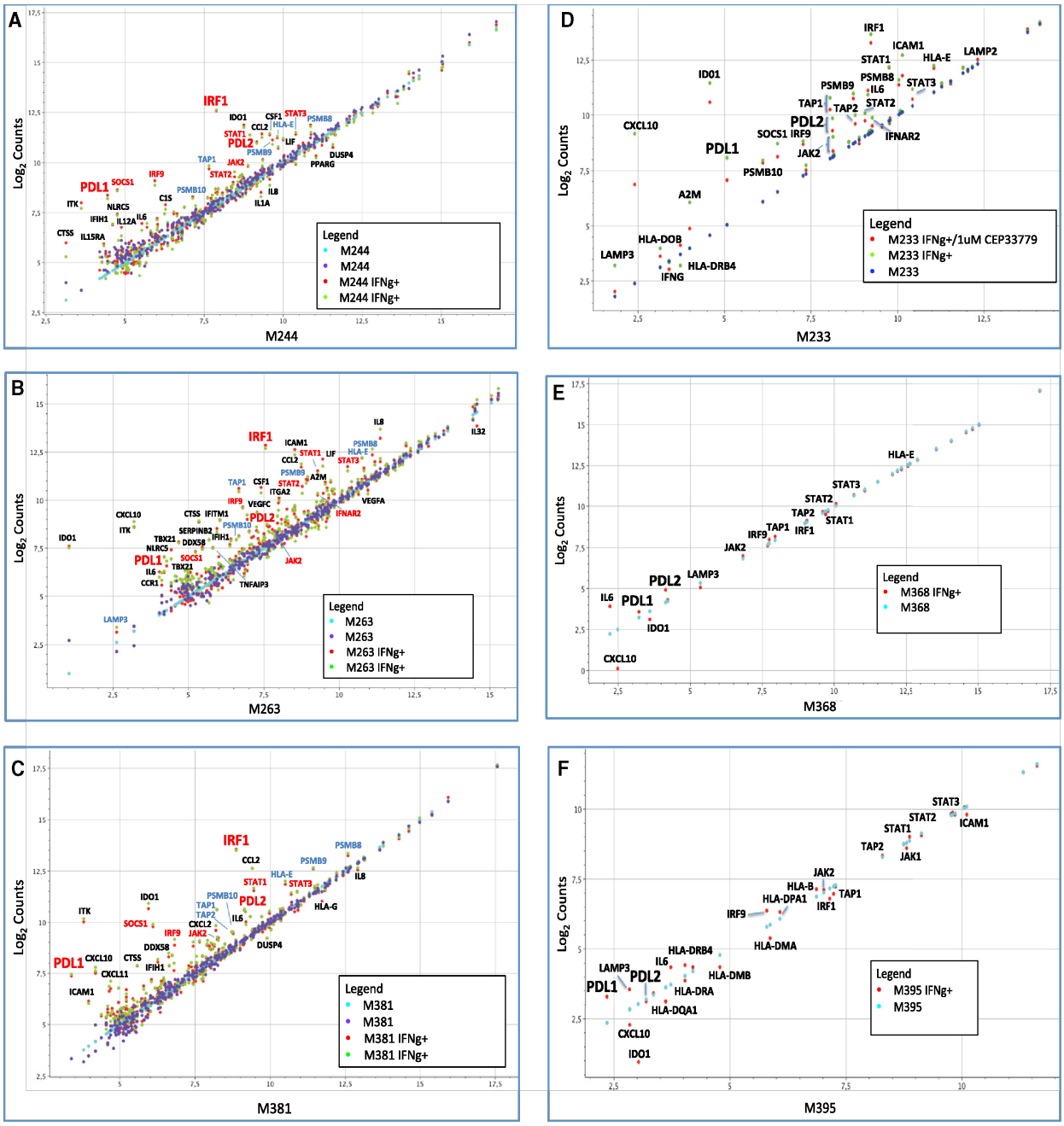

Figure 4. Selected mRNA Expression Profiling of Interferon-Gamma-Induced Genes

(A–C) Changes in selected gene expression upon interferon gamma exposure in three melanoma cell lines: M244 (A), M263 (B), and M381 (C). Purple and blue dots represent the expression level of the transcripts at basal level in two different biological duplicates (untreated cells), and red and green dots represent the expression level of the transcripts after 3 hr of interferon gamma treatment.

(D) Expression profile analysis of the good interferon gamma responder M233 cell line using the JAK2-specific inhibitor CEP33779. Dark blue dots represent untreated cells, green dots represent interferon-gamma-treated cells, and red dots represent cells treated with the JAK2 inhibitor CEP-33779 and interferon gamma. Data are presented as normalized counts (log2) of each transcript.

(E) Same analysis of the *JAK2* mutant cell line M368 with (red) or without (light blue) interferon gamma treatment.

(F) Expression profile of the *JAK1* mutant cell line M395 with (red) or without (light blue) interferon gamma treatment.

PD-L2 surface expression (Figures 5A–5C) revealed similar or even stronger effect of interferon beta, compared to interferon gamma, in two of the three analyzed cell lines, suggesting a shared role of type I and II interferon signaling and differential regulation for the PD-1 ligands, as previously reported in other cell types (Loke and Allison, 2003). Because the expression of interferon type I receptors is lower than that of type II receptors in all the analyzed cell lines, there must be contribution of

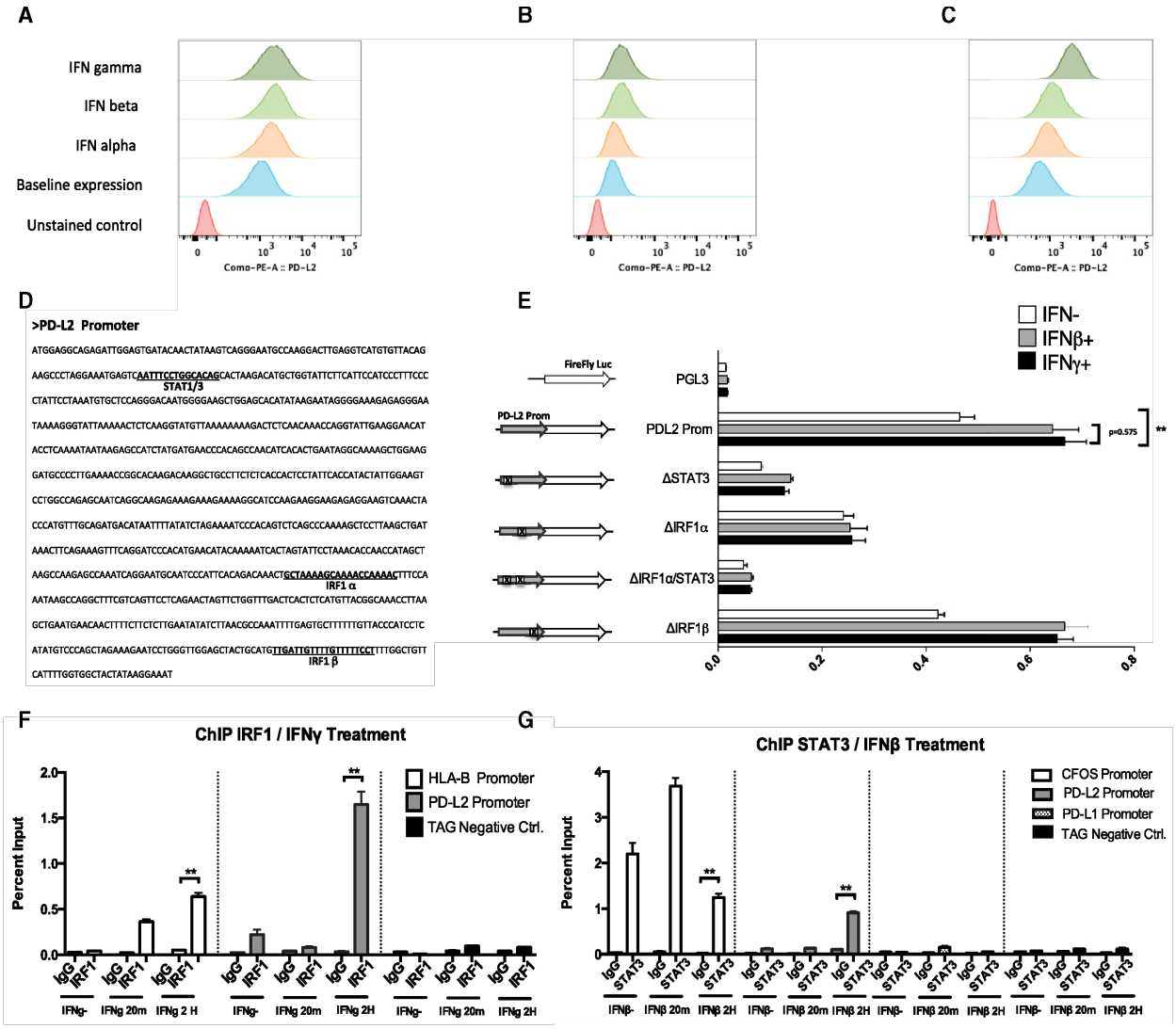

Figure 5. PD-L2 Expression and Promoter Function Analysis

(A–C) Flow cytometry analysis of PD-L2 surface expression upon interferon treatment in M244 (A), M263 (B), and M381 (C).

(D) Sequence of the PD-L2 promoter and position of the putative transcription factor binding sites.

(E) Transient reporter assay including deletions of STAT1/STAT3, IRF1, or double mutations for the putative binding sites. Analysis was performed in untreated cells (white bars) and under interferon beta (gray bars) and interferon gamma exposure (black bars).

(F) ChIP assay using IRF1 antibody in interferon-gamma-treated cells, including primers for the PD-L2 promoter (gray), HLA-B promoter as positive control (white), and TAG gene (black) as an irrelevant sequence for IRF1 binding.

(G) ChIP assay using STAT3 antibody in interferon-beta-treated cells, including primers for the C-FOS promoter as a positive control (white), the PD-L2 promoter (gray), the PD-L1 promoter (checkered), and TAG gene (black) as an irrelevant sequence for STAT3 binding.

Asterisks denote significance in an unpaired t test (*$p < 0.05$, **$p < 0.005$, ***$p < 0.001$), and error bars denote SD.

downstream elements to explain the similar or higher expression of PD-L2 in M244 and M263 under interferon beta exposure compared to interferon gamma exposure.

PD-L1 and PD-L2 are paralog genes, and their promoters share a similar architecture in terms of putative binding sites. We generated PD-L2 luciferase reporter constructs with specific deletions in STAT1/STAT3 and two IRF1 putative binding sites (α and β) (Figure 5D). First, we checked that PD-L2 promoter behaved very similar under interferon beta or gamma exposure (no statistically significant differences) in M381 and M244 cells (Figures 5E and S6), and then we performed reporter truncation assays comparing the PD-L2 reporter expression under interferon beta and gamma exposure or in untreated cells.

All mutations had a very similar effect on the PD-L2 promoter function independently of the type of interferon stimulation. Deletion of the IRF1α putative binding site decreased PD-L2 reporter expression upon interferon gamma induction, but at lower rates than on the PD-L1 promoter compared to the intact promoter (compare Figures 3B and 5E). In contrast, IRF1β site deletion had no effect on PD-L2 expression. Disruption of the

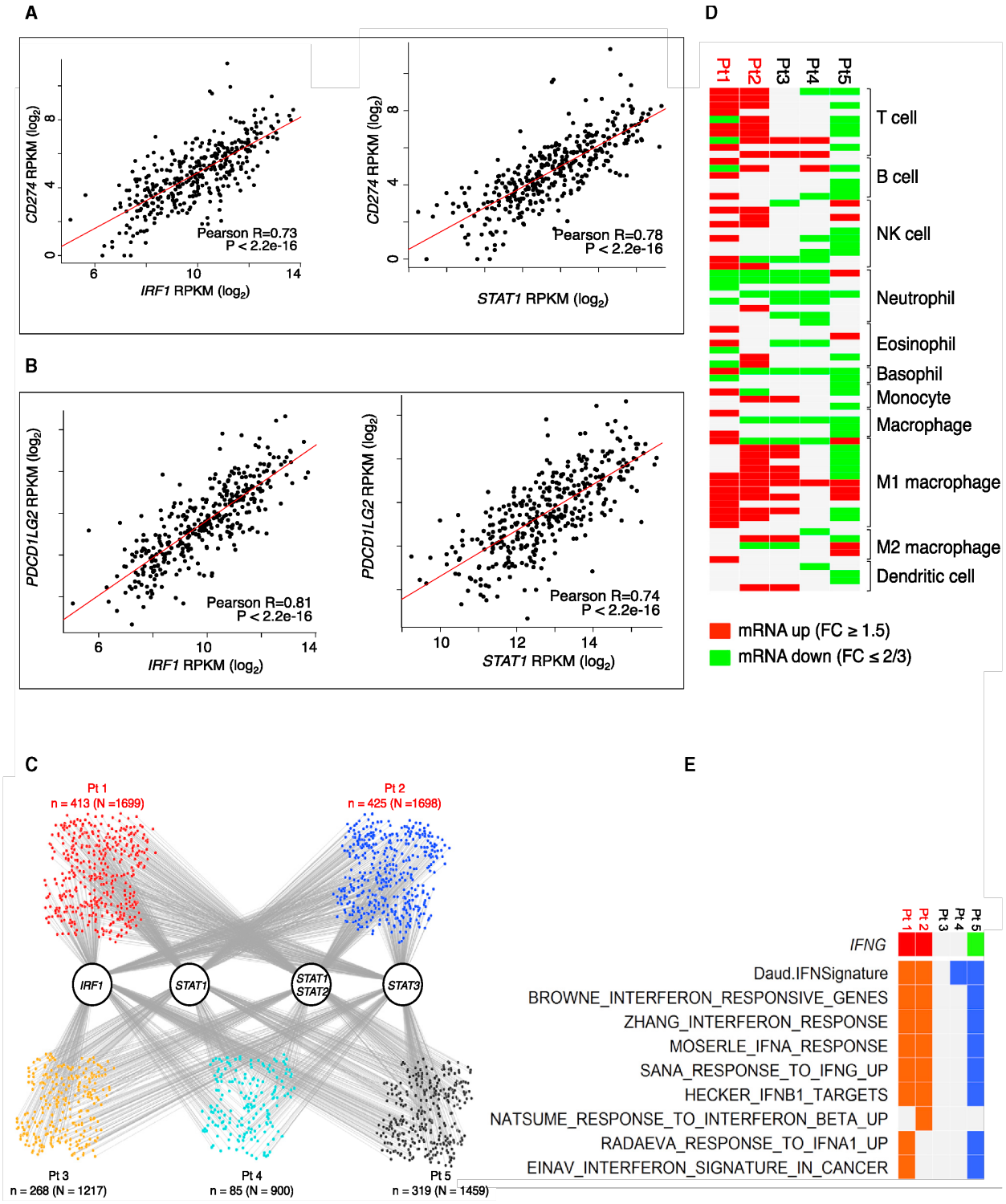

Figure 6. RNA-Seq Analysis of TCGA Tumors and Anti-PD-1-Treated Biopsies

(A) Pearson correlations between log2 normalized mRNA expression levels (RPKM) of *IRF1 and STAT1* versus *PD-L1* in the TCGA skin cutaneous melanoma RNA-seq database.

(B) Pearson correlations between log2 normalized mRNA expression levels (RPKM) of IRF1 and *STAT1* versus *PD-L2* in the TCGA skin cutaneous melanoma RNA-seq database.

(C) Potential target genes of IRF1, STAT1, STAT3, and STAT1:STAT2 heterodimer among all up-expressed genes in anti-PD1 on-treatment tumor samples (up-expression is defined by fold change ≥1.5). Gray lines indicate the occurrence of the respective transcription factor binding motifs in the target genes.

(legend continued on next page)

STAT1/STAT3 putative binding site dramatically decreased PD-L2 promoter activation. These data suggest opposite effects of these sites at the PD-L1 and PD-L2 promoters, which is consistent with a differential regulation of the two PD-1 ligands. Interestingly, the double mutation of these sites had the lower reporter expression of the PD-L2 promoter, suggesting the cooperation of both sites and their binding factors IRF1 and STAT3 in the regulation of the PD-L2 expression.

In order to confirm the IRF1 and STAT3 participation in PD-L2 regulation, ChIP analysis was performed upon interferon gamma or beta exposure for both PD-L1 and PD-L2 promoters in M381 cells (Figures 5F and 5G). Upon interferon gamma exposure, binding of IRF1 to the PD-L2 promoter was strong, yet weaker than PD-L1 promoter binding. We also demonstrated a moderated, interferon-beta-inducible binding of STAT3 to the PD-L2 promoter, but not to the PD-L1 promoter or under interferon gamma exposure (Figures 5G and S5B). These results support the key role of IRF1 with STAT3 contribution to the differential regulation of PD-L1 and PD-L2 expression in melanoma cells, respectively.

STAT1 and IRF1 Upregulation Correlates with PD-1 Ligand Expression and Interferon Signatures Enrichment in Biopsy Specimens of Patients Responding to Anti-PD-1 Blockade Therapy

To address whether our observations were recapitulated in human melanoma tumors, we analyzed RNA-sequencing (RNA-seq) data from The Cancer Genome Atlas (TCGA) skin cutaneous melanoma RNA-seq database (Figures 6A and 6B). We found a strong correlation between IRF1 and PD-L1 or PD-L2 expression (Pearson correlation: R = 0.73 and R = 0.83, respectively), as well as between STAT1 and PD-L1 or PD-L2 expression (R = 0.78 and R = 0.74, respectively). These data support our observations in the cell line analyses that the correlation between STAT1/IRF1 and PD-L1 expression is strong.

We analyzed by RNA-seq the differential expression of interferon gamma and interferon gamma responsive gene signatures (Figure 6E) and of immune cell marker genes (Figure 6D) in biopsy specimens from five patients responding (red, n = 2) or not responding (black, n = 3) to anti-PD-1 therapy. These biopsy specimens represented a range of baseline CD8 and PD-L1 expression both in the tumor center and the invasive margin that were felt to be representative of most cases with melanoma (Table S3). Biopsy specimens from patients responding to anti-PD-1 had enriched expression of interferon gamma responsive genes. The non-responding biopsy specimens did not show interferon gamma upregulation or increased interferon signatures, which is supportive of our in vitro data.

On the other hand, we observed at least 1.5 (log2) fold changes in the expression of immune cell marker genes in on-treatment tumors compared to their respective baselines (Figure 6D). For the on-treatment tumors of the two responders, there was a general increase in the mRNA expression levels of multiple immune lineage markers, especially T cell and natural killer (NK) cell. On the contrary, for the three non-responders, T cell and NK cell markers were either not changed or downregulated.

Finally, we analyzed the expression of target genes of the IRF1, STAT1, STAT2, and STAT3 transcription factors in anti-PD-1 on-treatment biopsy specimens (Figure 6C). The small nodes represent the up-expressed genes in each sample, with binding associations indicted by the gray lines connected to the transcription factors. The absolute numbers of upregulated genes with the motifs of IRF1, STAT1, STAT1/STAT2 dimer, and STAT3 were higher in the responder biopsy specimens than in those from biopsy specimens of patients who did not respond to therapy (n indicates the number of up-expressed genes with binding motifs of transcription factors, while indicates N the total number of up-expressed genes in each sample).

DISCUSSION

Blocking the inducible PD-L1 expression upon tumor-antigen-specific T cell infiltration is the key event leading to response to anti-PD-1 or anti-PD-L1 antibody therapy in patients with cancer (Herbst et al., 2014; Tumeh et al., 2014). The clinical significance of the current work mapping the pathways that allow interferons to regulate the expression of PD-L1 and PD-L2 is highlighted by recent evidence that biopsy specimens of patients with metastatic melanoma who do not respond to anti-CTLA-4 or anti-PD-1 therapy are enriched for mutations in the interferon receptor pathway (Gao et al., 2016; Shin et al., 2017) and the evidence that the selective pressure induced by a long-standing T cell response to melanoma with anti-PD-1 therapy can result in acquired resistance with loss-of-function mutations, with concomitant loss of heterozygosity, of *JAK1* or *JAK2* (Zaretsky et al., 2016). Therefore, a detailed understanding of the signaling pathways regulating the induction of PD-L1 and PD-L2 may help in defining additional mechanisms of primary or acquired resistance and test further improvements in this mode of therapy.

Our studies show that PD-L1 is mainly regulated by the type II interferon receptor singling pathway through JAK1 and JAK2, several STATs, and other modulators of the pathway and converged on the binding of IRF1 to the PD-L1 promoter. On the contrary, PD-L2 is regulated by both interferon beta and interferon gamma, with STAT3 and IRF1 being the transcription factors binding to its promoter in melanoma cells. This detailed knowledge may allow defining patients who cannot respond to PD-1 blockade therapy due to the cancer's inability to engage downstream interferon signaling, resulting in adaptive immune resistance when mutating or epigenetically silencing key molecules in this signaling, as demonstrated in preclinical models in vitro and in vivo (Dunn et al., 2005; Kaplan et al., 1998). Furthermore, this knowledge would allow defining new druggable molecules that could specifically modulate PD-L1 or PD-L2 signaling

(D) Tilling of differential immune cell marker genes in on-treatment anti-PD1 tumors compared to their respective baselines (red and green, up- and down-regulation of at least 1.5 (log2) fold changes.

(E) Tiling of differential *IFNG* expression (red and green, up- and down-expression) and interferon signature enrichment (orange and blue, positive and negative enrichments) in on-treatment tumors derived from patients receiving anti-PD1 treatment (red, patients who responded to treatment; black, patients who did not respond to treatment).

pathways, which may have advantages over current antitumor approaches given the lower cost of small molecules compared to antibodies. These agents may increase or decrease this signaling pathway, thereby having opposing potential uses in autoimmunity and transplantation tolerance or for cancer treatment.

Our studies document a differential regulation between the two PD-1 ligands depending on the cytokine signals, as well as cross talk between the interferon signaling pathways. Interferon gamma treatment resulted in a clear and repetitive upregulation pattern of the JAK2/STAT1/IRF1 axis and PD-L1, which is typical of the type II interferon canonical pathway. However, there was also upregulation of STAT2, STAT3 and IRF9 genes, more typically related to the type I interferon-signaling pathway, further highlighting the overlap between the pathways. We also found a very consistent IL-6 activation between the cell lines that could be contributing to the STAT3 upregulation via autocrine/paracrine action as previously described for other cancer cells (Sriuranpong et al., 2003).

To find the link between the interferon signaling pathways and the regulation of the expression of the PD-1 ligands, we dissected the promoters of both genes. It had been previously reported using electrophoretic mobility shift assays (EMSAs) that IRF1 binds to the PD-L1 promoter in vitro in human lung cancer cells (Lee et al., 2006). We carried out ChIP assays in M381 melanoma cells, and we confirmed a strong binding of IRF1 to the PD-L1 promoter in an interferon-gamma-inducible manner. The PD-L1 promoter truncation assay indicated the likely presence of a repressor at the STAT1/STAT3 in-silico-predicted putative binding site, although a ChIP assay failed to detect STAT3 binding to this region, indicating possible participation of additional factors. For the PD-L2 promoter, both a transient truncation reporter assay and a ChIP assay revealed STAT3 participation in the regulation of this promoter. Interestingly, STAT3 binding was only detected upon interferon beta induction, pointing out again the fact of the differential regulation of these two promoters.

The importance of the JAK1/JAK2-STAT1/STAT2/STAT3-IRF1 axis for the activation of the PD-1 ligands and many other interferon response genes is highlighted by the transcriptional profile of the two mutant melanoma cell lines that had loss of function of *JAK1* or *JAK2* genes and studies of the pharmacological inhibition of JAK2. Furthermore, we confirmed the relevance of our laboratory findings in patient-derived biopsy specimens. Tumor biopsy specimens from patients treated with PD-1 blocking antibody therapy upregulated interferon gamma signatures and target genes for IRF1, STAT1, STAT2, and STAT3 in anti-PD-1 on-treatment tumors. These data provide evidence of the importance of the related signaling pathway for an effective response to anti-PD-1 therapy. Whether this response is related exclusively to PD-1 ligand expression or is a consequence of antigen- presentation machinery regulation should be further investigated.

In conclusion, understanding the signaling pathway used by melanomas to respond to interferon exposure leading to the expression of PD-L1 and PD-L2 is of high importance to develop prognostic molecular markers and PD-1 blockade cancer immunotherapy. Genetic or epigenetic alterations affecting molecules in this pathway that result in lack of adaptive PD-1 ligand expression could be used for better patient selection for PD-1 blockade therapy. Modulation of the expression of factors involved in these pathways could define pharmaceutical targets to develop inhibitors that may block specific signaling resulting in adaptive immune resistance.

EXPERIMENTAL PROCEDURES

Cell Lines

Human melanoma cell lines of the M series were established from patient's biopsies under University of California, Los Angeles (UCLA) institutional review board (IRB) approval (11-003254), as previously described (Atefi et al., 2014). The double stable (DS) reporter cell lines DS244, DS263, and DS381 were generated by transducing M244, M263, and M381 cell lines with two different lentiviral particles (Figure 2A): EF1AProm-Renilla luciferase/RSV-BSD (GenTarget) and PD-L1Prom-DSRed-FireflyLuciferase/Neo lentivirus. Cells were infected at MOI 5–10 with 5 μg/mL polybrene (Santa Cruz Biotechnology) and then selected using 500–1,000 μg/mL G418 and 3–60 μg/mL of BSD during 3 weeks in RPMI media (Invitrogen, Thermo Fisher Scientific) with 10% fetal calf serum (FCS; Omega Scientific), 2 mM L-glutamine, and 1% penicillin, streptomycin (Invitrogen). Expression of both luciferases was validated after interferon gamma treatment for each generated reporter cell line as described in the reporter assay section (Figure S2).

Plasmids and Vectors

For the transient reporter analyses, PD-L1 and PD-L2 promoters were amplified by PCR from genomic DNA obtained from Jurkat cells using the primers listed in Table S1 and cloned into the multicloning site (MCS) of the PGL3 Basic Vector (Promega Corporation) as previously described (Sambrook et al., 1989; full methods can be found in Supplemental Experimental Procedures). Specific deletions of the putative binding sites were carried out using the Q5 Site-Directed Mutagenesis Kit (New England Biolabs), with primers and templates listed in Table S1. Normalization pRL-SV40P plasmid (Addgene plasmid 27163) was a gift from Ron Prywes (Chen and Prywes, 1999), who deposited the plasmid at the Addgene public repository.

For the stable reporter cell lines, the PD-L1Prom-DSRed-FireflyLuciferase/Neo lentiviral construct was cloned as described in Supplemental Experimental Procedures. shRNA lentiviral particles based on the pGIPZ lentiviral vector (Dharmacon) carrying hairpins for the specific genes were generated at UCLA's Molecular Screening Shared Resource (MSSR) from the shRNA Hannon collection. Plasmids were prepared using the PureLink HiPure Filter Plasmid Maxiprep Kit (Invitrogen) or NucleoSpin 96-well Miniprep kits (Macherey-Nagel), and lentiviral particles were produced as previously described (Kappes and Wu, 2001; Silva et al., 2005).

Surface Flow Cytometry Analysis of PD-L1 and PD-L2

Melanoma cell lines were seeded into six-well plates on day 1, targeting 70%–80% of confluence on the day of surface staining. On day 2, cells were exposed to 5,000 IU/mL interferon alpha (Merck Millipore), 500 IU/mL interferon beta (Merck Millipore), or 100 IU/mL interferon gamma (Becton Dickinson) for 18 hr. Interferon concentrations were defined after dose-response curve (PD-L1 mean fluorescence intensity as a function of interferon concentration) optimization processes for all three interferons (Shin et al., 2017).

On day 3, cells were trypsinized and incubated at 37°C for 2 hr with media containing the same concentrations of interferon alpha, beta, or gamma. After 2 hr of incubation, cells were stained with allophycocyanin (APC) anti-PD-L1 and phycoerythrin (PE) anti-PD-L2 antibodies on ice for 20 min and analyzed by flow cytometry using an LSRII (Becton, Dickinson and Company). Data were analyzed using FlowJo software (Tree Star). Experiments were performed at least twice for each cell line. Specificity of the PD-L1 antibody was previously reported (Atefi et al., 2014), while PDL2 antibody specificity was checked as described below using a PD-L2 siRNA approach (Figure S7).

siRNA Transfection

PD-L2 antibody specificity checking was performed on the two cell lines (M244 and M381), which were seeded on a six-well plate (target confluency of ~80%

on the day of flow cytometry analysis) on day 1. Cells were transfected with 25 nM of a PD-L2 siRNA (GE Dharmacon, SMARTpool: siGENOME PDCD1LG2 siRNA and non-targeting control siRNA) as per the manufacturer's protocol on day 2. On day 3, the selected groups were exposed to 100 IU/mL interferon gamma, and flow cytometry analyses were performed on day 4 as described above.

Western Blot

Western blotting was performed as previously described (Escuin-Ordinas et al., 2014). Primary antibodies were purchased from Cell Signaling Technology (CST). Immunoreactivity was revealed with an ECL-Plus kit (Amersham Biosciences) using the ChemiDoc MP system (Bio-Rad). Selected melanoma cells were maintained in 10-cm cell culture dishes and treated with 5,000 IU/mL interferon alpha, 500 IU/mL interferon beta, or 100 IU/mL interferon gamma for 30 min and 18 hr.

Transient Luciferase Reporter Assays

M381 cells were seeded in 24-well plates for 18 hr and then transfected in triplicate using the TransIT-X2 (Mirus Bio) according to the manufacturer's manual with 0.5 μg of each experimental plasmid and 0.5 μg of the Renilla pRL-SV40P plasmid used for normalization per well. After 24 hr in culture, relative luciferase units (RLUs) were measured in non-treated and interferon-treated cells (3 hr, 100 IU/mL interferon gamma; 500, IU/ml interferon beta) using the Dual-Glo Luciferase Assay System and a GloMax 96 Microplate Luminometer (Promega) according to the manufacturer's instructions. RLUs from firefly luciferase signal were normalized by RLUs from Renilla signal.

shRNA Lentiviral Screen

1,000–1,500 cells of each reporter cell line were seeded in 384-well plates and transduced with 15 μL of each virus containing a shRNA hairpin or with the same empty vector without any active hairpin as a control. After 72 hr of culture, transduced cells were treated with 100 U/mL interferon gamma for 8 hr and then stained with 35 μM propidium iodide (PI) and 5 μg/mL Hoechst (Invitrogen). Cell images were acquired using an Image press XL (Molecular Devices) with a 10× objective (0.6 numerical aperture [NA]) in the DAPI, GFP (virus encoded), and CY3 channel. Images were analyzed using the MetaXpress multi-wavelength cell-scoring algorithm with standard settings in order to score cells and calculate percent viability and efficiency of transduction. RLUs for firefly and Renilla were analyzed using the Dual Glo Luciferase Assay System (Promega) according to the manufacturer instructions in a Victor3V luminometer (Perkin Elmer) with 0.1 s integration time. Firefly RLUs were normalized to the Renilla signal and the percentage of transduction to take into account any possible difference in cell viability and virus titer. A probability-based RSA analysis was performed in order to minimize the impact of the shRNA off-target activities as described in the statistical analysis section. Relative downregulation compared to the control were calculated and plotted for each gene and cell line (Figures 3B–3D). A global score based ranking was generated taking into consideration the position of each gene in the 3 cell lines and then was mapped onto the interferon pathways using PathVisio (v 3.2.1) (Kutmon et al., 2015). Pathway representation was based on interferon type I signaling (*Homo sapiens*) from Wikipathways (WP585) and edited for size and clarity and to include type II interferon pathway components (Kutmon et al., 2016).

ChIP

Formaldehyde-cross-linked chromatin was prepared from 2×10^7 M381 melanoma cells, and ChIP was performed using the SimpleChip Plus Enzymatic Chromatin IP Kit (Magnetic Beads 9005) from CST according to the manufacturer's instructions. Antibodies were purchased from CST (normal rabbit immunoglobulin G [IgG] 2729, STAT3 12640) and Abcam (IRF1 ab26109). To calculate DNA enrichment in the ChIP assays, Real-time qPCR was performed in an ABI 7500 (Applied Biosystems, Thermo Fisher Scientific) or a CFX96 real-time PCR system (Bio-Rad) using the iQ SYBR Green supermix (Bio-Rad) and the primers for the PD-L1, PD-L2, and HLA-B promoters listed in Table S1. SimpleChip C-FOS and human tRNA-Leu anti-codon (TAG) primers were purchased from CST, and HLA-B primers were previously reported (Stefan et al., 2011).

Gene Expression qPCR Assays

Downregulation of the genes in the generated cells lines was measured by qPCR using TaqMan gene expression assays and the TaqMan RNA-to-CT 1-Step Kit (Applied Biosystems, Thermo Fisher Scientific) following the vendor's specifications. Total RNA was extracted from cell lines in the absence or presence of interferon-gamma (100 IU/mL) at 3 hr using the QIAGEN AllPrep DNA/RNA Mini Kit RNeasy kit according to the manufacturer's protocol (QIAGEN).

nCounter Transcriptional Profiling Analysis

Total RNA was extracted from human melanoma cell lines in the absence or presence of interferon gamma (100 IU/mL) at 3 hr as described above. nCounter (NanoString Technologies) analysis was performed at the Center for Systems Biomedicine, a part of the Integrated Molecular Technologies Core (IMTC) at UCLA analyzing the genes detailed in Table S2. mRNA transcripts of specific cellular genes, including housekeeping genes for normalization, were quantified in untreated M233, M244, M263, M368, M381, and M395 cells and after 3 hr of interferon gamma exposure. M233 cells were also co-incubated for 3 hr with 1 μM JAK2 pharmacological inhibitor CEP-33779 (Apex Bio). Results were analyzed using the 2.5 nSolver Software (NanoString Technologies).

Tumor Biopsies and Immunohistochemical Staining

Tumor biopsy specimens were obtained from patients receiving anti-PD-1 therapy under UCLA IRB 11-001918. Samples were immediately fixed in formalin followed by paraffin embedding and processed for snap-freezing in liquid nitrogen when an additional sterile piece of the tumor was present (Tumeh et al., 2014). For CD8 and PD-L1 analyses of tumor biopsy specimens, slides were stained with H&E, S100, CD8, and PD-L1 at UCLA's anatomic pathology immunohistochemistry laboratory. Immunostaining was performed on Leica Bond III autostainers using Leica Bond ancillary reagents and REFINE polymer 3,3′-diaminobenzidine (DAB) detection system. Percent positivity in the invasive margin or intratumoral area was calculated using the Indica Labs Halo platform as previously described (Tumeh et al., 2014).

CRISPR/Cas9-Mediated Knockout

The human melanoma cell line M233 was subjected to CRISPR/Cas9-mediated knockout of MAK14 (p38), CRKL, and PI3K by lentiviral transduction using particles encoding guide RNAs, a fully functional CAS9 cassette, GFP, and puromycin as selectable markers (Sigma-Aldrich), as previously described (Zaretsky et al., 2016). Two guide sequences were used per gene. GFP-positive single-cell clones were isolated using a FACSARIA sorter (Becton Dickinson). Disruption was confirmed by Sanger sequencing with tracking of indels by decomposition (TIDE) analysis (Netherlands Cancer Institute (NKI); https://tide.nki.nl) and finally by western blot.

RNA-Seq Gene Set Enrichment and Transcription Factor Enrichment Analysis

RNA-seq data were generated using 2 × 100 bp paired-end sequencing using the Illumina HiSeq2000 platform. Paired-end reads were mapped to the UCSC hg19 reference genome using Tophat2 (Kim et al., 2013); full methods are included in Supplemental Experimental Procedures.

Statistical Analysis

Descriptive statistics such as mean and SD were calculated and are presented in the figures. Unpaired t tests were performed for reporter assay analysis as well as comparing percent input in ChIP analysis. For the shRNA screening, a probability-based RSA analysis was performed in order to minimize the impact of off-target activities of the different shRNA hairpins used in the study (König et al., 2007). The activities of the top hit shRNAs of each gene identified by RSA algorithm were then summarized and presented. nCounter expression profile analysis was carried out using the 2.5 nSolver Software (NanoString Technologies). The normalization module of this software used the popular geNorm algorithm (Vandesompele et al., 2002) to identify the most stable subset of housekeeping genes. From this, a gene expression normalization factor was calculated for each sample based on the geometric mean of the selected housekeeping genes. The normalized expression values of each sample were

visualized and presented in scatterplots. Graph Pad Prism Version 6 was also used to generate plots and additional statistical analysis.

ACCESSION NUMBERS

The accession number for the RNA-seq data reported in this paper is GEO: GSE96619. The nCounter transcriptome is listed in Table S2.

SUPPLEMENTAL INFORMATION

Supplemental Information includes Supplemental Experimental Procedures, seven figures, and four tables and can be found with this article online at http://dx.doi.org/10.1016/j.celrep.2017.04.031.

AUTHOR CONTRIBUTIONS

A.R. and A.G.-D. supervised the project and developed the concepts. A.G.-D., D.S.S., B.H.M., J.M.Z., G.P., C.P.S., R.D., B.C.-A., T.G.G., and A.R. designed the experiments. A.G.-D. performed vector cloning, promoter truncation analysis, qPCR assays, transcriptional profile analysis, and reporter cell line generation. A.G.-D. and D.S.S. performed ChIP analysis. J.S. assisted in the construct cloning and performed truncation studies. D.S.S. performed flow cytometry analysis. A.G.-D., R.D., and J.M.Z. carried out shRNA screen analysis. D.S.S. and H.E.O. performed western blot analysis. L.S., W.H., and R.S.L. performed RNA-seq analyses. S.H.-L. performed pathological analyses in biopsies. X.W. carried out statistical analysis. A.G.-D. and A.R. wrote the manuscript. All authors contributed to the manuscript and approved the final version.

ACKNOWLEDGMENTS

This work was funded by NIH grants R35 CA197633 and P01 CA168585, the Parker Institute for Cancer Immunotherapy, the Dr. Robert Vigen Memorial Fund, the Ressler Family Foundation, the Samuels Family Fund, and the Garcia-Corsini Family Fund (to A.R.). A.R. was supported by a Stand Up To Cancer – Cancer Research Institute Cancer Immunology Dream Team Translational Research grant SU2C-AACR-DT1012). Stand Up To Cancer is a program of the Entertainment Industry Foundation administered by the American Association for Cancer Research. D.S.S. was supported by oncology (5T32CA009297-30), dermatology (5T32AR058921-05), and tumor immunology (5T32CA009120-39) training grants and a Tower Cancer Research Foundation grant. B.H.M. was supported by Juan Rodes Scholarship G83727016 from the Hospital 12 de Octubre, Madrid, Spain. Flow cytometry was performed in the UCLA Jonsson Comprehensive Cancer Center (JCCC) and Center for AIDS Research Flow Cytometry Core Facility, which is supported by NIH awards CA-16042 and AI-28697, and the JCCC, the UCLA AIDS Institute, and the David Geffen School of Medicine at UCLA. The NanoString experiments were run at the Center for Systems Biomedicine, a part of the Integrated Molecular Technologies Core (IMTC) supported by CURE/P30DK41301-26. We are grateful to Ron Prywes for the pRL-SV40P plasmid (Addgene plasmid 27163). Thanks to Bryan France and Bobby Tofig from the CNSI Molecular Screening Share Facility at UCLA for the help with the shRNA screen, Drs. Bin Liu and Kei Shuai from UCLA for guidance on interferon signaling and ChIP analyses, Shauna Gerold and Emmanuelle Faure-Kumar for assistance in NanoString data analysis, and Jeff Calimlim and the rest of the staff from the flow cytometry core laboratory at UCLA for the flow cytometry support.

Received: November 28, 2016
Revised: December 23, 2016
Accepted: April 12, 2017
Published: May 9, 2017

REFERENCES

Aaronson, D.S., and Horvath, C.M. (2002). A road map for those who don't know JAK-STAT. Science *296*, 1653–1655.

Atefi, M., Avramis, E., Lassen, A., Wong, D.J., Robert, L., Foulad, D., Cerniglia, M., Titz, B., Chodon, T., Graeber, T.G., et al. (2014). Effects of MAPK and PI3K pathways on PD-L1 expression in melanoma. Clin. Cancer Res. *20*, 3446–3457.

Chen, X., and Prywes, R. (1999). Serum-induced expression of the cdc25A gene by relief of E2F-mediated repression. Mol. Cell. Biol. *19*, 4695–4702.

Darnell, J.E., Jr., Kerr, I.M., and Stark, G.R. (1994). Jak-STAT pathways and transcriptional activation in response to IFNs and other extracellular signaling proteins. Science *264*, 1415–1421.

Decker, T., Lew, D.J., Mirkovitch, J., and Darnell, J.E., Jr. (1991). Cytoplasmic activation of GAF, an IFN-gamma-regulated DNA-binding factor. EMBO J. *10*, 927–932.

Domanski, P., and Colamonici, O.R. (1996). The type-I interferon receptor. The long and short of it. Cytokine Growth Factor Rev. *7*, 143–151.

Dong, H., Strome, S.E., Salomao, D.R., Tamura, H., Hirano, F., Flies, D.B., Roche, P.C., Lu, J., Zhu, G., Tamada, K., et al. (2002). Tumor-associated B7-H1 promotes T-cell apoptosis: a potential mechanism of immune evasion. Nat. Med. *8*, 793–800.

Dunn, G.P., Sheehan, K.C.F., Old, L.J., and Schreiber, R.D. (2005). IFN unresponsiveness in LNCaP cells due to the lack of JAK1 gene expression. Cancer Res. *65*, 3447–3453.

Escuin-Ordinas, H., Atefi, M., Fu, Y., Cass, A., Ng, C., Huang, R.R., Yashar, S., Comin-Anduix, B., Avramis, E., Cochran, A.J., et al. (2014). COX-2 inhibition prevents the appearance of cutaneous squamous cell carcinomas accelerated by BRAF inhibitors. Mol. Oncol. *8*, 250–260.

Friedman, R.L., and Stark, G.R. (1985). α-Interferon-induced transcription of HLA and metallothionein genes containing homologous upstream sequences. Nature *314*, 637–639.

Gao, J., Shi, L.Z., Zhao, H., Chen, J., Xiong, L., He, Q., Chen, T., Roszik, J., Bernatchez, C., and Woodman, S.E. (2016). Loss of IFN-γ pathway genes in tumor cells as a mechanism of resistance to anti-CTLA-4 therapy. Cell *167*, 397–404.

Herbst, R.S., Soria, J.-C., Kowanetz, M., Fine, G.D., Hamid, O., Gordon, M.S., Sosman, J.A., McDermott, D.F., Powderly, J.D., Gettinger, S.N., et al. (2014). Predictive correlates of response to the anti-PD-L1 antibody MPDL3280A in cancer patients. Nature *515*, 563–567.

Isaacs, A., and Lindenmann, J. (1957). Virus interference. I. The interferon. Proc. R. Soc. Lond. B Biol. Sci. *147*, 258–267.

Ivashkiv, L.B., and Donlin, L.T. (2014). Regulation of type I interferon responses. Nat. Rev. Immunol. *14*, 36–49.

Kaplan, D.H., Shankaran, V., Dighe, A.S., Stockert, E., Aguet, M., Old, L.J., and Schreiber, R.D. (1998). Demonstration of an interferon γ-dependent tumor surveillance system in immunocompetent mice. Proc. Natl. Acad. Sci. USA *95*, 7556–7561.

Kappes, J.C., and Wu, X. (2001). Safety considerations in vector development. Somat. Cell Mol. Genet. *26*, 147–158.

Kessler, D.S., Levy, D.E., and Darnell, J.E., Jr. (1988). Two interferon-induced nuclear factors bind a single promoter element in interferon-stimulated genes. Proc. Natl. Acad. Sci. USA *85*, 8521–8525.

Kim, J., Myers, A.C., Chen, L., Pardoll, D.M., Truong-Tran, Q.-A., Lane, A.P., McDyer, J.F., Fortuno, L., and Schleimer, R.P. (2005). Constitutive and inducible expression of b7 family of ligands by human airway epithelial cells. Am. J. Respir. Cell Mol. Biol. *33*, 280–289.

Kim, D., Pertea, G., Trapnell, C., Pimentel, H., Kelley, R., and Salzberg, S.L. (2013). TopHat2: accurate alignment of transcriptomes in the presence of insertions, deletions and gene fusions. Genome Biol. *14*, R36.

König, R., Chiang, C.Y., Tu, B.P., Yan, S.F., DeJesus, P.D., Romero, A., Bergauer, T., Orth, A., Krueger, U., Zhou, Y., and Chanda, S.K. (2007). A probability-based approach for the analysis of large-scale RNAi screens. Nat. Methods *4*, 847–849.

Kutmon, M., van Iersel, M.P., Bohler, A., Kelder, T., Nunes, N., Pico, A.R., and Evelo, C.T. (2015). PathVisio 3: an extendable pathway analysis toolbox. PLoS Comput. Biol. *11*, e1004085.

Kutmon, M., Riutta, A., Nunes, N., Hanspers, K., Willighagen, E.L., Bohler, A., Mélius, J., Waagmeester, A., Sinha, S.R., Miller, R., et al. (2016). WikiPathways: capturing the full diversity of pathway knowledge. Nucleic Acids Res. *44* (*D1*), D488–D494.

Lee, S.-J., Jang, B.-C., Lee, S.-W., Yang, Y.-I., Suh, S.-I., Park, Y.-M., Oh, S., Shin, J.-G., Yao, S., Chen, L., and Choi, I.H. (2006). Interferon regulatory factor-1 is prerequisite to the constitutive expression and IFN-γ-induced upregulation of B7-H1 (CD274). FEBS Lett. *580*, 755–762.

Lew, D.J., Decker, T., Strehlow, I., and Darnell, J.E. (1991). Overlapping elements in the guanylate-binding protein gene promoter mediate transcriptional induction by alpha and gamma interferons. Mol. Cell. Biol. *11*, 182–191.

Loke, P., and Allison, J.P. (2003). PD-L1 and PD-L2 are differentially regulated by Th1 and Th2 cells. Proc. Natl. Acad. Sci. USA *100*, 5336–5341.

Marzec, M., Zhang, Q., Goradia, A., Raghunath, P.N., Liu, X., Paessler, M., Wang, H.Y., Wysocka, M., Cheng, M., Ruggeri, B.A., and Wasik, M.A. (2008). Oncogenic kinase NPM/ALK induces through STAT3 expression of immunosuppressive protein CD274 (PD-L1, B7-H1). Proc. Natl. Acad. Sci. USA *105*, 20852–20857.

Novick, D., Cohen, B., and Rubinstein, M. (1994). The human interferon α/β receptor: characterization and molecular cloning. Cell *77*, 391–400.

Pachkov, M., Erb, I., Molina, N., and van Nimwegen, E. (2007). SwissRegulon: a database of genome-wide annotations of regulatory sites. Nucleic Acids Res. *35*, D127–D131.

Pardoll, D.M. (2012). The blockade of immune checkpoints in cancer immunotherapy. Nat. Rev. Cancer *12*, 252–264.

Platanias, L.C. (2005). Mechanisms of type-I- and type-II-interferon-mediated signalling. Nat. Rev. Immunol. *5*, 375–386.

Platanias, L.C., Uddin, S., Bruno, E., Korkmaz, M., Ahmad, S., Alsayed, Y., Van Den Berg, D., Druker, B.J., Wickrema, A., and Hoffman, R. (1999). CrkL and CrkII participate in the generation of the growth inhibitory effects of interferons on primary hematopoietic progenitors. Exp. Hematol. *27*, 1315–1321.

Qing, Y., and Stark, G.R. (2004). Alternative activation of STAT1 and STAT3 in response to interferon-γ. J. Biol. Chem. *279*, 41679–41685.

Ribas, A. (2015). Adaptive immune resistance: how cancer protects from immune attack. Cancer Discov. *5*, 915–919.

Saha, B., Jyothi Prasanna, S., Chandrasekar, B., and Nandi, D. (2010). Gene modulation and immunoregulatory roles of interferon γ. Cytokine *50*, 1–14.

Sambrook, J., Fritsch, E.F., and Maniatis, T. (1989). Molecular cloning: a laboratory manual (Cold spring harbor laboratory press).

Schroder, K., Hertzog, P.J., Ravasi, T., and Hume, D.A. (2004). Interferon-γ: an overview of signals, mechanisms and functions. J. Leukoc. Biol. *75*, 163–189.

Shin, D., Garcia-Diaz, A., Zaretsky, J., Escuin-Ordinas, H., Hu-Lieskovan, S., Palaskas, N.J., Hugo, W., Komenan, M.S., Chmielowski, B., Cherry, G., et al. (2015). Innate resistance of PD-1 blockade through loss of function mutations in JAK resulting in inability to express PD-L1 upon interferon exposure. J. Immunother. Cancer *3*, 311.

Shin, D.S., Zaretsky, J.M., Escuin-Ordinas, H., Garcia-Diaz, A., Hu-Lieskovan, S., Kalbasi, A., Grasso, C.S., Hugo, W., Sandoval, S., Torrejon, D.Y., et al. (2017). Primary resistance to PD-1 blockade mediated by JAK1/2 mutations. Cancer Discov. *7*, 188–201.

Silva, J.M., Li, M.Z., Chang, K., Ge, W., Golding, M.C., Rickles, R.J., Siolas, D., Hu, G., Paddison, P.J., Schlabach, M.R., et al. (2005). Second-generation shRNA libraries covering the mouse and human genomes. Nat. Genet. *37*, 1281–1288.

Smith, P.L., Lombardi, G., and Foster, G.R. (2005). Type I interferons and the innate immune response–more than just antiviral cytokines. Mol. Immunol. *42*, 869–877.

Sriuranpong, V., Park, J.I., Amornphimoltham, P., Patel, V., Nelkin, B.D., and Gutkind, J.S. (2003). Epidermal growth factor receptor-independent constitutive activation of STAT3 in head and neck squamous cell carcinoma is mediated by the autocrine/paracrine stimulation of the interleukin 6/gp130 cytokine system. Cancer Res. *63*, 2948–2956.

Stefan, M., Jacobson, E.M., Huber, A.K., Greenberg, D.A., Li, C.W., Skrabanek, L., Conception, E., Fadlalla, M., Ho, K., and Tomer, Y. (2011). Novel variant of thyroglobulin promoter triggers thyroid autoimmunity through an epigenetic interferon α-modulated mechanism. J. Biol. Chem. *286*, 31168–31179.

Stump, K.L., Lu, L.D., Dobrzanski, P., Serdikoff, C., Gingrich, D.E., Dugan, B.J., Angeles, T.S., Albom, M.S., Ator, M.A., Dorsey, B.D., et al. (2011). A highly selective, orally active inhibitor of Janus kinase 2, CEP-33779, ablates disease in two mouse models of rheumatoid arthritis. Arthritis Res. Ther. *13*, R68.

Tseng, S.-Y., Otsuji, M., Gorski, K., Huang, X., Slansky, J.E., Pai, S.I., Shalabi, A., Shin, T., Pardoll, D.M., and Tsuchiya, H. (2001). B7-DC, a new dendritic cell molecule with potent costimulatory properties for T cells. J. Exp. Med. *193*, 839–846.

Tumeh, P.C., Harview, C.L., Yearley, J.H., Shintaku, I.P., Taylor, E.J., Robert, L., Chmielowski, B., Spasic, M., Henry, G., Ciobanu, V., et al. (2014). PD-1 blockade induces responses by inhibiting adaptive immune resistance. Nature *515*, 568–571.

Vandesompele, J., De Preter, K., Pattyn, F., Poppe, B., Van Roy, N., De Paepe, A., and Speleman, F. (2002). Accurate normalization of real-time quantitative RT-PCR data by geometric averaging of multiple internal control genes. Genome Biol. *3*, H0034.

Velazquez, L., Fellous, M., Stark, G.R., and Pellegrini, S. (1992). A protein tyrosine kinase in the interferon α/β signaling pathway. Cell *70*, 313–322.

Zaretsky, J.M., Garcia-Diaz, A., Shin, D.S., Escuin-Ordinas, H., Hugo, W., Hu-Lieskovan, S., Torrejon, D.Y., Abril-Rodriguez, G., Sandoval, S., Barthly, L., et al. (2016). Mutations associated with acquired resistance to PD-1 blockade in melanoma. N. Engl. J. Med. *375*, 819–829.

Chapter 5:

Conclusion and

Future Directions

5.1 Conclusion

Our studies have shown the significant role of interferon signaling in mediating anti-tumor activity to immune check point immunotherapy. Interferon gamma signaling has pleotropic effects on cancer cell, including increased MHC (Major Histocompatibility Complex) class I and proteasome expressions, increased chemokine expression and growth inhibition/apoptosis. Benefit of inducible PD-L1 expression in response to interferon (T cell attack) outweighs other negative effects (immune sensitizing effects) on cancer cell survival. However, this selective pressure is flipped when the PD-1/PD-L1 axis is blocked by therapeutic application (acquired resistance) or immunoediting processes before therapeutic application (primary resistance).

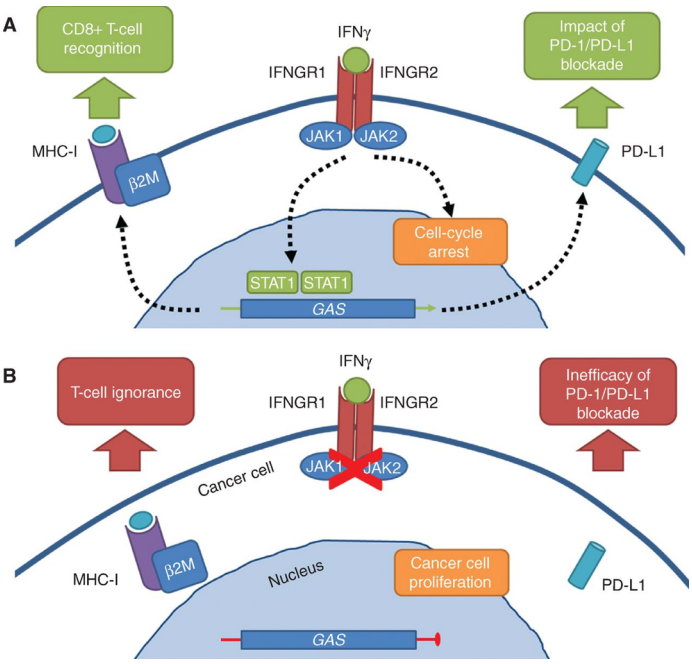

Figure 1. Impact of *JAK* mutations on IFNγ signaling. A, The binding of IFNγ to the interferon gamma receptor (IFNGR1/IFNGR2) activates downstream signaling via JAK1 and JAK2. Upon phosphorylation, a specific transcription profile will be initiated by a homodimer of the transcription factor STAT1, which will bind to the *GAS* promoter to induce the expression of IFN-stimulated genes. This transcription profile will result in cell-cycle arrest and an upregulation of MHC-I molecules and PD-L1 to the cancer cell outer membrane. **B,** Loss-of-function mutations of *JAK1* or *JAK2* can impair IFNγ downstream signaling and therefore allow for cancer cell proliferation, T-cell ignaorance by lack of MHC-I upregulation, and inefficacy of anti–PD-1/PD–L1 therapy due to absence of PD-L1 expression.
Aurelien Marabelle et al. Cancer Discov 2017;7:128-130

When cancer cell loses its adaptive Pd-L1 expression by disabled interferon signaling, we may think T cells may have better anti-tumor activity due to absence of PD-1/PD-L1 interaction. However, as Figure 1 showed, when cancer cell loses its interferon signaling, cancer cells become insensitive to T cell attacks (T cell ignorance). Therefore, treat those tumors with anti-PD-1/L1 antibodies would be ineffective and we propose that JAK1/2 loss of function mutations are a genetic mechanism of loss of adaptive PD-L1 expression that

leads to primary or acquired resistance to PD-1 blockade.

5.2 Future direction

As we have shown, the genetic alteration of JAK1/2 that leads to loss of adaptive PD-L1 expression and loss of interferon response is low. However, the frequency of loss of interferon signaling in cancer cell is likely under-appreciated considering epigenetic alteration as Bob Schreiber and his colleague showed that epigenetic inactivation of JAK1 or JAK2 allowed experimental carcinogen-induced cancers and some established human cell lines, especially in one of prostate cancer cell lines, to avoid immune response (1-3). Epigenetic modification is now increasingly recognized as one of the complex adaptations of cancer cells use to evade immune attack. Currently the strategy to prime cancer cells with epigenetic modifiers before immunotherapy, in particular with TCR engineered adoptive T cell transfer and checkpoint blockade, is being tested in the clinic (NCT01928576). Epigenetic modifiers appear to induce tumor antigen expression and recent studies show that it induces endogenous retroviral double strand RNA expression that triggers interferon

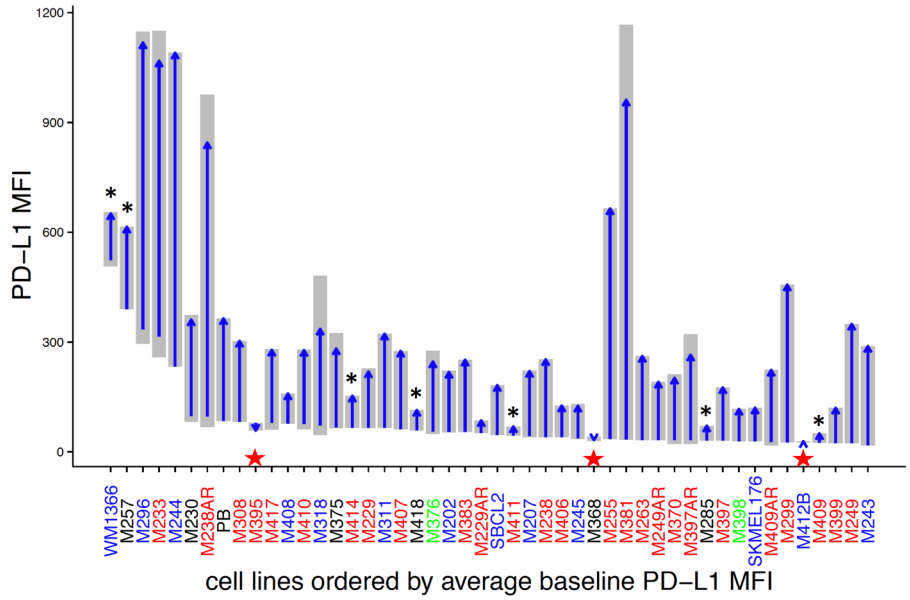

Figure 2. **PD-L1 response to interferon gamma**. Arrows represent average change from baseline upon interferon gamma exposure. Shades show the full range of measured values (n=2 or 3). Red stars indicate cell lines with no response and black stars indicate cell lines with poor response to interferons. Red: BRAF mutated; blue: NRAS mutated; green: BRAF and NRAS mutated; black: BRAF wild type, NRAS wild type. M395 harbored JAK1 loss of function mutation, M368 harbored JAK2 loss of function mutation, M412B did not harbor mutations in interferon signaling genes. (*Shin, et al, Cancer Discover, 2016*)

response in cancer cell (4, 5). Epigenetic modifiers also induce PD-L1 expression (6, 7). Our screening on 48 human melanoma cell lines showed variable degrees of PD-L1 up-regulation in response to interferon gamma, categorized into good (80%), poor (10-15%) and non-responding cell lines. Among 3 of the non-responding cell lines, we reported *JAK1* or *JAK2* loss of function mutations, and the third cell line did not have any loss of function mutations on JAK-STAT signaling genes, yet it did not up-regulate PD-L1 expression at all. These data indicate the potential role of epigenetics in regulating interferon response to those poorly responding and non-responding cell lines without genetic alterations.

With these observation, I am currently undertaking epigenetic profiling of melanoma cell lines based on its adaptive PD-L1 expression in response to interferon by utilizing cutting edge methodologies, such as ATAC (Assay for Transposase-Accessible Chromatin)-seq and fractionated RNA-seq (chromatin associated RNA), etc. These will be particularly useful to interrogate the active transcriptional programs along with accessible genome in each melanoma cell line in response to interferons. This ongoing work has great potential to characterize how cancer cells react to interferons which is a central question needs to be answered in order to understand response and resistance to immunotherapy.

5.3 References

1. Bach EA, Aguet M, Schreiber RD. The IFN gamma receptor: a paradigm for cytokine receptor signaling. *Annu Rev Immunol* **15**:563-91, 1997

2. Kaplan DH, Shankaran V, Dighe AS et al: Demonstration of an interferon gamma-dependent tumor surveillance system in immunocompetent mice. *Proc Natl Acad Sci* U S A **95**:7556-61, 1998

3. Dunn GP, Sheehan KC, Old LJ et al: IFN unresponsiveness in LNCaP cells due to the lack of JAK1 gene expression. *Cancer Res* **65**:3447-53, 2005

4. Roulois D, Loo Yau H, Singhania R et al: DNA-Demethylating agents taget colorectal cancer cells by inducing viral mimicry by endogenous transcripts. *Cell* **162**, 961-973, 2015

5. Chiappinelli KB, Strissel PL, Desrichard A et al: Inhibiting DNA methylation causes an interferon responses in cancer via dsRNA inducing endogenous retroviruses. *Cell*, **162**, 974-986, 2015

6. Wrangle J, Wang W, Koch A et al: Alteration of immune response of non-small celll lung cancer with azacitidine. *Oncotarget* **4,** 2067-79, 2013

7. Li H, Chiappinelli KB, Guzzetta AA et al: immune regulation by low doses of the DNA methyltransferase inhibitor 5-azacitidine in common epithelial cancers. *Oncotarget* **5**, 587-98, 2014